UNIVERSITÀ
DEGLI STUDI
DI PADOVA

UNIVERSITÀ DEGLI STUDI DI PADOVA

DIPARTIMENTO DI BIOLOGIA

SCUOLA DI DOTTORATO DI RICERCA IN BIOSCIENZE E BIOTECNOLOGIE

INDIRIZZO: BIOLOGIA CELLULARE

XXVI CICLO

SINGLE ORGANELLE FRET-BASED ANALYSIS OF INTRACELLULAR CALCIUM: DIFFERENT EFFECTS OF PRESENILINS CARRYING FAMILIAL ALZHEIMER'S DISEASE MUTATIONS

Direttore della scuola: Ch.mo Prof. Giuseppe Zanotti

Coordinatore: Ch.mo Prof. Paolo Bernardi

Supervisori: Ch.mo Prof. Tullio Pozzan

Dott.ssa Paola Pizzo

Dottorando : Andrea Kuan Cie Wong

INDEX

Riassunto

Il Calcio (Ca^{2+}) e' uno dei principali messaggeri intracellulari coinvolto quasi in tutti gli aspetti della vita cellulare. In particolare, il Ca^{2+} gioca un ruolo essenziale nello sviluppo neuronale, plasticità e trasmissione sinaptica, come anche nella regolazione delle vie metaboliche e dell'apoptosi.

Il primo obbiettivo del mio lavoro è stato studiare in dettaglio l'apparato di golgi (AG) come riserva intracellulare di Ca^{2+}.

Il complesso del Golgi può contenere più del 5% della totalità del Ca^{2+} cellulare a concentrazioni significativamente maggiori che in altre regioni cellulari. L'apparato del Golgi contiene tipicamente anche una moltitudine di proteine leganti Ca^{2+} e canali per il Ca^{2+}. L'uso di una sonda cameleon specificamente indirizzata al *trans*-Golgi, ci ha permesso di dimostrare direttamente l'eterogeneità funzionale dell'AG mettendo in luce le caratteristiche distinte di questo subcompartimento: l'accumulo di Ca^{2+} avviene esclusivamente tramite SPCA1 (e non tramite SERCA); inoltre, in risposta a generazione di IP_3 non c'è rilascio di Ca^{2+}, ma un suo piccolo accumulo come conseguenza dell'aumento di Ca^{2+} citosolico.

Usando una nuova sonda per il Ca^{2+} basata sulle GFP selettivamente indirizzata nel *cis*/*medial*-Golgi, (mGo-D1cpv), abbiamo dimostrato che il *medial*-Golgi si comporta in una maniera unica, rilasciandolo Ca^{2+} dopo stimolazione non solo di agonisti liberanti IP_3, ma anche attraverso il recettore rianodinico (RyR) e basandosi, per l'accumulo di Ca^{2+}, sia sulla SERCA che su SPCA1.

In conclusione, l'AG rappresenta uno store intracellulare di Ca^{2+} con un alto grado di complessità. In uno spazio di pochi micron e nonostante il suo continuo intermescolamento dei vari subcompartimenti, il set di proteine che regolano l'omeostasi Ca^{2+} cambia in maniera consistente, separando sub-regioni funzionali, con differenti proteine regolanti il Ca^{2+}, contriburndo alla sua omeostasi.

Il secondo obbiettivo del mio lavoro è stato studiare in dettaglio, utilizzando sonde cameleon specificamente indirizzate, l'effetto di mutazioni familiari del morbo di Alzheimer (FAD) nei geni delle presenilne (PSs) 1 e 2.

Nel nostro laboratorio è stato recentemente visto che la mutazione FAD PS2 riduce il contenuto di Ca^{2+} del principale store cellulare: il reticolo endoplasmatico (RE),

principalmente inibendo l'attività della SERCA, come dimostrato a livello di popolazione cellulare utilizzando la sonda Ca^{2+} equorina indirizzata al RE.

Per studiare l'effetto dell'espressione delle mutazioni FAD sull'omeostasi del Ca^{2+} nel RE in esperimenti FRET su singola cellula, abbiamo creato la nuova sonda cameleon indirizzata al RE (ERD4) con ottimizzate affinità al Ca^{2+} e range dinamico.

L'omeostasi del Ca^{2+} nei diversi subcompartimenti, a livello di singola cellula, sono stati studiati nella linea cellulare SH-SY5Y sovra-esprimendo PS2 wild type (wt), PS2-T122R, PS1 wt opppure PS1-A246E, e anche in fibroblasti umani da pazienti FAD-PS2-N141I e FAD-PS1-A246E (con i rispettivi fibroblasti di controllo da controlli sani della stessa età e sesso).

La concentrazione di Ca^{2+} ($[Ca^{2+}]$) di RE e *medial*-Golgi, in cellule a riposo, è fortemente ridotta dalle PS2 mutate o wt (quest'ultima solo in sovra-espressione), ma non dalla PS1 mutata. Nel *trans*-Golgi, invece, la $[Ca^{2+}]$ in cellule a riposo risulta non essere alterata in nessun caso.

Inoltre, il tasso di accumulo di Ca^{2+} in questi stores viene ridotto dalle PS2 mutate o wt (quest'ultima solo in sovra-espressione) e, solo nel *medial*-Golgi, il tasso di fuoriuscita del Ca^{2+} è potenziata. Questi risultati rafforzano la nostra ipotesi di un effetto inibitorio da parte della PS2 mutata sull'attività della SERCA. Tali risultati sono anche consistenti con il fatto che, all'interno del Golgi, solo il compartimento *cis*/*medial* ha il recettore IP_3 e la pompa SERCA, mentre il *trans*-Golgi è mancante di entrambi.

In conclusione, i nostri dati fanno luce sull'eterogeneità molecolare di diversi store intracellulari per il Ca^{2+} (e in distinti subcompartimenti dello stesso organello) e aggiungono nuovi dettagli per comprendere i meccanismi attraverso cui le PSs influenzano l'omeostasi del Ca^{2+} e la patogenesi delle FAD.

In prospettiva futura, queste sonde cameleon saranno utilizzate per studiare alterazioni sull'omeostasi del Ca^{2+} indotte da mutazioni FAD-PS2 e, eventualmente, in vivo utilizzando vettori virali.

Summary

Calcium (Ca^{2+}) is one of the major intracellular messengers that impacts nearly every aspect of cell life. In particular, it plays essential roles in neuronal development, synaptic transmission and plasticity, as well as in the regulation of metabolic pathways and cell fate decisions.

The first goal of my work was to study more in details the Golgi apparatus (GA), as an intracellular Ca^{2+} store.

The Golgi complex may store up to 5% of the total cellular Ca^{2+} at higher concentrations and contains several different luminal Ca^{2+}-binding proteins and Ca^{2+}-release channels. The use of a specific Cameleon Ca^{2+} sensor targeted to the trans-Golgi, allowed us to directly demonstrate the functional GA heterogeneity by showing the distinct behaviour of this sub-compartment: it takes up Ca^{2+} almost exclusively via SPCA1 (and not by SERCA); it does not release Ca^{2+} in response to IP_3 generation, but rather accumulates the cation as a consequence of the cytoplasmic Ca^{2+} rise.

Using a novel GFP-based Ca^{2+} probe selectively localized to the *medial*-Golgi (mGo-D1cpV), we have demonstrated that this sub-compartment behaves in a unique way, releasing Ca^{2+} upon cell stimulation not only with IP_3-generating agonists, but also through Ryanodin receptors (RyRs) and relying, for its Ca^{2+} uptake, on both SERCA and SPCA1 pumps.

The GA represents, thus, an intracellular Ca^{2+} store with an high complexity level. In a space of a few microns and despite its continuous inter-mixing dynamics, the Ca^{2+} toolkit undergoes major changes and distinct, separate functional sub-regions, with different Ca^{2+} features, contribute to its Ca^{2+} handling.

The second aim of my work was to study, at the single cell level by employing specifically targeted cameleon Ca2+ probes, the effect of Familial Alzheimer's Disease (FAD) presenilin 1 and 2 (PS1, PS2) mutants on Ca^{2+} homeostasis in different sub-cellular compartments: the endoplasmic reticulum (ER), the *medial* and *trans*-Golgi.

Ca^{2+} dyshomeostasis has been demonstrated in AD, in particular in the rare genetically inherited FAD cases (mostly due to mutations in PS1 and PS2 genes).
In our lab has been recently shown, by employing an ER-targeted aequorin Ca^{2+} sensor at the cell population level, that FAD-PS2 mutants reduce the Ca^{2+} content of the major intracellular Ca^{2+} store, the ER, mostly by inhibiting SERCA activity.
In order to deeper investigate the effect of the expression of FAD-PS mutants on ER Ca^{2+} handling in single cell FRET-experiments, we created a novel ER-targeted cameleon Ca^{2+} probe (ER-D4) with optimized Ca^{2+} affinity and dynamic range. In addition, the new cameleon Ca^{2+} probe targeted to the *medial*-Golgi, above described, was also used for a similar purpose.
Ca^{2+} handling by the distinct intracellular compartments, at single cell level, was evaluated in SHSY5Y cell line over-expressing PS2 wild type (wt), FAD-PS2-T122R, PS1 wt or FAD-PS1-A246E and also in human fibroblasts from a FAD-PS2-N141I and a FAD-PS1-A246E patient (and corresponding controls from individuals of the same age and sex).
Ca^{2+} concentration ($[Ca^{2+}]$) of the ER and the *medial*-Golgi, in resting cells, is strongly reduced by PS2, but not PS1, mutants expression, while that of the trans-Golgi compartment results unaffected by both mutants.
The Ca^{2+} uptake rate in these stores is reduced by PS2 mutants expression and, only within the *medial*-Golgi, also the Ca^{2+} leak rate is potentiated.
These findings strength our previous data showing the inhibitory effect of FAD-PS2 on SERCA activity. They are also consistent with the fact that, within the Golgi, only the medial-compartment is endowed with IP_3 receptors and SERCA pumps, whereas the trans-Golgi is devoid of both.
In conclusion, the data highlight the molecular heterogeneity of different intracellular Ca^{2+} stores (and in distinct sub-compartments of the same organelle) and provide new insights for the comprehension of the mechanisms through which PSs influences cellular Ca^{2+} homeostasis and FAD pathogenesis.
In the future, these cameleon probes will be applied to study Ca^{2+} alterations induced by FAD-PS2 mutations and, eventually, in vivo by means of viral vectors.

Introduction

1. Ca^{2+} signalling

In milion years of adaptation to different environments cells have developed different and complex signal systems that changes both in time and space (Clapham D.E., 2007). Calcium (Ca^{2+}) is one of the most important second messengers able to regulate many different cellular functions (Berridge M.J. et al., 2003).

Normally, in resting condition, cells maintain a huge Ca^{2+} gradient between their cytoplasm, that has a Ca^{2+} concentration ($[Ca^{2+}]$) of ~100 nM, and the extracellular medium (1.5-2 mM) and some intracellular organelles, that can reach concentrations of several hundreds micromolar. In order to maintain this gradient, cells extrude Ca^{2+} from the cytoplasm through different energy-dependent mechanisms (Fig. 1). Cytosolic $[Ca^{2+}]$ is strictly controlled by different systems which extrude it through the plasma membrane (exchangers and pumps), bind it (buffers) or compartimentalize it within different subcellular compartments (pumps) (Berridge M.J. et al., 2003). Eukaryotic cells may manage and sequester Ca^{2+} into intracellular organelles, mainly in the endoplasmic reticulum (ER) and the Golgi apparatus (GA), but also peroxisomes, mitochondria and endolysosomal compartments (Fig. 1) (Prins D. and Michalak M., 2011). Changes in intracellular $[Ca^{2+}]$, caused by its influx from the extracellular medium or release from intracellular stores, may trigger different cellular events, such as exocytosis, muscle contraction, fertilization and transcription activation.

1.1. Intracellular Ca^{2+} stores and dynamics

Ca^{2+} may be compartmentalized within subcellular endomembrane compartments, accumulating or releasing Ca^{2+} and also by shaping its transients. The main Ca^{2+} store is the ER, but also the GA, mitochondria, peroxisomes and endolysosomes are strictly involved in Ca^{2+} signalling (Pozzan T., et al., 1994; Rizzuto R. and

Pozzan T., 2006). Each organelle has its own distinct Ca^{2+} molecular toolkits and Ca^{2+} handling proprieties (Zampese E. and Pizzo P., 2011).

1.1.1 The Endoplasmic Reticulum

The ER is a complex and continuous membrane network, with a luminal space that may comprise up to 10% of the whole cell volume. The ER is involved in many different pathways such as carbohydrate and steroid metabolism, biotransformation and protein processing (Csala M. et al, 2006).

In many cell types, increases in cytosolic [Ca^{2+}] can be mainly due to the release of Ca^{2+} from the ER.

The ER contains a high intra-luminal [Ca^{2+}] that has been measured with different metodologies in different cell types, from 200 µM up to 1mM (Meldolesi J. and Pozzan T. 1998).

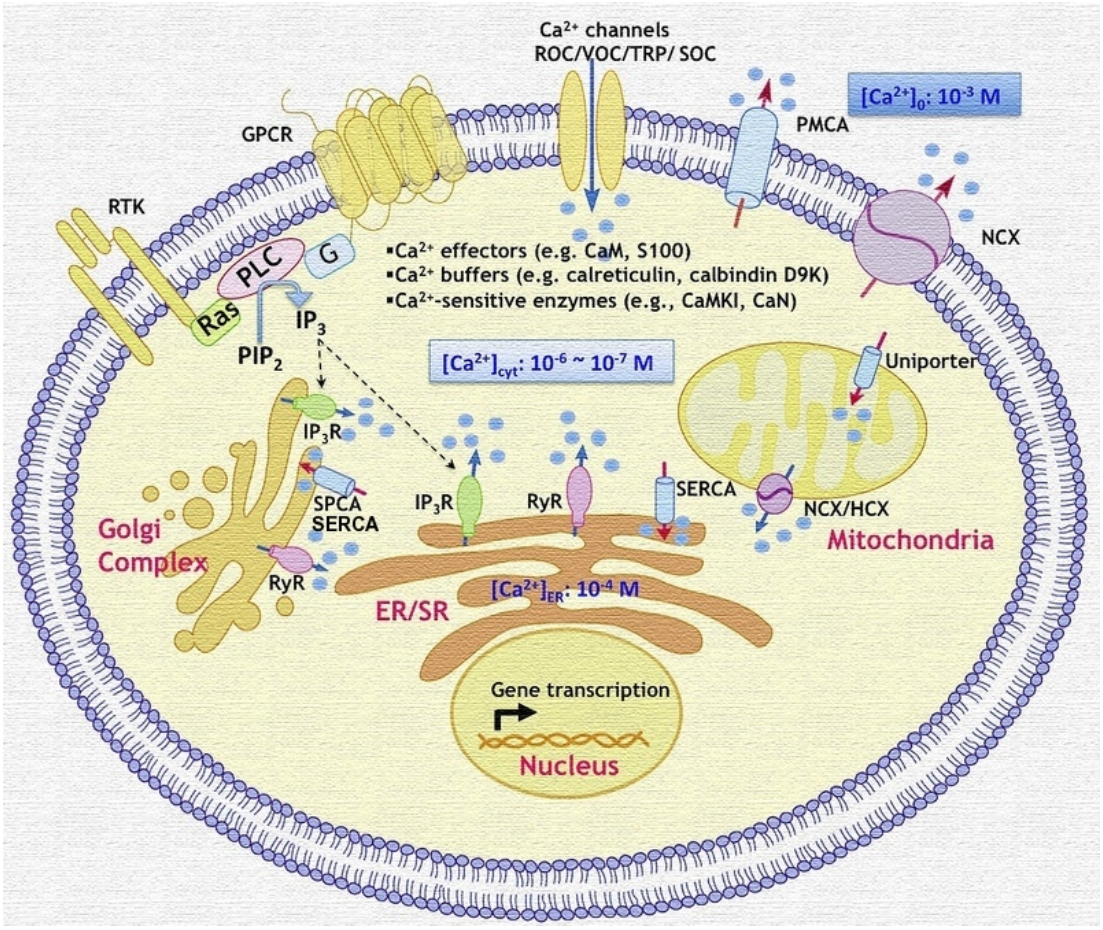

Fig. 1: Ca^{2+} signalling, dynamics and homeostasis.

This compartment contains several proteins able to regulate molecular trafficking from and toward the ER (proteins, ions, etc.), regulated, in their role, by the fine control of [Ca^{2+}].

Ca^{2+} accumulation by the ER depends on the activity of SERCAs (Sarco/ endoplasmic reticulum calcium ATPases): a family of transmembrane proteins that can pump actively 2 Ca^{2+} ions in the ER lumen exploiting the energy of one molecule of ATP (Wuytack F., et al., 2002). In mammals three genes (ATP2A1, ATP2A2, ATP2A3) are present encoding the three SERCA proteins, that have also different splicing variants. There is a different tissue-specific expression pattern of the SERCA variants that can also change during development. The SERCA2b is almost ubiquitous and it is considered the housekeeping isoform (Brini M. and Carafoli E., 2009). There are several drugs able to inhibit the SERCAs, such as the irreversible inhibitor thapsigargin (Tg) (Thastrup O. et al, 1990) and the reversible inhibitors cyclopiazonic acid (CPA) (Seidler N.W. et al, 1989) and 2,5-di-(ter-butyl)-1,4-benzohydroquinone (t-BHQ) (Oldershaw K.A. and Taylor C.W.,1990).

Within the ER different Ca^{2+} buffering proteins are present, such as calreticulin (CRT), calnexin (CNX), calsequestrin (CSQ) (in the sarcoplasmic reticulum), glucose-related protein 78 (GRP78) and 94 (GRP94), etc. All these proteins have multiple Ca^{2+} binding sites but with a low Ca^{2+} affinity (K_d about 1mM). These latter features provide a double advantage: buffering a large amount of Ca^{2+} and a rapid diffusion of the cation within the organelle and the consequent prompt release upon opening of Ca^{2+} releasing channels (Zampese E. and Pizzo P., 2011).

Ca^{2+} is released from the ER through two main family of channels: the inositol 1,4,5-triphosphate (IP_3) receptor (IP_3R), ubiquitously expressed, and the ryanodine (Ry) receptors (RyRs).

IP_3 is a cell common second messenger which release is triggered by different extracellular stimuli (hormones, growth factors, neurotransmitters, etc) that bind and activate plasma membrane G-coupled protein receptors. These latter proteins, in turn, activate the phospholipase C (PLC) that acts on phosphatidyl

inositol bis-phosphate (PIP_2) producing two distinct second messengers: IP_3 and diacyl-glycerol (DAG) (Fig. 2).

IP_3 diffuses in the cytoplasm and binds to IP_3R, ligand-gated Ca^{2+} release channels, localized primarily in the ER membranes (Maeda N. et al., 1991). The activation of the channel induces a rapid flux of Ca^{2+} from the ER lumen to the cytosol and, as a second effect, increases its Ca^{2+} sensitivity. Indeed, Ca^{2+} itself is the most important modulator of the IP_3R which shows a biphasic modulation: at low cytosolic [Ca^{2+}] (250-300 nM) the channel is activated, potentiating the IP_3 response, while at higher concentration (>10 μM), occuring upon Ca^{2+} release at receptor close proximity, the channel is blocked (Foskett J.K. et al, 2007).

The activity of the IP_3R may also be modulated through phosphorylation by different kinases (PKA, PKC, etc.) (da Silva C.P. and Guse A.H., 2000) or interaction with different intraluminal (Chromogranin, ERp44, etc.) and cytosolic (Huntingtin, Cytochrome c, etc.) proteins (Choe C.U. and Ehrlich B.E., 2006).

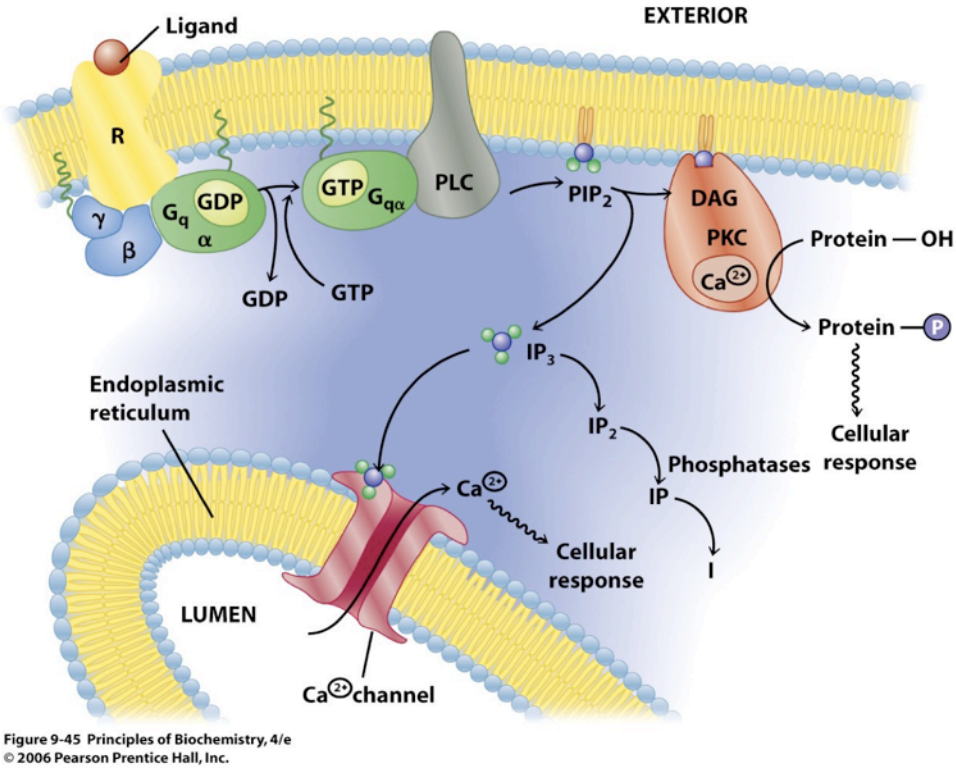

Fig. 2: Molecular mechanisms of IP_3 and DAG second messengers cascade activation (*Principles of Biochemistry,* 4/e. Pearson Prentice Hall, Inc. 2006).

To date, in mammalian cells, IP_3Rs are known to be coded by three different genes with different alternative spliced isoforms. The sequences of the three genes have an homology of approximately 60–80%. Different cells have distinct and overlapping IP_3R patterns of expression that vary during differentiation and they can express more than one isoform (Foskett J.K. et al., 2007). The different isoforms are probably involved in shaping different types of signalling events (Hattori M. et al., 2004).

An IP_3R molecule contains: (I) a large cytoplasmic N-terminus (~85% of the protein), that includes the IP_3 binding region (Mignery G.A. et al., 1990) and a "regulatory"/"coupling" domain which has phosphorylation sites and binding sites for nucleotides and proteins; (II) a central hydrophobic region that forms six membrane-spanning helices that contribute to the ion-conducting pore of the channel; (III) a relatively short cytoplasmic C-terminus that contains a suppressor domain, that may inactive the channel (Foskett J.K. et al, 2007).

The complete IP_3R channel is a homo- or hetero-tetramer of four IP_3R molecules (Joseph S.K. et al., 1997; Patel S. et al., 1999). In this tetrameric structure (Fig. 3) the 5th and 6th helices of the tran-smembrane region and the cytosolic C-terminus are critical for creating the basic pore structure (Michikawa T. et al., 1994; Ramos-Franco J. et al., 1999).

When IP_3 binds the N-terminus of the channel, it induces conformational changes that activate the gate, enabling ions flow through the channel. The molecular identity of the gate and the mechanisms that couple ligand binding to the opening/closing of the gate are still unknown (Foskett K.J. et al., 2007).

As previously described, the N-terminus cytoplasmic part of the protein contains the regulatory domain, that integrates different cellular signalling pathways or metabolic states with the IP_3R functionality (Zampese E. and Pizzo P., 2011).

Several molecules - such as homer, protein phosphatases (PP1, PP2A), RACK1, chromogranin, Na+/K+-ATPase, carbonic anhydrase-related protein (CARP) and IRBIT - interact with the IP_3R and modulate its activity, suggesting that the receptor can form multi-molecular complexes and function as a centre for signalling cascades (Mikoshiba K., 2007).

The other major Ca^{2+}-releasing channel in the ER membranes is the RyR. RyRs are large conductance channels capable of creating rapid transient increases of cytosolic Ca^{2+}. RyRs play a vital role in muscle excitation–contraction (E-C) coupling. They release Ca^{2+} from the sarcoplasmic reticulum (SR) into the cytosol, which sets off a cascade of events resulting in muscle contraction (Lamb G.D., 2000). E-C coupling refers to the close interaction between the dihydropyridine receptor (DHPR) L-type Ca^{2+} channels and RyRs, where depolarization of the plasma membrane, due to L-type Ca^{2+} channels, is coupled to opening of RyRs (Beam K.G. and Bannister R.A., 2010).

Structurally, the RyR is a homotetramer of 2 MDa formed by monomer of ~ 5000 amino acids. Most of the mass of the RyR, similarly to the IP_3R, forms a large

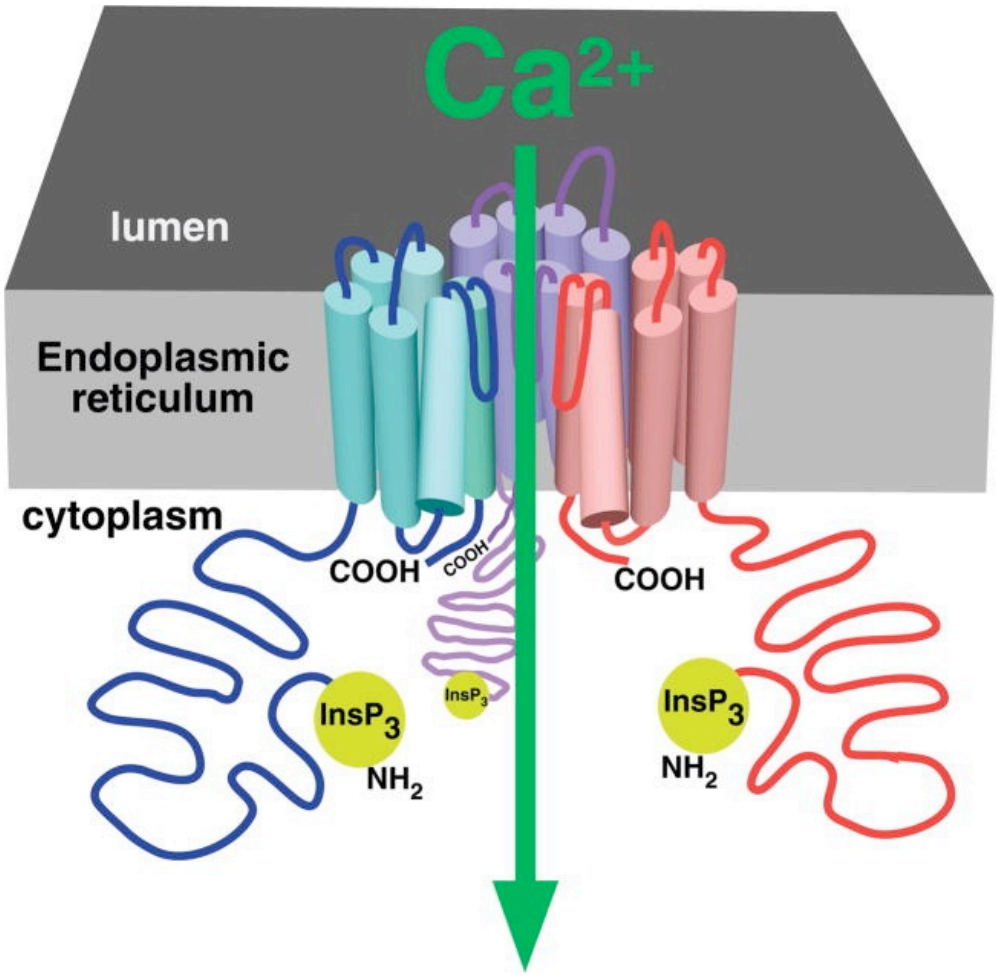

Fig. 3: The IP_3R Ca^{2+} release channel. The cartoon depicts three of four IP_3R molecules (in different colours) in the tetrameric structure. Part of the luminal loop connects transmembrane helices 5 and 6 of each monomer creating the permeation pathway for Ca^{2+} efflux from the ER lumen (Foskett J.K. et al., 2007).

cytoplasmic assembly that is connected to the trans-membrane region. The cytoplasmic region has distinctive structural domains and intervening cavities that permit the interaction with modulators (Fig. 4). The clamp-shaped regions, located at the corners of the cytoplasmic assembly, contain domains for the inter-digitation of neighboring RyRs and for the interaction with some modulators (Hamilton S.L. and Serysheva I.I., 2008).

The RyR and the IP_3R share an overall 17% sequence identity and the identity increases up to 35% within the predicted transmembrane region of the two proteins. The two receptors show similarities in their function and regulation: indeed both permeate Ca^{2+} and are regulated by it in a biphasic manner [Roderick H.L. et al., 2003]; structurally, both are trans-membrane proteins that share a high sequence homology in their ion-conducting pore (formed by 2 transmembrane helices from any monomer of the receptor) and both have conserved domains outside the trans-membrane region (Ponting C.P., 2000).

While in skeletal muscle RyR1 opening is primarily (or exclusively) due to the E-C coupling with DHPR, the major gating mechanism of RyR2 and RyR3 is the Ca^{2+}-induced Ca^{2+} release (CICR): in this case, the opening of RyRs is due to the local plasma membrane Ca^{2+} increase, occurring in the proximity of Ca^{2+} channels, as initially demonstrated for cardiac muscle cells (Fill M. and Copello J.A., 2002).

1.1.2 The Golgi Apparatus

The GA is the main sorting and processing site along the secretory pathway, ensuring that lipids and proteins synthesized in the ER are properly modified (*e.g.*, glycosylated, phosphorylated, processed and packaged into carrier vesicles) and eventually directed to their final destination within or outside the cell (P. Pizzo et al., 2011).

The GA can be schematically viewed as a three composed organelles (*cis*-, *medial*- and *trans*-Golgi) and consists of multiple membranous cisternae arranged in close apposition forming multiple polarized stacks. Indeed, the GA has a *cis*-side associated with a tubular reticular network of membranes (*cis*-

Golgi network, CGN), a medial area of disc-shaped flattened cisternae, and a *trans*-side associated with another tubular reticular membrane network (*trans*-Golgi network, TGN) (fig. 5) (Pizzo P. et al., 2011).

The GA is a highly dynamic structure, where the steady-state structure of Golgi stacks depends on the balance of anterograde and retrograde vesicle trafficking between the various GA cisternae, the ER and other cellular compartments (P. Pizzo et al., 2011).

Functionally, the GA is an obligatory station for post-translational modification of proteins and lipids: it contains numerous glycosyl-transferases, glycosidases, sulphatases, kinases and pro-protein convertases (such as furin) that cleave protein precursors into their mature forms (Schafer W. et al., 1995).

The polarized morphology of GA parallels specific functionalities: for example, glycosyl-transferases act sequentially in consequent compartments and, in general, enzymes that need to act early in glycan biosynthetic pathways are

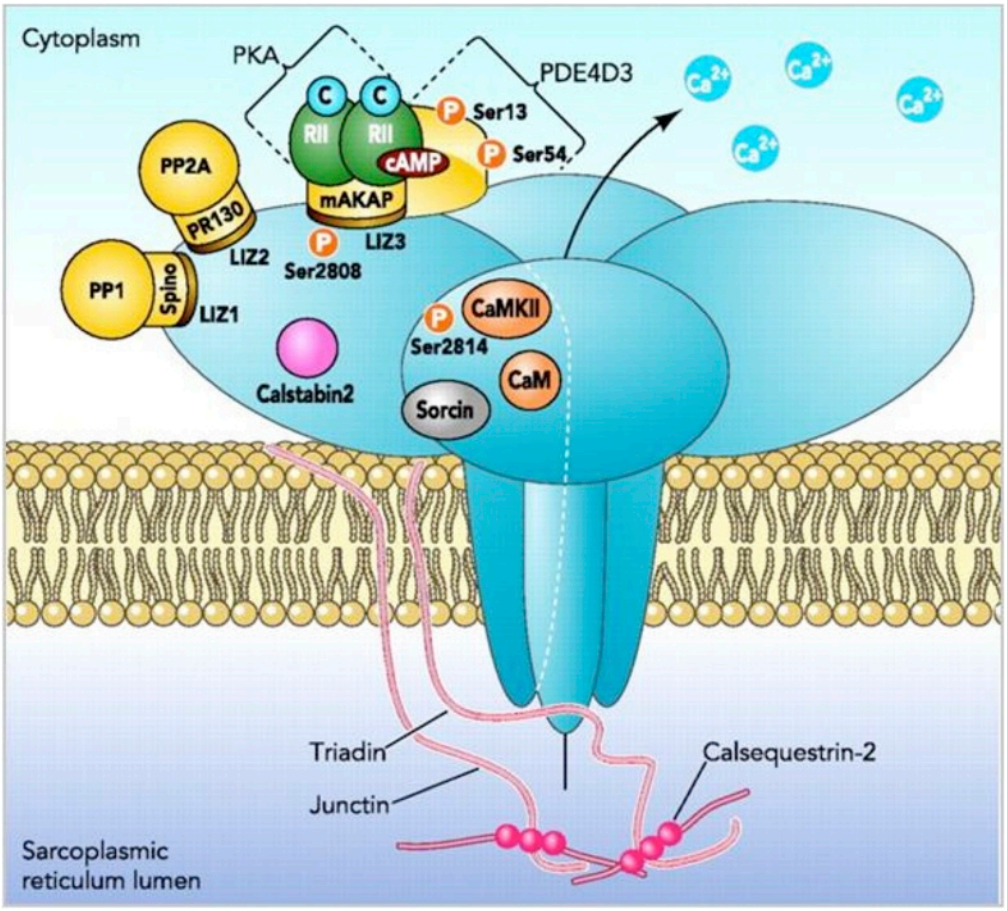

Fig. 4: The RyR macromolecular signalling complex

located within *cis*- and *medial* compartments of the GA, whereas enzymes that need to act later tend to reside within the *trans*-Golgi cisternae and the TGN (Breton C. et al., 2001).

In the last two decades, numerous direct and indirect evidence supported the idea that the GA plays a key role as intracellular Ca^{2+} store, containing up to 5% of whole cell Ca^{2+} (Chandra S. et al., 1991, Pezzati R. et al., 1991). Furthermore, processing enzymes located in the GA show a strong Ca^{2+} dependency of their activity, such as retrograde membrane traffic from the Golgi to the ER (Oda K., 1992) and selective aggregation of regulated secretory proteins in the TGN is also critically depended on GA Ca^{2+} content (Chanat E. and Huttner W.B., 1991).

The first direct demonstration that the GA is a dynamic Ca^{2+} store capable of releasing Ca^{2+} upon cell activation came when a new aequorin based Ca^{2+} probe

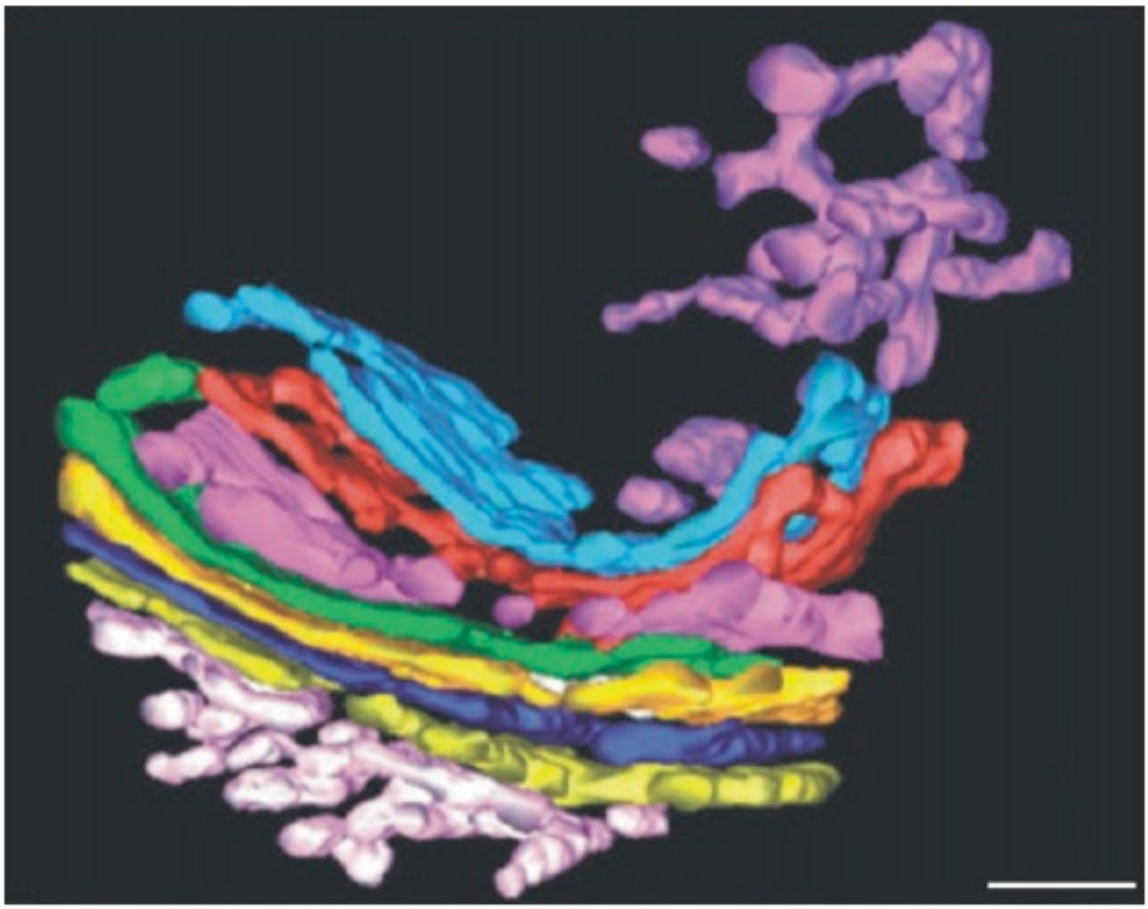

Fig. 5: Three-dimensional tomographic reconstruction of the Golgi complex. The *cis*-Golgi network (white) and the stack with the terminal three *trans*-Golgi cisternae (pink, red and cyan) are shown. The *trans*-Golgi network (violet) appears as a tubular network that emerges from the lateral part of the last *trans*-cisterna (cyan) (Pizzo P. et al., 2011)

specifically targeted into the GA lumen was developed (Pinton P. et al., 1998). With this tool was demonstrated that a high [Ca^{2+}] is maintained in the GA lumen of a resting cell, and that the Ca^{2+} uptake in the GA is depended on the combined activity of two Ca^{2+} pumps: the SERCA pump typical of the ER, and the secretory pathway Ca^{2+} ATPase1 (SPCA1). Furthermore, Ca^{2+} within the GA could be discharged rapidly and extensively upon stimulation with an IP_3-generating agonist.

Experiments from different groups have confirmed that the GA is an ER-like Ca^{2+} store and indirectly supported the idea that its integrity is important for shaping cytosolic Ca^{2+} responses (Lin P. et al 1999; Callewaert G. et al., 2003). Furthermore, Ca^{2+} handling within the GA was demonstrated to be heterogeneous: Vanoevelen J. and Missiaen L. experiments showed that the SPCA1-containing Ca^{2+} sub-compartment was insensitive (or mildly sensitive) to IP_3-generating agonist stimulations and therefore not involved in setting up cytosolic Ca^{2+} signals (Vanoevelen J. et al., 2004; Missiaen L. et al., 2004).

The GA contains several Ca^{2+} handling proteins known to be expressed in the ER, such as SERCA2 pumps and IP3Rs (Pizzo P. et al., 2011); also RyRs have been shown to be expressed in this compartment (Cifuentes F. et al., 2001).

For Ca^{2+} uptake, in addition to SERCA the GA expresses also another ATP-dependent Ca^{2+} pump: the SPCA (Pizzo P. et al., 2011). In human cells, two different genes encoding for SPCA have been identified: ATP2C1 (that have 4 protein variants) and ATP2C2.

SPCAs are single subunit integral membrane proteins with a large cytosolic head, containing an actuator (A), a nucleotide-binding (N), and a phosphorylation (P) domain, and with 10 hydrophobic trans-membrane helices (M1–M10).

Within the trans-membrane region, SPCAs contain one high-affinity binding site for Ca^{2+} and Mn^{2+}, providing both cations to the GA. This is a very important because Mn^{2+} is absolutely required for the correct glycosylation of secretory proteins in the GA (Kaufman R.J. et al., 1994).

The GA is also equipped with luminal Ca^{2+}-binding proteins. CALNUC is the most abundant and better characterized of the GA Ca^{2+} binding proteins (Lin P. et al., 1998). Other identified GA Ca^{2+} binding proteins are Cab45, a luminal

soluble protein important for vesicular sorting (Scherer P.E. et al, 1996); p45/ NEFA, a luminal protein strongly associated to GA membranes (Karabinos A. et al., 1996) and calumenin, a protein present also in the ER and in the secretory pathway, that interacts with SERCA and RyR2 modulating their activity (Jung D.H. et al. 2006; Sahoo S.K. et al, 2009).

The GA is thus equipped with all the necessary molecular components for its function as a Ca^{2+} store (Ca^{2+} pumps, Ca^{2+} releasing channels and luminal Ca^{2+}-binding proteins), and their differential distribution within GA cisternae suggests that the GA does not behave uniformly in terms of Ca^{2+} handling.

Recently, in our lab, direct evidence of the GA heterogeneity have been obtained, using a novel genetically encoded fluorescent Ca^{2+} indicator specifically targeted to the *trans*-Golgi lumen, the GoD1cpv. With this probe, it has been demonstrated that within the *trans*-Golgi is present the only SPCA1 (and not the SERCA) to takes up Ca^{2+} and the release of Ca^{2+} does not happened in response to IP_3 generation (Fig. 6A), rather, the cytoplasmic Ca^{2+} rise that follows this latter event, leads the *trans*-Golgi Ca^{2+} accumulation (Fig. 6B) (Lissandron V. et al., 2010).

Furthermore, cells that express high level of RyRs (*i.e.*, neonatal primary cardiomyocytes) showed, upon activation of these latter channels by caffeine or in response to CICR, a release of Ca^{2+} within the *trans*-Golgi (fig. 6C) (Lissandron V. et al., 2010).

From these findings is clear that the *trans*-Golgi appears as an intracellular Ca^{2+} store quite distinct from the ER, but also from the other GA sub-compartments.

In cells that do not express RyRs, the *trans*-Golgi behaves simply as a Ca^{2+} sink, taking up Ca^{2+} by SPCA1 when cytosolic Ca^{2+} increases, while it represents a mobilizable Ca^{2+} store when RyRs are functionally present, for example in cardiomyocytes (Lissandron V. et al., 2010).

The $[Ca^{2+}]$ within the *trans*-Golgi, calculated in HeLa cells using the GoD1cpv, is 130 µM (Lissandron V. et al., 2010), lower than the $[Ca^{2+}]$ measured with aequorin in the whole GA of the same cell type (around 200–300 µM) (Pinton P. et al., 1998). Considering the data of several other groups showing the Ca^{2+} values calculated for the different intracellular organelles (with different probes

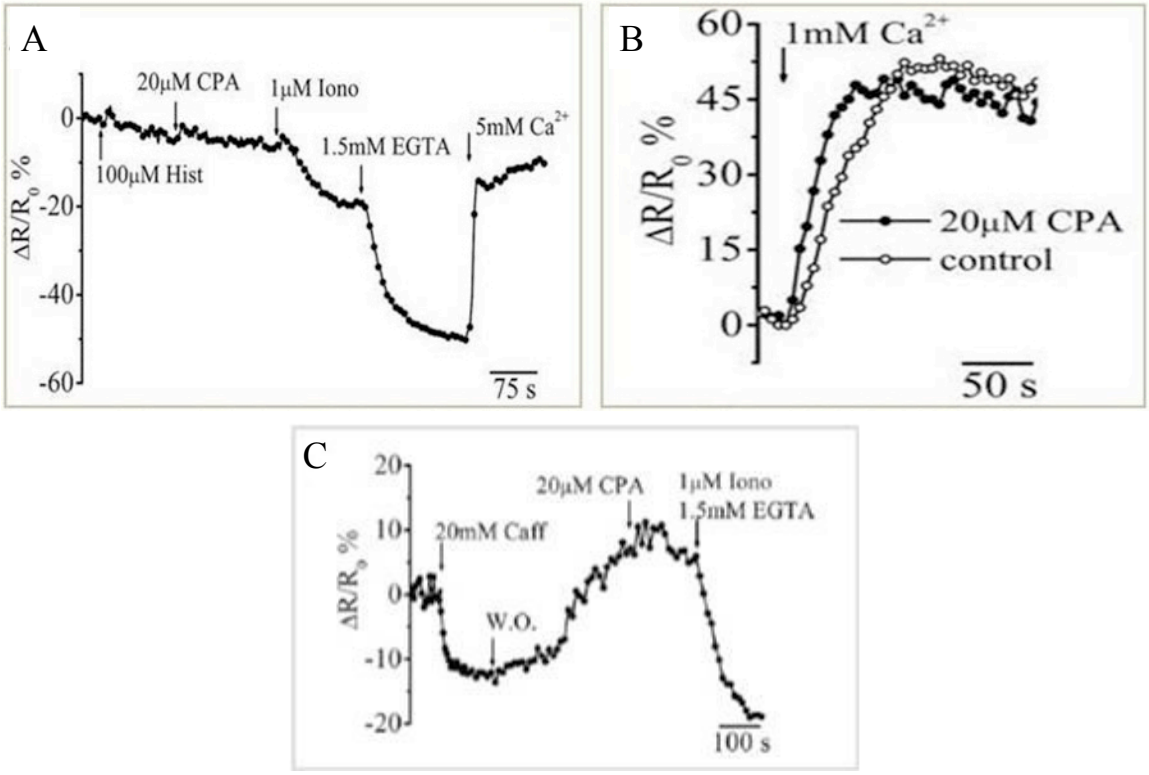

Fig. 6: A representative transGo-D1cpv FRET change curve in response to different stimuli (panel A) and a representative Ca^{2+} refilling kinetic of the *trans*-Go (panel B) in HeLa cells. *Trans*-Golgi Ca^{2+} response in cardiac myocytes upon ryanodine receptor stimulation (panel C) (Lissandron V. et al., 2010).

and in different cell types), it appears that a gradient in the luminal Ca^{2+} concentration through the secretory pathway is present. This gradient decreases from the ER (3–400 μM), passing across the whole GA (200–300 μM) and the *trans*-Golgi (130 μM), to the secretory vesicles (80 μM) (fig. 7) (Lissandron V. et al., 2010; Pinton P. et al., 1998; Mitchell K.J. et al., 2001; Pizzo P. et al., 2011).

The complexity of the GA morphology, and of its sub-compartments specific enzymatic repertoire, is paralleled by the expression of different molecular Ca^{2+} toolkit in each sub-compartment (Ca^{2+} pumps, channels and buffering proteins). The informations on the *cis*- and *medial*-Golgi are still based on indirect data and one attained goal of my work has been to characterize them, in term of Ca^{2+} handling, using specific targeted Ca^{2+} probes for these sub-compartments.

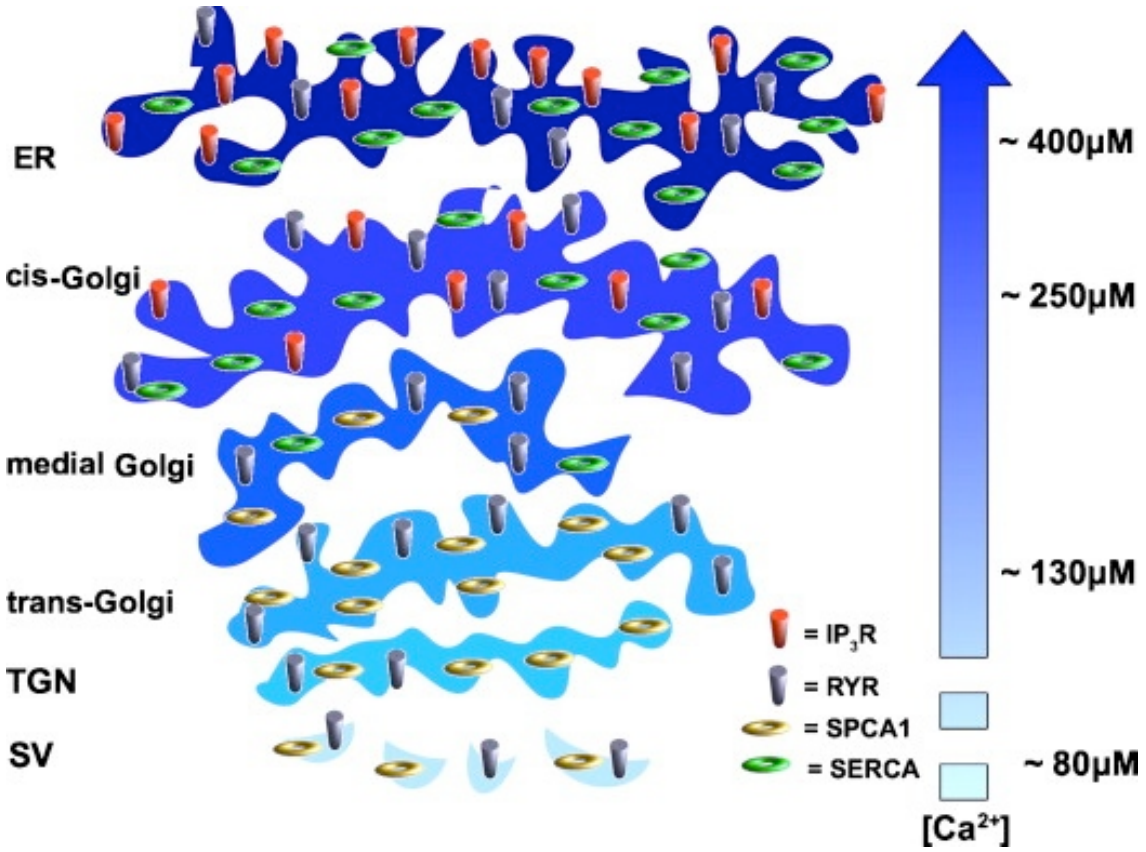

Fig. 7: Ca^{2+} concentration and molecular tool-kit gradient through the secretory pathway (P. Pizzo et al., 2011).

1.1.3 Mitochondria, peroxisomes and lysosomal compartments

Mitochondria are cellular organelles responsible of the generation of energy; moreover, they are also important intracellular Ca^{2+} modulators. The organelle can take up Ca^{2+} in his matrix by the action of the uniporter (mitochondrial Ca^{2+} uniporter, MCU) that transports Ca^{2+} at the cost of the high electrochemical H^+ gradient across the mitochondrial membrane ($\Delta\Psi$ ~ -180 mV) generated by the respiratory chain (De Stefani D. et al., 2011). Within the mitochondrial matrix Ca^{2+} is stored not bound to Ca^{2+} buffering proteins but instead precipitated out as an insoluble salt, $CaPO_4$. The handling of Ca^{2+} by mitochondria is very complex, and one worth highlighting aspect is how mitochondria communicate with the ER with respect to Ca^{2+} fluxes (Prins D. and Michalak M., 2011).

Mitochondrial [Ca^{2+}] has been accurately measured evidencing that, upon an agonist-evoked transient cytosolic [Ca^{2+}] increase, mitochondria respond with a transient Ca^{2+} increase that reaches values even 100-fold higher than the cytosolic one (Rizzuto et al, 1992). These evidence led to the hypothesis that ER and mitochondria are often tightly apposed in regions known as mitochondria-associated membranes (MAM), where [Ca^{2+}] can reach very high levels, as in the proximity of IP3-sensitive channels (Rizzuto et al., 1993). Interestingly, resting cytoplasmic Ca^{2+} levels promote dissociation of the two organelles whereas higher Ca^{2+} levels enhance their association, suggesting that mitochondria may act as buffers to soak up Ca^{2+} released from the ER lumen (Wang et al., 2000). Ca^{2+} entry into mitochondrial matrix exerts different physiological functions ranging from activation of three mitochondrial dehydrogenases (the pyruvate, α-keto-glutarate and isocitrate dehydrogenase), thus positively regulate ATP synthesis, to obtain buffering and modulation of cytosolic Ca^{2+} variations (Giacomello et al., 2007).

Recent results indicate that peroxisomes are capable of taking up and storing Ca^{2+} within their lumen at concentrations much higher than those found in the cytoplasm (Raychaudhury B. et al. 2006; Drago I. et al. 2008). However, it is not yet known how Ca^{2+} is stored within these organelles and whether specific peroxisomal Ca^{2+} buffering proteins exist (D. Prins and M. Michalak, 2011).

Recently, the nicotinic acid adenine dinucleotide phosphate (NAADP) has been shown to act as a second messenger, mobilizing intracellular Ca^{2+} stores by activation of two-pore channels (TPCs) in endosomal membranes (Calcraft P.J. et al. 2009). Endosomes and lysosomes may thus be considered as Ca^{2+} storage organelles; however, the mechanism of lysosomal Ca^{2+} buffering has not been yet described (D. Prins and M. Michalak, 2011).

1.2 Extracellular Ca^{2+} entry into cells

A cytosolic [Ca^{2+}] rise can trigger a fast activation of different signalling pathways; these [Ca^{2+}] increases can be due to the opening of Ca^{2+} channels, located on the plasma membrane or within organelles membranes, allowing Ca^{2+}

to follow its electrochemical gradient. Most ion channels are gated (*i.e.*, capable of making transitions between conducting and non-conducting conformations), permitting their activation upon an appropriate electrical or chemical stimuli. Ca^{2+} channels have generally been classified on the nature of the activation stimulus in voltage-gated and ligand-gated Ca^{2+} channels (Piertrobon et al., 1990; Fasolato et al., 1994).

1.2.1 Voltage-operated Ca^{2+} entry

Voltage-operated Ca^{2+} channels (VOCCs) can be opened upon plasma membrane depolarization, transforming electrical signals into chemical signals. In the nervous system they control a broad array of functions including neurotransmitter release, neurites outgrowth, synaptogenesis, neuronal excitability, differentiation, plasticity, etc. VOCCs are present also in other cell types, such as cardiac and smooth muscle cells, where their activation initiate contraction directly by increasing cytosolic [Ca^{2+}] and indirectly by activating CICR by RyRs in the SR (W.A. Catterall, 2011); in skeletal muscle cells, where these channels interact directly with RyRs within the SR and activate them to initiate rapid contraction (Catterall W.A., 1991); in endocrine cells, where VOCCs mediate Ca^{2+} entry that initiates secretion of hormones (Yang S.N. and Berggren P.O., 2006).

VOCCs are multi-subunits complexes made up of a pore-forming and voltage-sensing α1 subunit and several auxiliary subunits, including 2δ and β subunits and, in some cases, also γ subunits. They constitute a complex family of channels comprising a larger number of different subtypes, which have in common a steep voltage dependence of the open probability and a very high selectivity for Ca^{2+} over Na+ and K+ ions in physiological solution (Carafoli 2005). They are located in the plasma membrane in excitable cells (*e.g.*, in neurons and heart cells), and are classified in different subtypes depending on voltage and inhibitors sensitivity: L-, N-, T-, P/Q-, and R- type.

1.2.2 Ligand-operated Ca^{2+} entry

Ligand-gated Ca^{2+} channels are characterized by a lower selectivity for Ca^{2+} over other monovalent cations if compared to VOCCs. This family of Ca^{2+} channels is usually divided into two subgroups:

1- The receptor-operated Ca^{2+} channels, which possess a ligand-binding site in the same polypeptide or in the same molecular complex forming the channel itself. The extracellular binding of the ligand, either hormone or neurotransmitter, may trigger channels opening and the further Ca^{2+} entry (Clapham 2007).

3- Second-messenger Operated Ca^{2+} channels, which are activated by second messengers produced or released after activation of G-protein or enzyme-coupled receptors. The most common second messengers are: cAMP, cGMP, IP_3, DAG, arachidonic acid and Ca^{2+} itself (Clapham 2007).

1.2.3 Store-operated Ca^{2+} entry

Depletion of intracellular Ca^{2+} stores via different way, such as Ca^{2+} release associated to the IP_3 cascade or by the inhibition of SERCA pump, results in the activation of Ca^{2+} influx via the so-called store-operated Ca^{2+} channels (SOCCs) (Vaca L., 2010), that may re-establish the Ca^{2+} content of the stores depleted and resets the system.

One key event in this process is the signal that communicate the depleted state of intracellular Ca^{2+} stores to the plasma membrane channels (Putney J.W. Jr., 2007). STIM1 is the molecular link between the ER Ca^{2+} depletion event and the store-operated Ca^{2+} entry activation that, in turn, depends on the activation of Ca^{2+} release-activated Ca^{2+} (CRAC) channels in the plasma membrane.

STIM1, initially characterised as a phosphoprotein, includes a single transmembrane domain located in the ER in resting cells. Within the N-terminal, the luminal part of the protein, a single EF-hand Ca^{2+}-binding motif acts as luminal ER Ca^{2+} sensor (Liou J. et al., 2005).

The direct CRAC molecular interactor of STIM1 is Orai1 that comprise the CRAC channel pore-forming subunit (Cahalan M.D., 2009). Orai1 is formed by four trans-membrane segments that form the Ca^{2+} selective plasma membrane channel (Cahalan M.D. et al., 2005).

In resting cells, STIM1 is uniformly distributed within the ER membrane, displays tubular structures and binds to the microtubule-plus-end-tracking protein EB1 at those sites where microtubule ends come in contact with the ER (fig. 8) (Grigoriev I. et al, 2008). After sensing the Ca^{2+} depletion within the ER, STIM1 forms oligomers and then redistributes into punctuate clusters close to the plasma-membrane (fig. 8) (Liou J. et al., 2005). Recently, it has been shown that oligomerisation of about four STIM1 proteins is the critical step transmitting ER store depletion to activating store-operated Ca^{2+} entry (fig. 8). In particular, four Orai1 molecules create the pore-forming subunit of the CRAC channel that opens upon stimulation by STIM1, upon the interaction of the C-terminus of STIM1 and N-terminus of Orai1 (fig. 8) (Lewis R.S., 2007).

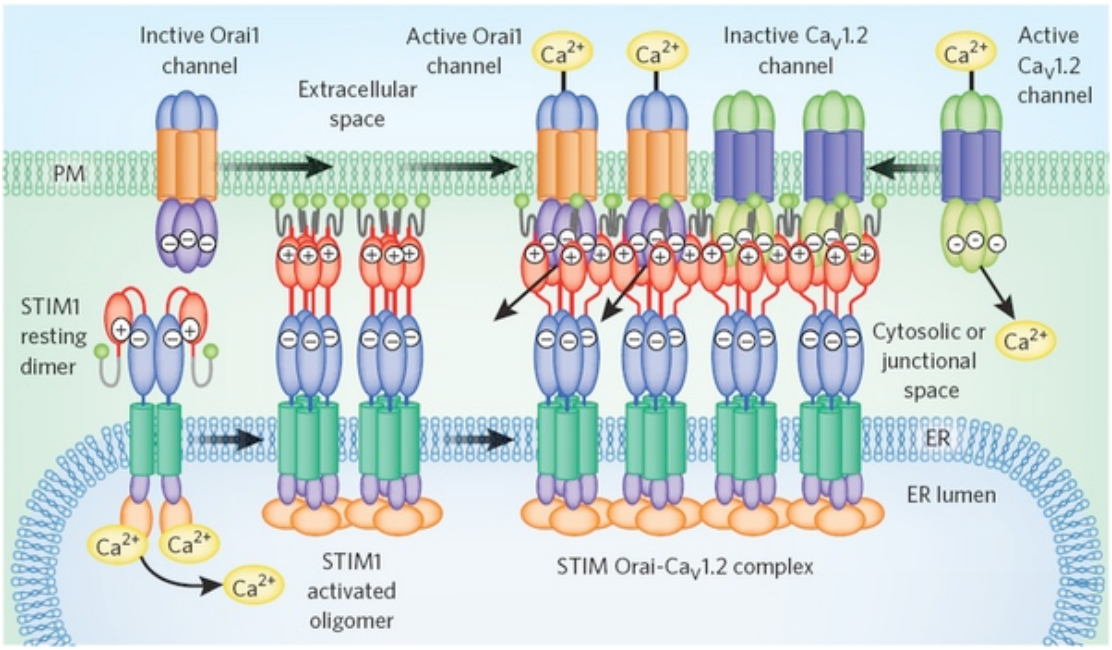

Fig. 8: The functional units of store-operated Ca^{2+} entry assemble in response to store depletion (Saboloff J. et al., 2011).

2. Genetically encoded Ca^{2+} sensors

As explained in privious section, Ca^{2+} is one of the most important cellular second messangers, and the development of tools and methods to valuate Ca^{2+} in living cells became crucial in last decades for the study of this molecule.

Up to now several probes have been devised, which are classifiable in chemical (or synthetic) Ca^{2+} sensors (such as quin-2, fura-2, fluo-4, calcium green, etc) and genetically encoded Ca^{2+} indicators (GECIs).

This latter class are defined as indicators that are produced by translation of a nucleic acid sequence and they are composed solely of natural protein or peptide motifs. In order to convert a Ca^{2+} signal into an optical readable signal, GECIs consist of at least one light-emitting protein and a Ca^{2+} responsive element, where Ca^{2+} binding changes the optical properties of the protein(s). These protein-based indicators are typically incorporated into cells by gene transfer techniques (McCombs J.E. and Palmer A.E., 2008).

GECIs have the intrinsic advantage that they may be targeted to specific intracelular site and organelles (such as mitochindria, ER, GA, etc), just adding a specific targeting sequence at one or both protein ends.

This class of Ca^{2+} sensors comprise three main sub-groups (Fig. 9):

1- bioluminescent reporters. This group of GECIs, based on the aequorin photoprotein (Rizzuto R. et al., 1994), are able to generate light by a chemical reaction that requires reconstitution of the indicator with a co-factor (coelenterazine);

2- single fluorescent proteins indicators. These probes are composed by a Ca^{2+}-responsive elements, such as calmodulin (CaM), or a portions of it, which are inserted into a fluorescent protein (FP). Ca^{2+} binding alters the protonation state of the FP changing the spectral properties of the chromophore. These indicators include the camgaroos, G-CaMPs, pericams, “Case” sensors and grafted EF-hands (McCombs J.E. and Palmer A.E., 2008);

3- FRET-based sensors. Substancially, this group is composed solely by the “cameleon-type” probes, in which a Ca^{2+}-responsive elements are inserted

between two fluorescent proteins. Upon Ca^{2+} binding, an alteration in the efficiency of fluorescence resonance energy transfer (FRET) occurs (Miyawaki A. et al., 1997).

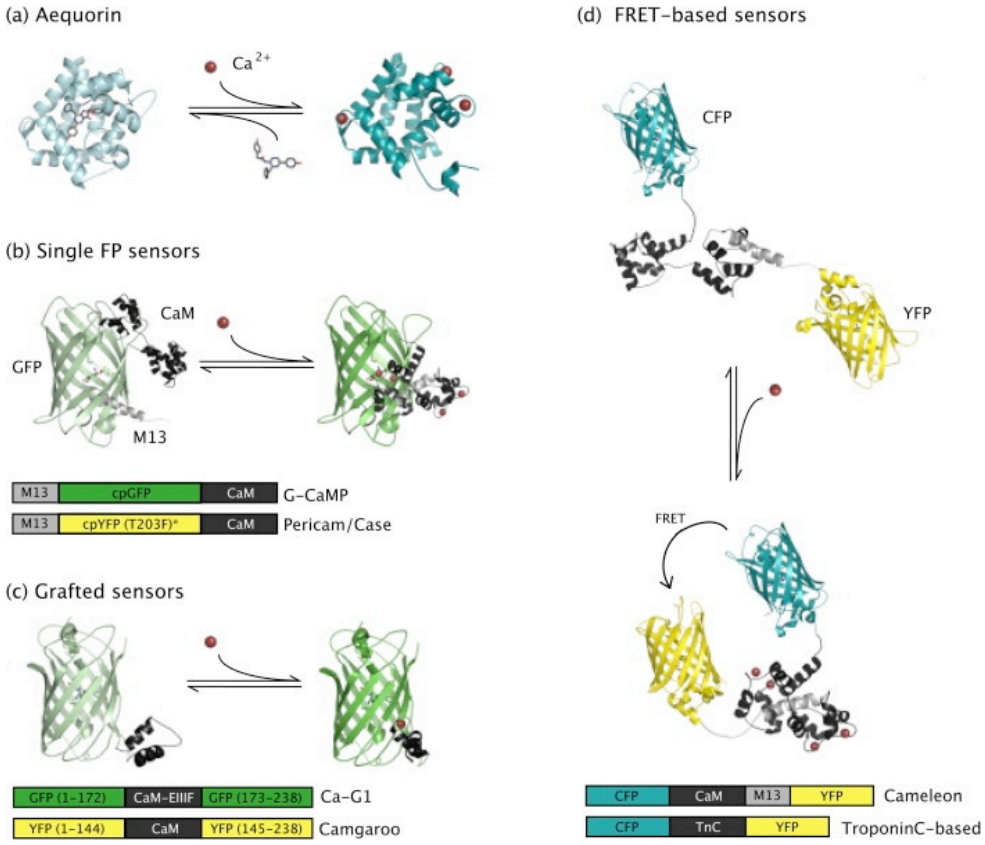

Fig. 9: Models of the three sub-groups of GECIs. **(a)** The aequorin photoprotein is shown in complex with coelenterazine. Upon Ca^{2+} binding it undergoes a conformational change emitting blue light with the release of coelenteramide; **(b)** single FP sensors which employ CaM and a CaM binding peptide (M13) linked to a FP. Upon Ca^{2+} binding CaM-M13 induce a conformational change that alter the chromophore protonation state which result in a changing of the probe fluorescence intensity; **(c)** grafted sensors utilizing EF hands or portions of CaM inserted into a fluorescent protein. Binding of Ca^{2+} induces a change in the protein conformation and a shift in the protonation state of the chromophore; **(d)** in FRET-based probes a Ca^{2+} binding domain is located between two fluorescent proteins. In presence of Ca^{2+}, the Ca^{2+} binding domain change its conformation that brings the two FPs close enough to increase the FRET efficiency (McCombs J.E. and Palmer A.E., 2008).

2.1 FRET-based cameleon probes

Cameleons (fig. 9) are tandem repeats of GFP mutants with overlapping excitation/emission spectra linked together by a Ca^{2+} sensor based on CaM, a glycyl-glycine linker, and the CaM binding peptide of myosin light chain kinase M13 (M13) (Miyawaki A. et al., 1997). In this design, Ca^{2+} binding promotes the reversible association of CaM and M13, promoting fluorescence resonance energy transfer between the two GFP variants (Demaurex N., 2005).

The first probes generated, yellow cameleons (YC), used cyan and yellow fluorescent proteins (CFP and YFP) as FRET donor and acceptors. The reversible changes in FRET can be detected as changes in the yellow over cyan emission fluorescence, and the probes function as ratiometric emission Ca^{2+} indicators. The original YC comprised probes of different affinities, ranging from 1 to 300μM (YC2, YC3 and YC4), but all probes suffered from a poor dynamic range and were sensitive to pH and to chloride ions. YC were subsequently made pH resistant by YFP mutagenesis (YC2.1 and YC3.1) and brighter by replacing YFP with citrine (YC3.3) or with Venus, a YFP mutant with fast and efficient maturation (YC2.12 and VC6.1). Although these cameleons were greatly improved over the original design, they still displayed insufficient signal-to-noise ratio when targeted to organelles (Demaurex N., 2005).

To further increase the dynamic range of cameleons, Nagai et al. generated several circularly permuted YFP mutants in an attempt to optimize the relative orientation of the two FRET partners (Nagai T. et al., 2004). By introducing new termini into the surface exposed loop regions of the β-barrel of Venus, they generated several YC variants with improved dynamics. The best construct, YC 3.6, which contains a YFP circularly permutated at position 173 (173cpVenus), matures efficiently, is resistant to acidification, and displays a monophasic Ca^{2+} sensitivity with a Kd of 250 nM. The cp173Venus cameleon has much better dynamics than all previous cameleons when expressed in cells, with an impressive 5.6-fold increase in ratio between Rmin and Rmax. The expanded dynamic range of YC3.6 is a clear advantage to image Ca^{2+} dynamics in cells and tissues with adequate spatiotemporal resolution.

Moreover A.E. Palmer et al. generated a series of indicators that resist endogenous CaM and have varying Ca^{2+} affinities to be useful in monitoring Ca^{2+} in distinct subcellular locations as well as in microdomains of high Ca^{2+} (Palmer A.E. et al., 2006). Their goal in redesigning the cameleon was to reengineer the binding interface between CaM and a target peptide to generate selective and specific binding pairs that could not be perturbed by wild-type (wt) CaM. They previously reversed the salt bridge interactions between basic residues in the target peptide and acidic residues in CaM to generate a mutant calmodulin-peptide pair that was unaffected by large concentrations of excess CaM. This redesigned pair led to a Ca^{2+} indicator (D1) with a relatively weak affinity for Ca^{2+} (Kd = 60 µM) and has been used to monitor Ca^{2+} directly in the ER in individual living cells (Palmer A.E. et al., 2004).

Subsequently, they computationally designed steric bumps in the target peptide and complementary holes in CaM in order to generate a series of indicators (D2, D3, and D4) with varying Ca^{2+} affinities (fig. 10), including a high-affinity indicator that cannot be perturbed by excess CaM. These indicators show significant improvements in the ability to monitor Ca^{2+} in different subcellular

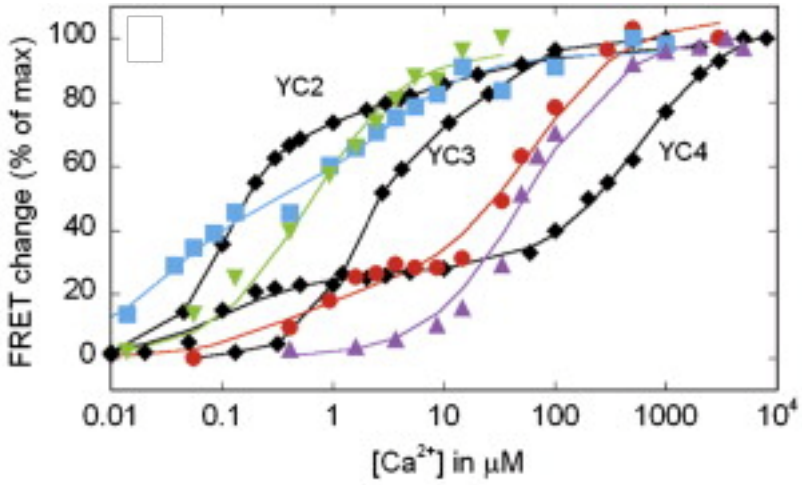

Fig. 10: In Vitro Characterization of the Redesigned Cameleons Ca^{2+} titration curves of original and redesigned cameleons. The original cameleons (YC2, YC3, and YC4; black diamonds) are labeled on the graph. The first redesign, D1, is presented as red circles, and the computational designs are presented as follows: D2cpv, blue squares; D3cpv, green, upside-down triangles; D4cpv, purple triangles.

locations such as the plasma membrane of neurons and the mitochondria (Palmer A.E. et al., 2006).

To date, cameleons have been targeted the cytosol (D1cpv probe) (Leite M.F. et al., 2003), the ER (ER-D1 probe), the nucleoplasm (H2BD1cpv probe) (Leite M.F. et al., 2003), to the mitochondria (4mt-D1cpv probe) (de Brito O.M. and Scorrano L., 2008), to the *trans*-Golgi (Go-D1cpv probe) (V. Lissandron et al., 2010), to the peroxisomal matrix (KVK-SKL-D3cpv probe) (Schrader M. and Yoon Y., 2007).

All these probes have been successfully used to monitor Ca^{2+} dynamics in their specific sub-cellular compartments.

3. The Alzheimer's disease

Alzheimer's disease (AD) was first described little more than 100 years ago. It is the most common cause of dementia with an estimated prevalence of 30 million people worldwide, a number that is expected to quadruple in 40 years.

In the 105 years since Alzheimer's original case report and particularly in the past three decades, much has been learned about Alzheimer's disease (AD). However, there currently is no effective treatment that delays the onset or slows the progression of AD (Holtzman D.M. et al., 2011).

3.1. Clinical and pathological features of AD

Dementia is an acquired syndrome characterized by a loss or decline in memory and other cognitive abilities. It represents a decline from a person's previously established level of intellectual function that is sufficient to interfere with the everyday performance of that individual. AD is the most common cause of dementia, estimated to contribute to about 60–70% of cases (Barker W.W. et al., 2002).

The essential feature of AD, intra-individual decline in cognitive abilities, has an insidious onset over several months with subsequent gradual but relentless

progression though successive stages of dementia severity. The time course of AD dementia averages 7–10 years and inevitably the illness culminates in death. Impaired recent memory usually is an initial symptom of AD but other cognitive deficits, such as executive dysfunction manifested by changes in attention and problem solving abilities, are typically also present. As dementia progresses, language dysfunction, visuospatial difficulty, loss of insight, and personality changes (withdrawal, decreased initiative, occasionally depression) frequently are apparent. There also is impaired ability to function at routine tasks at home, such that even basic activities of daily living (e.g., dressing, bathing, grooming) require supervision or assistance. In the severe stage of Alzheimer dementia, individuals are totally dependent on caregivers for all activities of daily living and, in advanced disease, often become mute, non-ambulatory, and unable to swallow or control bladder and bowel function (Holtzman D.M. et al., 2011).

The key neuropathological elements of AD were described by Alois Alzheimer in 1906 and at about the same time by Oskar Fischer (Goedert M., 2009). At the macroscopic level, there is abundant atrophy of the brain (Figure 11).

Amyloid plaques are accumulations of molecules in the extracellular space of the brain (fig. 12). The principal proteinaceous component of this plaques is the

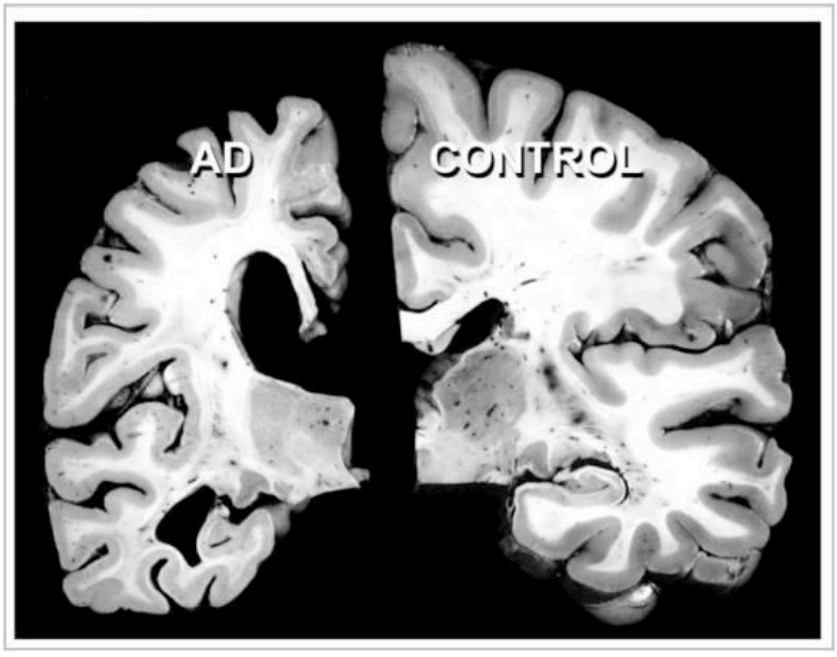

Fig. 11: Postmortem brain section from an AD case (left) compared with that of a cognitively normal individual (right).

amyloid-β (Aβ) peptide, a 38–43 amino acid peptide derived from a much larger protein, the amyloid precursor protein (APP). Within plaques, Aβ is present in aggregated (insoluble) forms including fibrils as well as oligomers (Kayed R. et al., 2003).

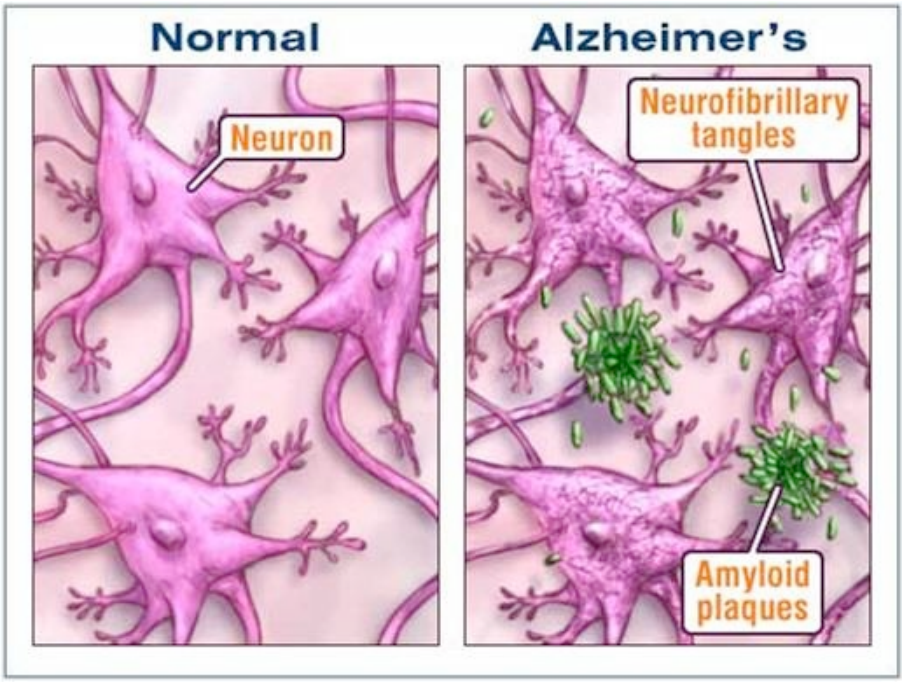

Fig. 12: The neurofibrillary tangles and tha amyloid plaques depositions in AD neurons.

These "neuritic" plaques are surrounded by swollen, degenerating neurites (axons and dendrites). In areas surrounding neuritic plaques, there is also "gliosis" with hypertrophy and an alteration of the morphology as well as the proliferation of astrocytes and microglia (immune cells of the CNS). It is likely that this inflammatory response contributes to brain injury although there is evidence that glial cells also play a protective role (Lucin K.M. and Wyss-Coray T., 2009) (fig. 13).

In addition to the deposition of Aβ in plaques in AD, nerve cell bodies as well as their processes in specific brain regions develop neurofibrillary tangles (NFTs) (fig. 12), neuropil threads, and neuritic dystrophy (Braak H. and Braak E., 1997). NFTs (present in neuronal cell bodies) and neuropil threads (present in neuronal processes) are intracellular structures composed predominantly of a hyperphosphorylated, aggregated form of the microtubule binding protein, tau.

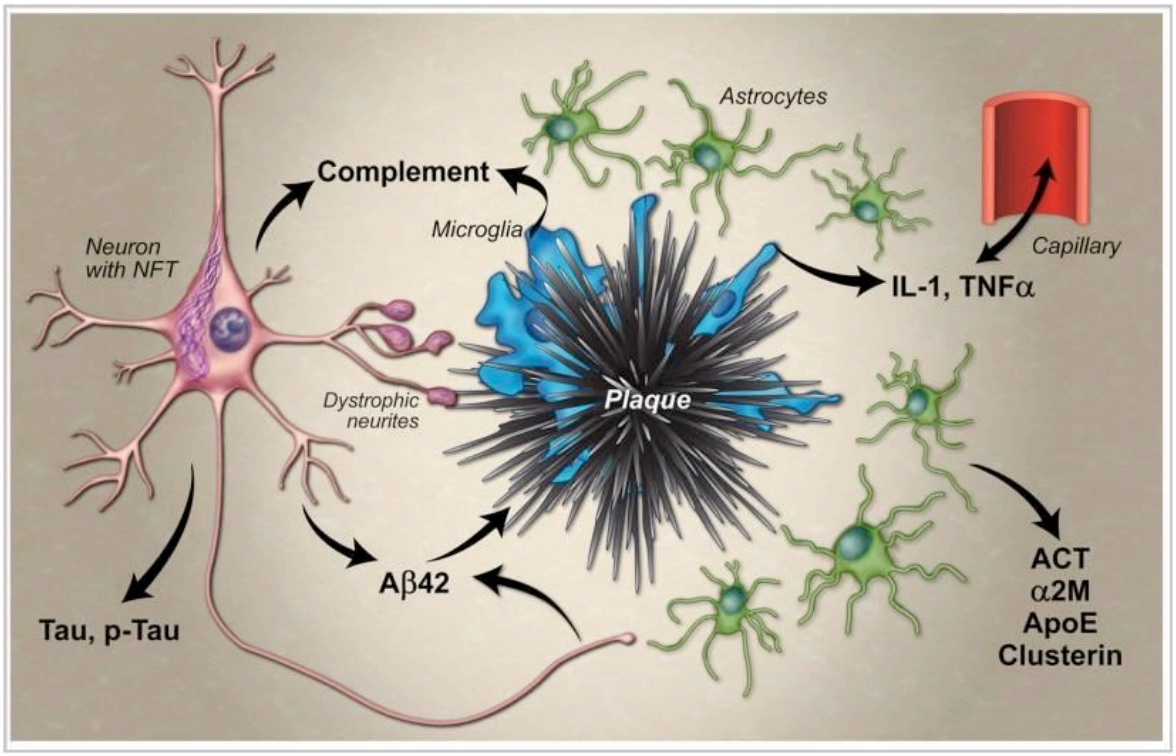

Fig. 13: Diagram illustrating aspects of the neuropathology of AD.

Tau is synthesized and produced in all neurons and is also present in glia. The normal function of tau is to bind to tubulin and stabilize microtubules. However, in AD, tau becomes hyperphosphorylated and this form of tau disassociates from microtubules and has a tendency to self-aggregate forming NFTs in cell bodies and dystrophic neurites.

Data strongly suggest that neurofibrillary pathology contributes to neuronal dysfunction and correlates with the clinical progression of AD (Holtzman D.M. et al., 2011).

Clinically, most cases of symptomatic AD begin after age 65 years with incidence increasing with age. These cases are often referred to as “sporadic” or “late-onset” AD (LOAD). This form of AD accounts for >99% of all cases. In addition to LOAD, a very small percentage (<1%) of AD occurs within families and is inherited in an autosomal dominant fashion and are termed FAD. In these families, dementia onset is usually between the ages of 30–60 years. APP was identified as the first gene in which mutations in the coding sequence cause FAD (Levy E. et al., 1990). These mutations within the APP gene provided an

important clue regarding the likely mechanism leading to increased Aβ accumulation in the brain in FAD.

In addition to APP, mutations in 2 other genes have been identified in which specific mutations result in the rare, autosomal dominant forms of FAD: presenilin-1 (PS1) (Levy-Lahad E. et al., 1995) and presenilin-2 (PS2) (Sherrington R. et al., 1995). These genes encode highly homologous transmembrane proteins in which multiple mutations have been identified in FAD families. Mutations in PS1 are the most common identified cause of FAD.

A molecular connection between presenilins and Aβ production was uncovered in the late 1990s. A normal function of presenilins is to form a γ secretase complex with 3 other proteins, Anterior pharynx-defective1 (APH-1), Presenilin enhancer 2 (PEN2), and nicastrin (Takasugi N. et al., 2003). The γ secretase complex directly cleaves the transmembrane protein Notch, APP, and other substrates, and its activity is required for Aβ formation (Holtzman M.D. et al., 2011).

Thus, AD is thought to be a disorder of protein aggregation in which the aggregation and accumulation in the brain of Aβ and tau are key players in AD pathophysiology. However, there are many additional cellular pathways, processes, and molecules involved in AD pathogenesis that have emerged and will continue to be discovered, that play important roles in the disease (Holtzman D.M. et al., 2011).

3.2. Molecular causes of AD

The pathogenesis of AD is complex and involves many molecular, cellular and physiological phenomenon, firstly the accumulation of β amyloid and the hyperphosphorilation of tau. Although for many years ‘Aβ-centric’ hypotheses dominated AD research (Pritchard S.M. et al., 2011), the importance of tau in the pathogenesis of AD is now much more appreciated (Small S.A. and Duff K., 2008), and seems to increase as new findings emerge. In addition, the calcium hypothesis support the proposal of an early, central role of calcium dysregulation in the pathogenesis of AD.

3.2.1. The amyloid hypothesis

The amyloid plaques associated with AD were first purified and found to consist of multimeric aggregates of Aβ polypeptide containing about 40 amino acid residues in the mid-1980s (Glenner G.G. and Wong C.W., 1984).

Cloning of the complementary DNA (cDNA) of Aβ revealed that Aβ is derived from a larger precursor protein (Tanzi R.E. et al. 1987). The full-length cDNA of APP was later isolated and sequenced and it was predicted to be a glycosylated integral membrane cell surface receptor protein with 695 amino acids (Kang J. et al., 1987).

The Aβ peptide was found to be a cleavage product derived from the transmembrane domain of this large precursor protein, the APP.

The APP protein is a type I integral membrane protein with a large extracellular portion, a hydrophobic transmembrane domain, and a short C-terminus designated the APP intracellular domain (AICD).

APP undergoes post-translational processing, involving several different secretases and proteases, via two major pathways.

In the non-amyloidogenic pathway, APP is sequentially cleaved by α-secretase and γ-secretase. α-cleavage, which cuts APP at the 17th amino acid inside the Aβ peptide sequence (fig. 14), releases a large secreted extracellular domain (sAPP-

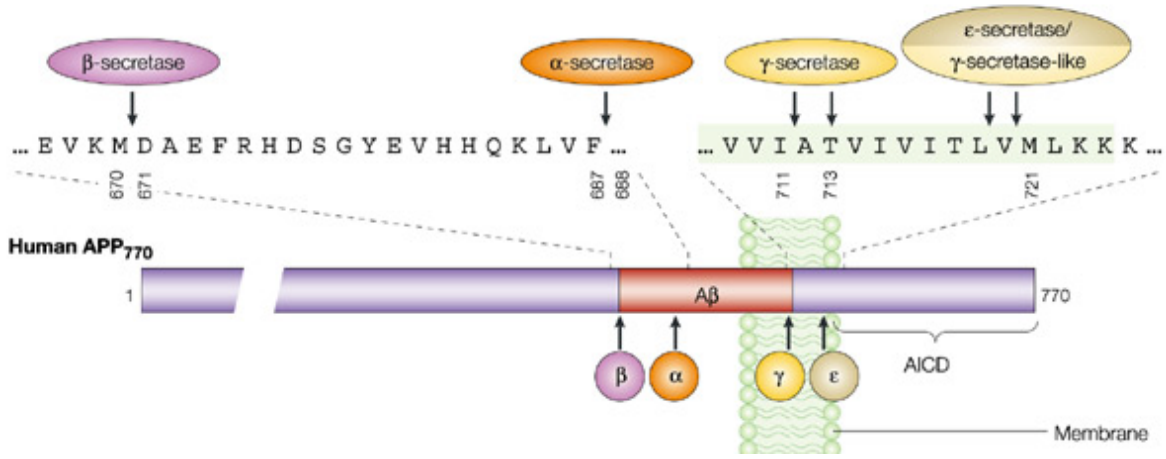

Fig. 14: Proteolytic processing of APP

α) and a membrane-associated C-terminal fragment consisting of 83 amino acids (C83). APP C83 is further cleaved by γ-secretase to release a P3 peptide and the AICD, both of which are degraded rapidly (Zhang H. et al., 2012).

In the amyloidogenic pathway, APP is primarily processed by β-secretase at the first residue or at the 11th residue (so called β' site) of the Aβ peptide sequence (fig. 14), shedding sAPPβ and generating a membrane associated C-terminal fragment consisting of 99 amino acids (C99) (Cole S.L. and Vassar R., 2007).

γ-Secretase further cleaves C99 to release AICD and the amyloidogenic Aβ peptide which aggregates and fibrillates to form amyloid plaques in the brain.

As APP was found to be constitutively cleaved at the α-site to yield sAPP-β, three members of the α disintegrin and metalloproteinase (ADAMs), ADAM-10, ADAM-17 and ADAM-9 have been proposed as the α-secretase (Koike H. et al. 1999).

ADAMs are type I integral membrane proteins that belong to the zinc protease super family and have been implicated in the control of cytokine and growth factor shedding.

ADAM10 is widely expressed in the brain and in other tissues and a several fold increase in sAPP-β levels in cell lines overexpressing ADAM10 can be observed (Kojro E. et al. 2001).

Moderate neuronal over-expression of human ADAM10 increases sAPP-β production while reducing Aβ generation/plaque formation in mice carrying the human APP V717I mutation, while expression of a catalytically-inactive form of the ADAM10 mutation increases the size and number of amyloid plaques in mouse brains (Postina R. et al. 2004). These findings suggest that ADAM10 may be responsible for constitutive α-cleavage activity. However, although sAPP-β generation is not affected in ADAM9/17 knock-down cell lines nor in mice carrying deficient ADAM9/17 genes, over-expression of ADAM9/17 does increase the level of sAPP-α under some conditions, suggesting that ADAM9 and ADAM17 are more likely involved in the regulated β-cleavage of APP rather than in constitutive α-cleavage (Zhang H. et al, 2012).

Aβ generation is initiated by β-cleavage at the ectodomain of APP, resulting in the generation of an sAPP-β domain and the membrane associated APP C-

terminal fragment C99. The putative β-secretase, β-site APP cleaving enzyme 1 (BACE1), was first identified and characterized in 1999 (Sinha S. et al., 1999).
BACE1 is a type I transmembrane aspartyl protease with its active site on the luminal side of the membrane. The originally identified full length BACE1 has 501 amino acids (BACE1-501) and is predominantly expressed in perinuclear post-Golgi membranes, vesicular structures throughout the cytoplasm, as well as on the cell surface (Ehehalt R. et al., 2002).
Knocking out the BACE1 gene prevents Aβ generation and completely abolishes Aβ pathology in mice expressing the Swedish mutation of human APP (Cai H. et al. 2001). The expression level and activity of BACE1 were also found to be elevated in AD patients (Holsinger R.M. et al. 2002).
Both α-cleavage and β-cleavage generate short APP C-terminal fragments that are further processed by γ-secretase.
Distinct from α-/β-secretases, γ-activity involves a large proteinase complex (fig. 15) consisting of at least four major protein components (PS1 or PS2, PEN2, APH1 and Nicastrin) (Vetrivel K.S. et al. 2006).

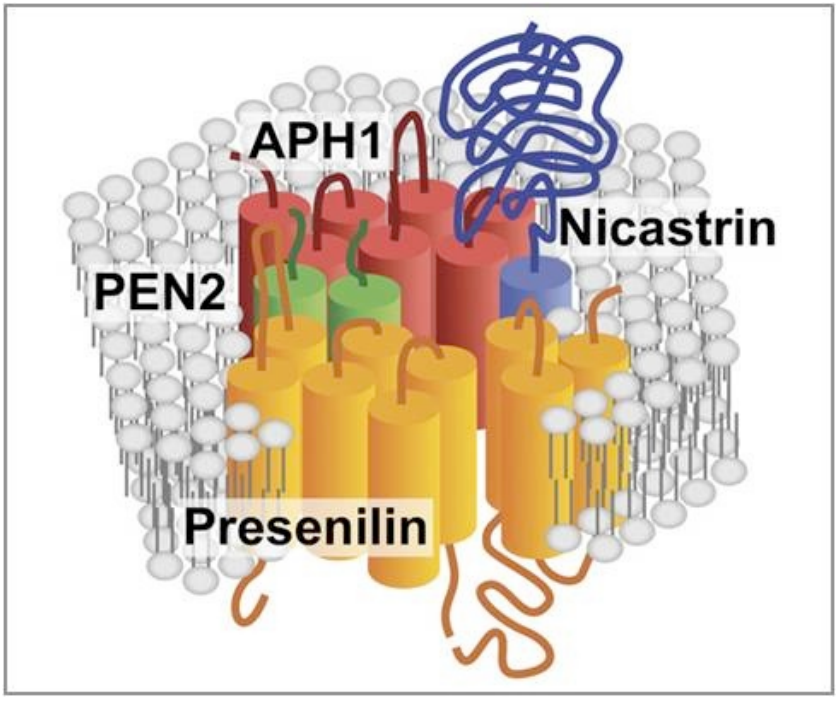

Fig. 15: The γ-secretase complex

Presenilins (PSs) were identified and cloned in the mid-1990s (Levy-Lahad E. et al., 1995; Sherrington R. et al., 1995).

Genetic mutations of PSs are found in a large portion of FAD cases, indicating its crucial role in AD. Although other proteins are required for the γ-secretase complex, PSs are believed to contain the actual protease activity (Zhang H., 2012).

PSs (fig. 16) are multi-transmembrane proteins and can be cleaved at the cytoplasmic loop between the sixth and seventh transmembrane regions to generate an N-terminal and a C-terminal fragment during post-translational maturation (Thinakaran G. et al., 1996). The two fragments interact with each other after the cleavage and they are both necessary for γ-secretase activity.

Nicastrin, identified as a protein that interacts with PS in 2000 (Yu G. et al., 2000), is a type I membrane glycoprotein with a large ectodomain. Nicastrin undergoes a glycosylation/maturation process that causes a conformation change in its ectodomain, which is crucial for the assembly and maturation of the γ-secretase complex and γ-activity. Mature nicastrin can bind to the ectodomain of APP C-terminal fragments derived through α-/β-secretase cleavage and may act as a substrate receptor of γ-secretase (Shirotani K. et al. 2003).

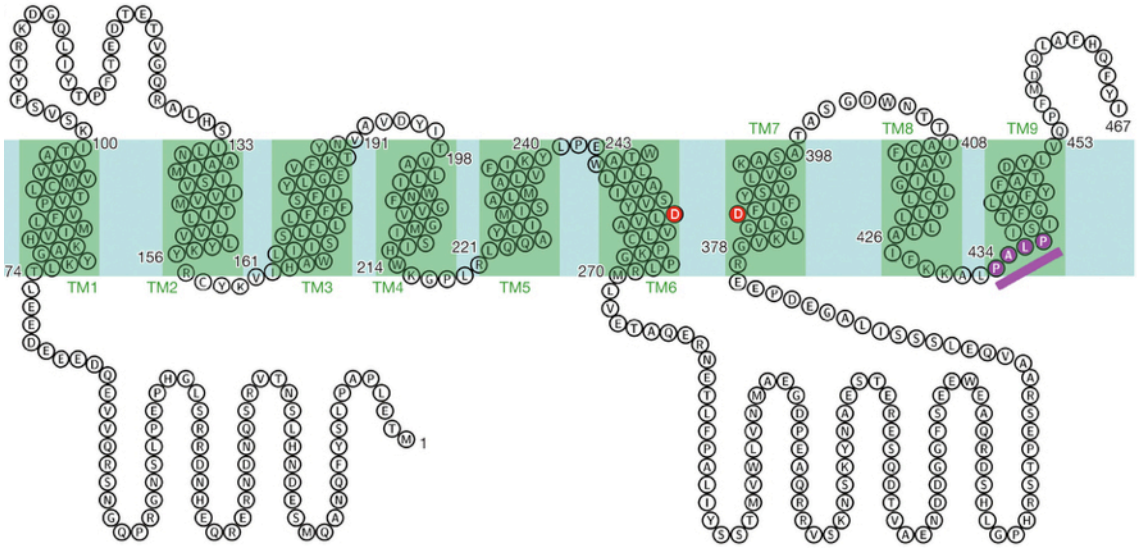

Fig. 16: Schematic representation of Presenilin

PEN2 and APH1 are another two γ-secretase complex components that were originally identified as the enhancers of PSs (Francis R. et al., 2002).

APH1 is a multiple transmembrane protein with seven transmembrane domains and a cytosolic C terminus. APH1 interacts with immature nicastrin and PS to form a relatively stable pre-complex which is then translocated to the *trans*-Golgi from the ER/*cis*-Golgi for further maturation (Lee S.F. et al., 2002).

PEN2 is a hairpin-like protein with two transmembrane domains and with both ends in the lumen. PEN2 is found to mediate the endoproteolysis of PS (Luo W.J. et al., 2003).

γ-Secretase cleaves APP at multiple sites and in sequential steps to generate Aβ peptides of different lengths (fig. 14).The majority of Aβ peptides produced are 40 amino acids long, however, peptides ranging from 38 to 43 amino acids are found in vivo. Besides the dominant γ-cleavage site at 40 and 42 residues, ζ-cleavage at 46 and ε-cleavage at 49 residues are also thought to be mediated by γ-secretase. Accordingly, various AICDs (C50, C53, C57 and C59) can be generated during these multi-site cleavages executed by γ-secretase. However, all of the endogenous AICD forms are rarely detected, probably because of their rapid degradation (Zhang H., 2012).

Strong evidence suggests that the γ-secretase complex resides primarily in the ER, Golgi/TGN, endocytic and intermediate compartments–most of which (except the TGN) are not major subcellular localizations for APP

(Cupers P. et al., 2001). In addition to cleaving APP, γ-secretase cleaves a series of functionally important transmembrane proteins, including Notch, cadherin, tyrosinase, ErbB4, CD44, etc (Zhang Y. et al., 2011).

The cleavage of various substrates appears to be dependent on the subcellular compartment; APP is mainly cleaved in the TGN and early endosomal domains whereas Notch is primarily cleaved at the plasma membrane (Tarassishin L. et al., 2004). Thus a disturbance in the localization of the γ-secretase complex may play some role in abnormal Aβ generation and AD pathogenesis (Zhang Y. et al., 2011).

3.2.2. The hyperphosphorilated tau hypothesis

AD belongs to a group of neurodegenerative diseases collectively designated as ‘‘tauopathies’’, because they are characterized by the aggregation of abnormally phosphorylated tau protein. The mechanisms responsible for tau aggregation and its contribution to neurodegeneration are still unknown. Thereby, understanding the way of regulation of tau is of high interest in the determination of the possible causes of the formation of tau aggregates and to elaborate protection strategies to cope with these pathological lesions (Martin L. et al., 2011).

Tau protein (tubulin-associated unit) was identified in 1975 (Weingarten M.D. et al., 1975). Tau is a microtubule-associated protein highly conserved and exclusively found in higher eukaryotes.

Tau is mainly expressed in neuron and its primary role, by interacting with microtubules, is to stabilize neuronal cytoskeleton.

Tau protein is subdivided into four regions (fig. 17): (I) an acidic region in the N-terminal part; (II) a proline-rich region; (III) a region responsible for tau binding with microtubules that contains four repeat domains R1, R2, R3 and R4 also called MBDs (microtubule-binding domains); and (IV) a C-terminal region.

Each repeat domain contains a conserved consensus motif KXGS, which can be phosphorylated at serine (Ozer R.S. and Halpain S., 2000). Indeed, this Serine phosphorylation, within MBD region, decreases tau affinity for microtubules and consequently prevents its binding to microtubules which results in the destabilization of the neuronal cytoskeleton (Sengupta A. et al., 1998).

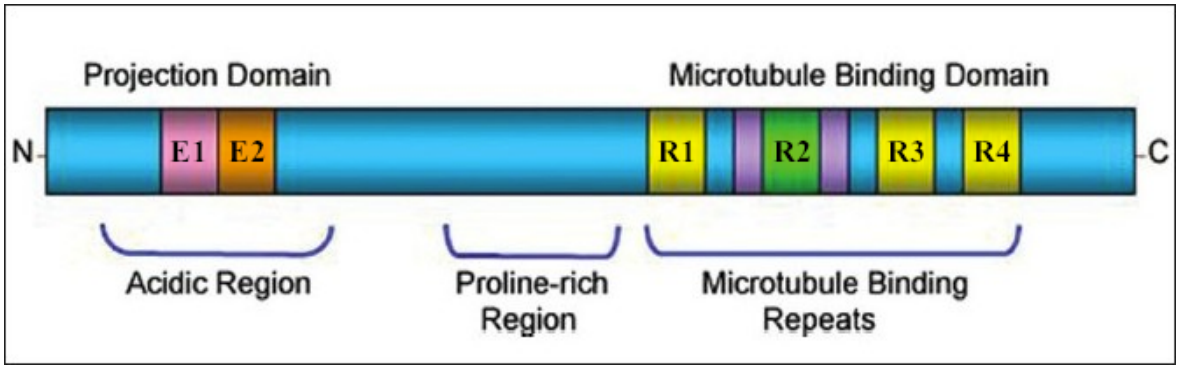

Fig. 17: Schematic representation of functional domains of longest tau isoform (2N4R).

Cytoskeleton destabilization is well known to cause disruption of tau-dependent cellular functions including axonal growth, vesicle and organelle transport as well as nervous signal propagation along the nerve network formed by microtubules (LaPointe N.E. et al., 2009).

Phosphorylation specifically modulates tau aggregation by disrupting its binding to microtubules and subsequently by promoting tau self- aggregation (Martin L. et al., 2011).

Various kinases and phosphatases regulate tau phosphorylation. Each tau phosphorylation site is subjected to the action of one or more protein kinase. Tau kinases are grouped into three classes: protein kinases PDPKs (proline-directed protein kinases), protein kinases non-PDPKs and protein kinases specific for tyrosines.

Alterations in the expression and/or the activity of tau kinases such as GSK3β, CDK5, DYRK1A, p38 and CK1 have been reported in the brains of AD patients, suggesting that one or several of them could be involved in the tau hyperphosphorylation (Chung S.H., 2009).

3.2.3. The Ca^{2+} hypothesis

A perturbed Ca^{2+} homeostasis has been demonstrated in AD and in particular, mutations in PSs have variably been correlated to alteration of Ca^{2+} signaling and different molecular targets have been identified, suggesting a physiological role for these proteins in intracellular Ca^{2+} pathway (Zampese E. et al., 2009).

PS, present as two homologous proteins PS1 and PS2, is an essential component of the APP cleaving enzymes γ-secretase. As an integral membrane protein, it is abundantly co-expressed with markers of ER, GA, endo-exocytic vesicles and only a minor fraction is present at the plasma membrane level (Vetrivel K.S. et al., 2004).

However, both, PS1 and PS2, are regarded as a multi-faceted proteins whose roles can be functionally distinguished and independent of their enzymatic activity. In particular, several experimental evidence suggest that PSs are also involved in the regulation of cellular Ca^{2+} homeostasis (Zampese E. et al., 2009).

Since their discovery, different FAD-lined PS mutants were reported to induce alterations of cellular Ca^{2+} handling in several cell models and in particular, it was observed that the FAD-mutant PS1-L286V, when expressed in PC12 cells, causes an increased Ca^{2+} release upon different stimulation (Furukawa K. et al., 1998). Then, other two FAD mutations in PS1 (A246E and M146V) were described to cause larger Ca^{2+} release from intracellular stores and increase excitotoxicity in neurons from transgenic mice expressing the mutant protein (Stutzmann G.E. et al., 2006). The idea that FAD-linked PS mutations are somehow correlated to altered Ca^{2+} signaling was further supported by the fact that these mutations could modify the sensitivity (or expression) of ER Ca^{2+} release channels (RyR and IP_3R) in different cell models, in neurons from transgenic AD mice as well as in isolated brain microsomes. This "Ca^{2+} overload" hypothesis is actually the only "Ca^{2+} hypothesis" for AD pathogenesis, stating that FAD-linked PS mutations, by increasing the store Ca^{2+} content, cause excessive Ca^{2+} release from the ER, increase sensitization to Aβ and exocitotoxic stimuli and eventually lead to cell death via Ca^{2+}-dependent mechanisms (Zampese E. et al., 2009).

However, different studies reported either no alteration or a reduced store Ca^{2+} content in cells expressing wt or FAD-mutant PSs. In particular, it was demonstrated that the FAD-linked PS2 mutations M239I and T122R reduce rather than increase Ca^{2+} release in fibroblasts from FAD patients and in cell lines stably or transiently expressing the PS2 mutants (Zatti G. et al., 2004; Giacomello M. et al., 2005;). In addition, an extended investigation of other FAD-linked PS mutants by directly monitoring the ER and the Golgi Ca^{2+} content in different cell lines confirmed that the FAD-linked PS2 mutations cause a reduction in the Ca^{2+} level of these organelles and none of the PS1 mutations cause an increase (Zatti G. et al., 2006). Similar results have been obtained in rat cortical neurons transiently expressing FAD-mutant PSs (Zatti G. et al., 2006).

The absence of elevated ER $[Ca^{2+}]$ in these models suggests that the enhanced Ca^{2+} release observed by other groups, upon expression of various FAD-linked PS mutants, might depend on different mechanisms, not necessarily due to an increased amount of Ca^{2+} within the stores (Zampese E. et al., 2009).

Despite, a dysregulation of store Ca^{2+} handling seems the common feature of a heterogeneous group of FAD-linked PS mutants.

The hypothetical mechanisms through which PS mutants exert their effect on Ca^{2+} homeostasis are numerous. For instance, a model that was suggested in accordance with the Ca^{2+} overload supports the idea that PSs represent one of the molecular components of the elusive Ca^{2+} leak channel of the ER membrane and the FAD-linked PS mutants, by reducing the leak, increase the ER Ca^{2+} content (Zampese E. et al., 2009). Moreover, in addition to the ER Ca^{2+} release channel and modulation of CCE, other mechanisms have been implicated, on the basis of either physical or functional interactions with proteins involved in cellular Ca^{2+} handling (Zampese E. et al., 2009), such as sorcin (Pack-Chung E. et al., 2000), calsenilin (Buxbaum J.D. et al., 1998), calcindin (Guo Q. et al., 1998). In particular, recent data by our lab have demonstrated that PS2 mutations linked to FAD reduce ER and GA Ca^{2+} levels, in particular by inhibiting SERCA pump (Zatti et al., 2006 and Brunello et al., 2009). To support this idea, endogenous PS seems to interact with SERCA and modulate its function and the absence of both PSs impaire SERCA pumping activity (Green K.N. et al., 2008).

Materials and methods

Constructs

To monitor ER Ca^{2+} levels, a new probe (D4ER) was created starting from the D1ER (Rudolf et al. 2006) cDNA (containing the calreticulin signal sequence MLLPVLLLGLLGAAAD at the 5' of CFP, and an ER retention sequence, KDEL, at the 3' end of citrine) by substituting the central part of the sequence, containing the mutant peptide and calmodulin, with that coming from the D4cpv (Palmer et al. 2006), upon SphI/SacI enzymatic restriction and ligation.

To monitor *cis*/*medial*-GA Ca^{2+} levels, a new probe (mGo-D1cpv) was created, inserting the first 32 N-terminal amino acids (AA) of the resident Golgi enzyme β-1,6-N-acetylglucosaminyltransferase (C2gnT) (MLRTLLRRRLFSYPTKYYFM VLVLSLITFSVL), was introduced before the start codon of the D1cpv cDNA (kindly provided by Dr. R. Tsien) in the HindIII - BamHI restriction sites, after its isolation from the GFP fused construct kindly provided by Dr. A. El-Battari (Zerfaoui et al., 2002).

To monitor *trans*-GA Ca^{2+} levels, the transGoD1cpv (tGo-D1cpv) probe was used. The targeting sequence of the *trans*-Golgi enzyme sialyl-transferase (MIHTNLKKKFSCCVLVFLLFAVICVWKEKKKGSYYDSFKLQTKEFQVLKSL GKLAMGSDSQSVFSSSTQ) was introduced before the start codon of the D1cpv cDNA (kindly provided by R. Tsien) in the HindIII restriction site, after its isolation from the Go-Aeq construct (Pinton et al., 1998).

Cell culture and transfection

SH-SY5Y cells and BHK cells were grown in DMEM containing 10% FCS, supplemented with L-glutamine (2 mM), penicillin (100 U/ml), and streptomycin (100 µg/ml), in a humidified atmosphere containing 5% CO_2.

HL-1 cells were grown in Claycomb medium (SLD #6467; Sigma) containing 10% FBS, norepinephrine (100 mM), L-glutamine (2 mM), penicillin (100 U/ml), and streptomycin (100 mg/ml).

Human fibroblasts from patients were grown in DMEM containing 20% FCS, supplemented with L-glutamine (2 mM), penicillin (100 U/ml), and streptomycin (100 µg/ml), in a humidified atmosphere containing 5% CO_2.

Cells were seeded onto glass coverslips (18 mm diameter) and transfection was performed at 60-70% confluence using Lipofectamine™ 2000 Transfection Reagent (Life Technologies) for SH-SY5Y and HL-1 cells and TransIT®-LT1 transfection reagent (Mirus Bio LCC) for BHK cells, with 2 µg of DNA (0.5 µg of cameleon codifying DNAs and 1.5 µg of pcDNA3 or PSs codifying DNAs); fibroblasts were transfected by electroporetion, using the Neon Transfection System (MPK500, Invitrogen). FRET measurements have been usually performed 24-48 h after transfection.

SPCA1 siRNA transfection in SH-SY5Y cells and Western Blot

The day before transfection, SH-SY5Y cells were plated in order to ensure 50% confluence on the day of transfection. Functionally validated siRNA directed against SPCA1 (CATCGAGAAGTAACATTGCCTTTA) and siGENOME RISC-Free Control siRNA were from Thermo scientific. SPCA1 siRNAs (100 nM each) or control siRNA were transfected using Lipofectamine™ 2000 Transfection Reagent (Life Technologies).

Proteins were resolved by SDS-PAGE, blotted onto a PVDF membrane and probed with selected antibodies (mouse monoclonal anti-ATP2C1, Sigma-Aldrich); mouse monoclonal anti-β-actin (Sigma-Aldrich).

Cell imaging

Cells expressing the fluorescent probes were analyzed using a DM6000 inverted microscope (Leica, Wetzlar, Germany) with a 40X oil objective (HCX Plan Apo, NA 1.25). Excitation light produced by a 410nm LED (Led Engin #LZ1-00UA00

LED) was filtered at the appropriate wavelength (425 nm) through a band pass filter, and the emitted light was collected through a beamsplitter (OES s.r.l., Padua, Italy) (emission filters HQ 480/40M (for CFP) and HQ 535/30M (for cpv-YFP) and a dichroic mirror 515 DCXR). The beamsplitter permits the collection of the two emitted wavelengths at the same time, thus preventing any artefact due to movement of the organelles. All filters and dichroics were from Chroma Technologies (Bellow Falls, VT, USA). Images were acquired using an IM 1.4C cool camera (Jenoptik Optical Systems) attached to a 12-bit frame grabber. Synchronization of the excitation source and cool camera was performed through a control unit ran by a custom-made software package, Roboscope (developed by Catalin Cubotaru at VIMM, Padua, Italy); this software was also used for image analysis. Exposure time and frequency of image capture varied from 200 ms to 400 ms, depending on the intensity of the fluorescent signal of the cells analyzed and on the speed of fluorescence changes.

Cells were mounted into an open-topped chamber and maintained in an extracellular medium (modified Krebs-Ringer Buffer, mKRB; in mM: 135 NaCl, 5 KCl, 1 $MgCl_2$, 0.4 KH_2PO_4, 1 $MgSO_4$, 20 HEPES, 11 glucose, pH 7.4). Classical experiments started in 1 mM $CaCl_2$; after perfusion with 300 µM EGTA, cells were stimulated by perfusion of bradykinin (BK, 100 nM) and/or CPA (20 µM); thereafter, the Ca^{2+} ionophore ionomycin (1 µM) was applied (not with the ERD4 probe) to completely discharge the stores; finally digitonin (40 µM, to obtain plasma membrane permeabilization) in Ca^{2+}-free intracellular-like medium [130 mM KCl, 10 mM NaCl, 1 mM $MgCl_2$, 2 mM succinic acid and 20 mM Hepes, 7,05 pH, at 37°C] and then a saturating $CaCl_2$ concentration (3 mM) were applied, in order to verify the dynamic range of the probe.

For Ca^{2+} pumping experiments a Ca^{2+}-buffer solution was prepared by adding to the intracellular medium: 1 mM H-EDTA, 1 mM $MgCl_2$, 2 mM EGTA and 350 µM $CaCl_2$. 100 µM ATP-Na was added fresh to this Ca^{2+}-buffered solution. The free [Ca^{2+}] (100 nM) was estimated by MaxChelato r2.5 and checked by fluorimetric measurements with fura-2.

All media were perfused through a temperature controller (Warner Instruments, TC-324B) set to have a constant temperature of 37°C in the chamber.

Immunocytochemistry

Cells decorated with anti-GM130 (BD Bioscience Pharmigen, San Jose CA, USA), anti-TGN46, anti-Giantin (AbCam, Cambridge UK), anti-calreticulin (Pierce #PA3-900) and anti-PS2 (Santa Cruz Biotechnology, Dallas Texas, USA) antibodies were fixed in Phosphate Buffered Saline (PBS) containing 4% paraformaldehyde for 15 min, incubated with 50 mM NH_4Cl for 20 min, permeabilized with 0.1% Triton X-100 in PBS 3 min and then blocked with 2% BSA and 0.2% gelatine for 30 min; anti-GM130 (1:1000), anti-Giantin (1:300) and anti-calreticulin (1:100) were added for 1 hour at room temperature, anti-TGN46 (1:200) and anti-PS2 (1:500) were added for 2h at 37°C. Samples were treated with Alexa Fluor 488 (555, 568 or 647) conjugated goat anti-mouse, anti-rabbit or rabbit anti-goat IgG (Molecular Probes Invitrogen, Eugene OR) for 1 hour at room temperature and mounted with Mowiol (Sigma-Aldrich Saint Louis, MI). Images were collected at Leica TCS-SP5-II confocal system, equipped with a PlanApo 100×/1.4 numerical aperture objective. For all images, pinhole was set to 1 Airy unit. The Argon laser line (488 nm) was used to excite the Cameleon sensors or AlexaFluor488 the He/Ne 543 nm laser was used to excite the AlexaFluor555/568 and the AlexaFluor647 was excited by the HeNe 633nm laser line. Video microscopy was performed at 1024×1024 pixels per image, with a 100Hz acquisition rate. Images were elaborated with ImageJ program (Wayne Rasband, Bethesda,USA). Z-stacks were acquired with a step of 0.42 μm.

Materials

Restriction and modification enzymes were purchase from NEB Inc. (Ipswich, MA). CPA, digitonin (Dig), BK, ATP-Na, thapsigargin, bis-phenol and caffeine were purchased from SIGMA-Aldrich; ionomycin (Iono) from Calbiochem and NAADP from Tocris. All other materials were analytical or highest available grade.

Statistical analysis

Off-line analysis of FRET experiments was performed with ImageJ software (Wayne Rasband, Bethesda, USA). Cpv-YFP, citrine-YFP and CFP images were subtracted of background signals and distinctly analyzed after selecting proper regions of interest (ROIs) on each cell; subsequently, a ratio between cpv-YFP (or citrine-YFP) and CFP emissions was calculated (R=F530/F480). Data are presented as a normalized $\Delta R/R_0$ %, where R_0 is the R value at the beginning of the experiment (t_0) and ΔR is the R value at each time (t) of the experiment minus R_0, or as % of minimum and maximum FRET.

All the data are representative of at least five different experiments. Data were analyzed by Origin 7.5 SR5 (OriginLab Corporation). Averages are expressed as mean ± s.e.m. (n = number of independent experiments; $*$ = $p < 0.05$, $**$ = $p < 0.01$, $***$ = $p < 0.001$, unpaired Student's t test).

Results

1. Ca^{2+} handling among within the medial-Golgi

In order to study in details, and at the single cells level, the effects of FAD-mutants PSs on intracellular Ca^{2+} handling, we firstly characterized the cis/ medial-Golgi sub-compartement using a new created Cameleon Ca^{2+} probe specifically targeted to this intracellular sub-organelle.

1.1. A new cameleon probe specifically targeted to the *medial*-Golgi

In order to specifically evaluate the [Ca^{2+}] in the *medial* part of the GA, in our lab a new cameleon Ca^{2+} probe was generated, taking advantage of the first 32 N-terminal AA of the resident Golgi enzyme β-1,6-N-acetylglucosaminyltransferase (C2gnT), which have been shown to represent the minimal *cis*/*medial*-Golgi targeting determinant when fused to a GFP (Zerfaoui et al., 2002). This sequence was inserted at the 5' of the cDNA coding for the cameleon D1cpv (Fig. 18 A).

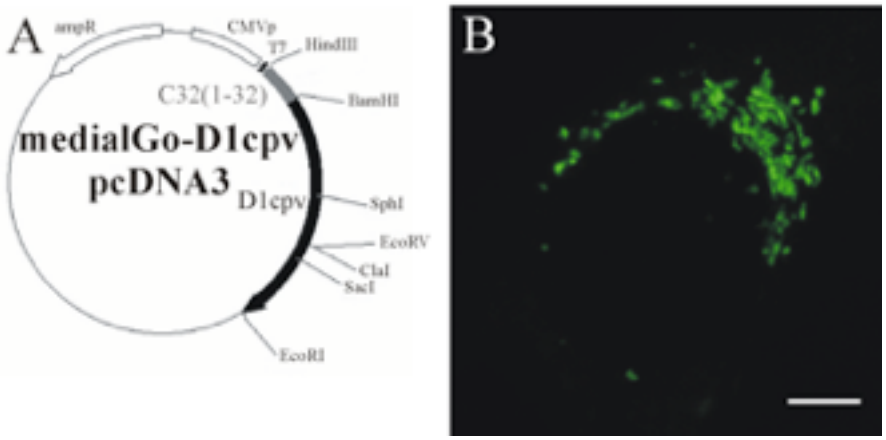

Fig. 18: **(A)** The first 32 AA of the Golgi enzyme β-1,6-N-acetylglucosaminyltransferase (C32), were cloned upstream of the cDNA coding for the cameleon D1cpv. **(B)** Z-projection confocal image (10 sections) of a SH-SY5Y cell expressing the new mGoD1cpv excited at 488 nm. Scale bar, 10 μm.

As shown in figure 18B, when the human neuroblastoma cell line SH-SY5Y was transiently transfected with the cDNA for the new Golgi cameleon, our probe localized in cisternae-like structures and small vesicles localized in the perinuclear region, thus appearing as a Golgi complex like structure.

Figure 19 shows the new Golgi probe expressed in SH-SY5Y cells (Fig. 19 A, D and G) that were fixed and immuno-labelled with antibodies against *bona fide* markers for *cis*- (GM130, Fig. 20 B), *cis*/*medial*- (Giantin, Fig. 19 E) and *trans*- (TGN46, Fig. 19H) Golgi compartments. There is a good overlap of the probe fluorescence with that of the *cis*/*medial*-Golgi marker Giantin (Fig. 19 F), while a partial separation was observed towards the signals of GM130 (Fig. 19C) and TGN46 (Fig. 19I).

Statistical analysis (by ImageJ) of confocal Z-stacks of cells marked as above, to quantify the signal of co-localizations of the new probe against the three markers (Fig. 20A), reveals a Pearson's coefficient (an index of co-localization that varies from -1, no co-localization, to +1, complete overlapping; Adler J. and Parmryd I., 2010) demonstrating a partial overlap of our probe versus the three endogenous markers, but with higher value for Giantin *(cis*/*medial-Golgi*) and TGN46 (*trans*-Golgi), compared to that for GM130 (*cis*-Golgi).

The spatial resolution of confocal microscopy is about 0.4 µm on the X/Y axis, but only 1 µm, at the best, on the Z axis. Given that the diameter of the GA cisternae can be significantly smaller than these values, the question is whether the co-localization of the new probe with the different markers is real or only apparent.

Indeed, when we calculated the Pearson's coefficient for the three endogenous Golgi marker proteins (GM130, Giantin, TGN46), one to each other, a high co-localization index between the *cis*/*medial*- and the *trans*-GA marker was found, while the signals coming from the *cis*- and the *trans*-compartment of the GA (and from the *cis*- and the *medial*-) appeared better separated (Fig. 20 B), although it is known that they are localized in distinct GA sub-compartments.

A further co-localization analysis was carried out to investigate more precisely the localization of the new probe within the GA: SH-SY5Y cells were treated with the microtubule depolymerizing agent nocodazole, which induces the

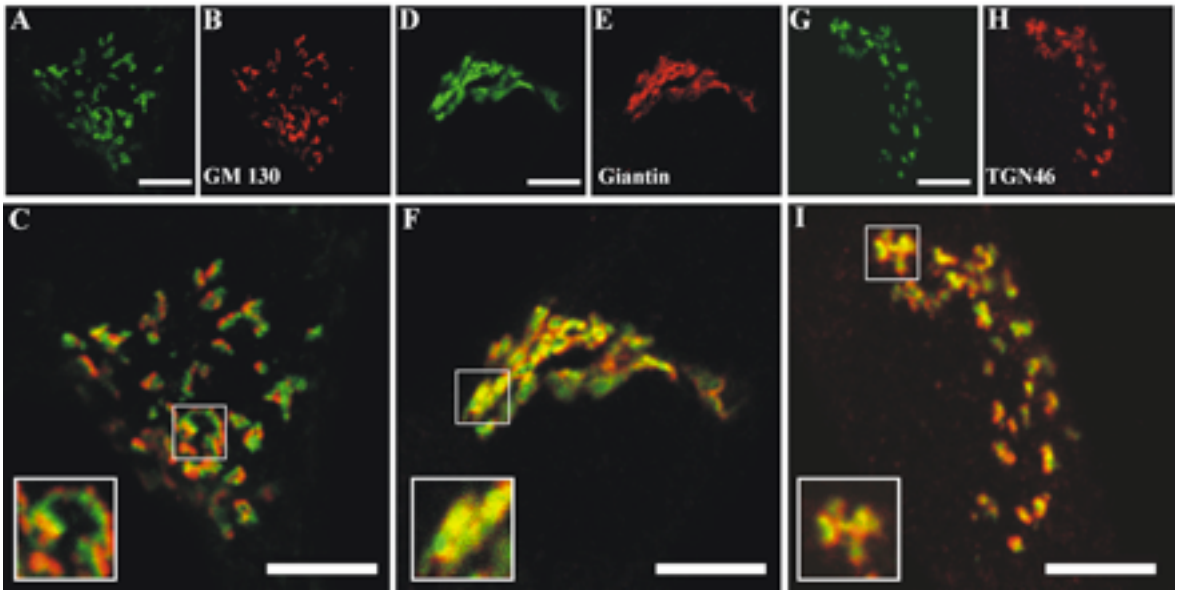

Fig. 19: Confocal fluorescence images of the Golgi Ca^{2+} probe express SH-SY5Y cells either excited at 488 nm (**A**, **D** and **G**) or decorated with antibodies against the *cis*-Golgi marker GM130 **(B)**, the *medial*-Golgi marker Giantin **(E)** and the *trans*-Golgi marker TGN46 **(H)**, and excited at 543 nm. Merging of the two upper images **(C, F** and **I)**. Insets in each panel show magnifications of selected cisternae. Scale bar, 10 µm.

accumulation of dispersed individual Golgi stacks in the cytoplasm, improving the recognition of different GA sub-compartments (Thyberg J and Moskalewski S., 1999). In figure 21A, SH-SY5Y cells treated with nocodazole, fixed and then triple immuno-labelled for GM130, Giantin and TGN46, were analyzed as above. In this case, the co-localization of the three endogenous markers appears more distinct and, particularly, when the vesicles were image *en face*, a typical 3 colour staining was often evident, with the Giantin signal closer and partially overlapped to that of TGN46, while the GM130 signal was more clearly separated from the other two.

Similarly, cells expressing the probe were treated, fixed and immuno-labelled, with the same two antibodies towards the *cis*- and the *trans*-GA marker (Fig. 21 B). In several structures, the spatial separation among the three signals was striking evident. On the contrary, if the same protocol was applied, but the cells were immuno-labelled with antibodies against GM130 and Giantin (Fig. 21 C), the probe signal appears almost completely separated from the first marker, but completely largely overlapped with the second.

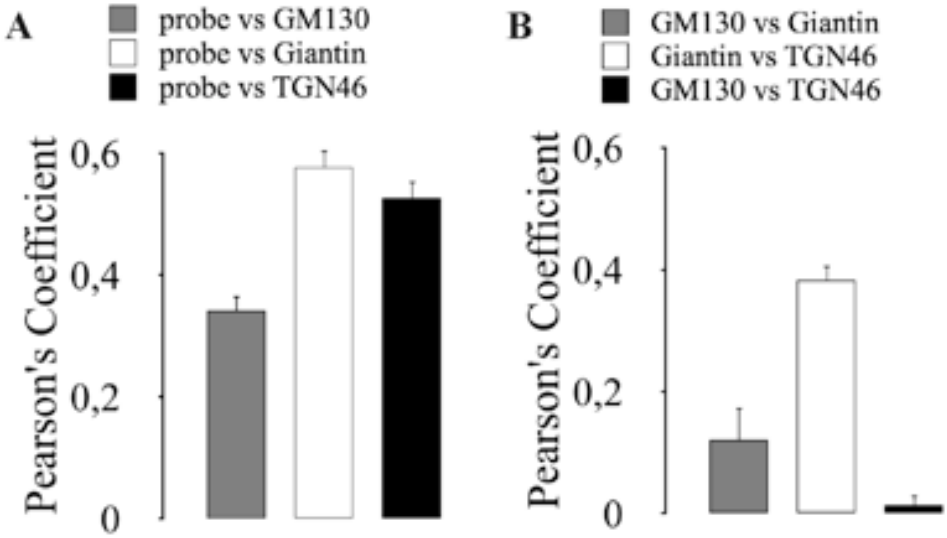

Fig. 20: Pearson's coefficients for signal co-localization between **(A)** the new probe and the three Golgi markers GM130, Giantin and TGN46, or **(B)** between the three markers for different Golgi compartments. The values were calculated from Z-axis confocal stacks by the Image-J JACoP plug-in; mean ± SEM; n (number of cells) ≥ 10.

In conclusion, the new probe appears to be almost completely excluded from the cis-Golgi compartments, while it well overlapped with vesicles marked with Giantin (*cis*/*medial*-Golgi). A partial overlapping between the probe distribution and TGN46 (*trans*-Golgi) was observed, similar to that between the trans-GA marker and Giantin. Accordingly, for simplicity, the new probe from now on is named medialGo-D1cpv (mGo-D1cpv).

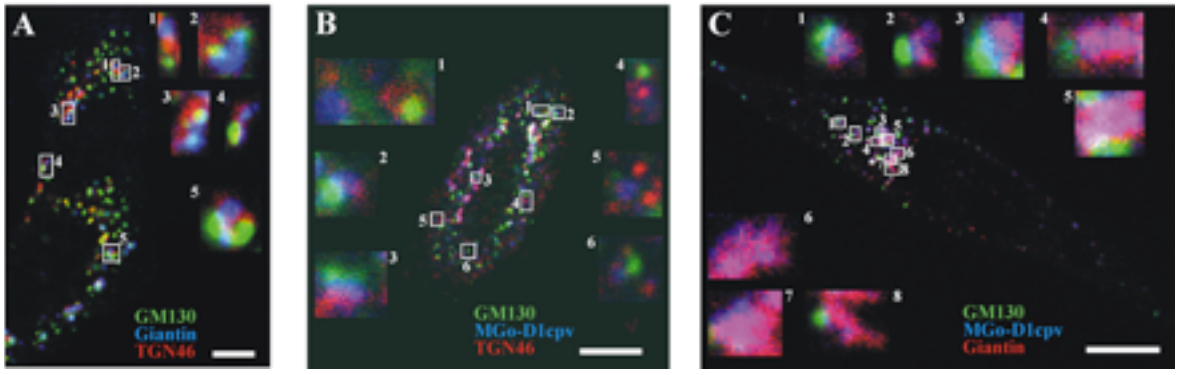

Fig. 21: Confocal fluorescence images corresponding to cells treated with nocodazole and expressing the mGo-D1cpv (and excited at 488 nm; B and C, blue). Cells were decorated with antibody against the *cis*-Golgi marker GM130 (and excited at 647 nm; A, B, C, green), the *medial*-Golgi marker Giantin (and excited at 488 nm; A, blue; or at 543 nm; C, red) and the *trans*-Golgi marker TGN46 (and excited at 543 nm; A and B, red). Insets in each panel show magnifications of en face vesicles. Bar, 10 µm.

1.2. Calibration of the new mGo-D1cpv

I In order to determine the absolute value of [Ca^{2+}] within the *medial*-GA, the *in situ* calibration of the new probe was carried out, performing passive Ca^{2+} loading experiments permeabilizing cells with digitonin in an intracellular-like medium containing different Ca^{2+} concentrations and no energy source (Fig. 22 A and B).

The experimentally calculated Kd for the new probe is 27.4 μM (Fig. 22, panel C) and the mean Ca^{2+} level that matched the cpv-YFP/CFP fluorescence emission ratio of mGo-D1cpv expressing SH-SY5Y cells at rest before permeabilization was 235 ± 30 μM (mean ± s.e.m., n = 24 for every point).

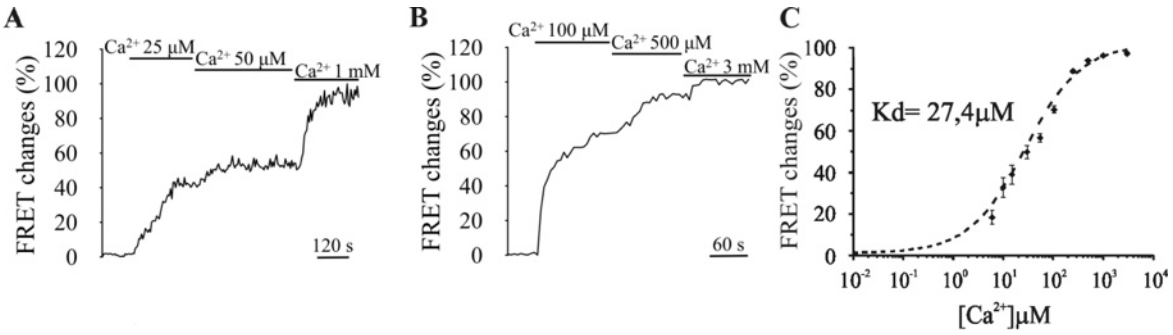

Fig. 22: Representative kinetics of FRET changes (% of max) in permeabilized SH-SY5Y cells transiently expressing the mGo D1cpv **(A-B)**. Where indicated, digitonin-permeabilized cells were bathed with an intracellular-like medium without energy source and containing different [Ca^{2+}]; 3mM $CaCl_2$ was finally added to reach the maximum value. **(C)** *In situ* calibration curve for the mGo D1cpv, obtained perfusing the cells with different [Ca^{2+}]-containing intracellular-like medium as described in A. Mean ± s.e.m., n ≥ 3 for each Ca^{2+} concentration.

1.3 Ca^{2+} handling in the medial-Golgi

Functional experiments were carried out in SH-SY5Y cells transiently transfected with the cDNA encoding mGo-D1cpv. Cameleon-probes are FRET-based indicators and FRET occurs between the two GFP mutants (the CFP and the cpv-YFP). This phenomenon is caused by the interaction between Ca^{2+}, Calmodulin (CaM) and its target peptide M13. Variations in [Ca^{2+}] can be followed as variations in the ratio between cpv-YFP and CFP fluorescence emission. Changes in [Ca^{2+}] can be conveniently expressed as $\Delta R/R_0$ or R% of the maximal fluorescence obtained upon normalization by the minmum (Ca^{2+} free medium) and maximum (3 mM [Ca^{2+}]) FRET. A drop in the $\Delta R/R_0$ value indicates a decrease in [Ca^{2+}] within the organelle.

Figure 23 shows typical $\Delta R/R_0$ changes in mGo-D1cpv expressing SH-SY5Y cells after addition of different stimuli. The perfusion in a Ca^{2+}-free EGTA-containing (300 µM) medium of an IP3-generating stimulus, such as bradikinin (BK; Fig. 23 B), results typically in small $\Delta R/R_0$ decreases (a drop of 10 ± 0.4%, mean ± s.e.m., n = 14; Fig. 32 E) within the GA region. The following addition of the Ca^{2+} ionophore ionomycin causes a rapid and large decrease in terms of $\Delta R/R_0$ (a drop of 70 ± 2.1%, mean ± s.e.m., n = 37; Fig. 23 E) within the *medial*-Golgi, down to a level that was not significantly affected by the subsequent permeabilization of the plasma membrane with digitonin.

We then tested the effect on medial-Golgi Ca^{2+} handling of the SERCA inhibitor cyclopiazonic acid (CPA), added alone (Fig. 23 C) or in combination with BK (Fig. 23 D): the SERCA inhibitor alone resulted in a slow decrease of $\Delta R/R_0$ down to a new steady state value approximately halfway between the value at resting condition and the minimum obtained after cell permeabilization with digitonin in Ca^{2+}-free, EGTA-containing medium (-40 ± 3.4%, mean ± s.e.m., n = 21; Fig. 23 E); however, when the addition of the SERCA inhibitor was rapidly followed by BK, the slow CPA-induced $\Delta R/R_0$ decrease was strongly accelerated (Fig. 23 D) until a new steady-state value, similar to that reached upon CPA addition alone, was reached (-40 ± 1%, mean ± s.e.m., n = 9; Fig. 23 E). Addition of ionomycin, after CPA, induced, in both cases, a further large drop in

the $\Delta R/R_0$ signal (Fig. 23 C and D). In Figure 23 E, the averaged decreases in $\Delta R/R_0$ values obtained in SH-SY5Y cells expressing the mGo-D1cpv upon different stimulations are reported.

The partial depletion of the medial-Golgi by SERCA inhibitors suggests that this Golgi compartment is endowed with additional mechanisms for its Ca^{2+} uptake, one of which sensitive to the drugs. The existence in the medial-Golgi of a Ca^{2+} uptake mechanism other than the SERCA was then investigated. First, cells expressing the mGo-D1cpv were treated (in a Ca^{2+} free, EGTA-containing medium) with ionomycin to completely deplete Ca^{2+} from the lumen; ionomycin was then washed away, cells were treated with the irreversible SERCA inhibitor thapsigargin (Tg, 1 µM) and finally 1mM $CaCl_2$ was added to the medium. For comparison, the same procedure was employed in parallel cells expressing an ER targeted cameleon Ca^{2+} probe, the ER-D4.

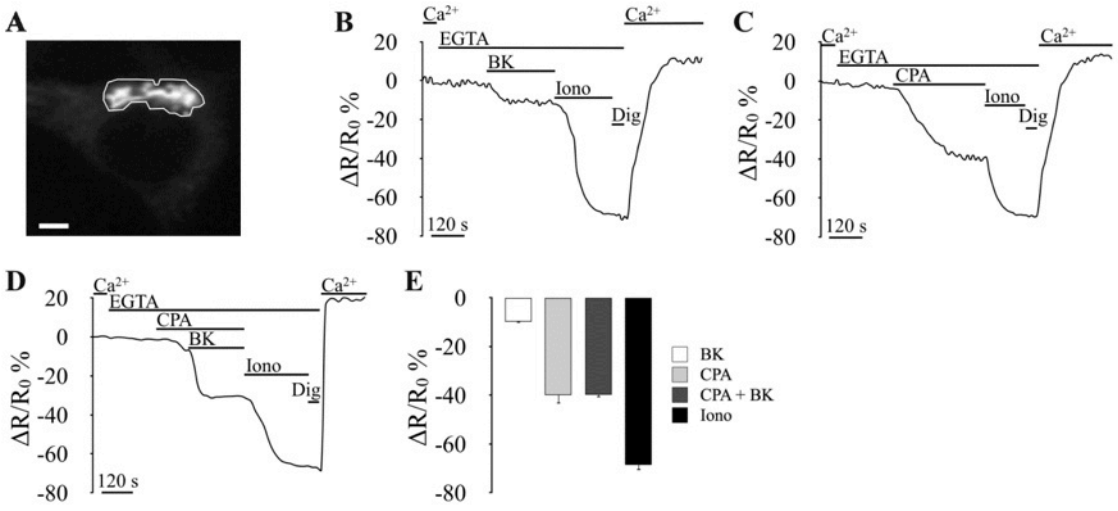

Fig. 23: Image of a SH-SY5Y cell expressing the mGo-D1cpv probe. Bar, 10 µm **(A)**. Representative $\Delta R/R_0$ variations in medialGo-D1cpv expressing SH-SY5Y cells in response to different stimuli. Where indicated 1 mM $CaCl_2$, 300 µM EGTA, 100 nM bradikinin (BK), 20 µM cyclopiazonic acid (CPA), 1 µM ionomycin (Iono), 50 µM digitonin (Dig) were perfused **(B-C-D)**. Statistical medial-Golgi $\Delta R/R_0$ reduction in SH-SY5Y cells upon different stimulation (mean ± s.e.m.; $n \geq 9$) **(E)**.

Figure 24 A shows that, while a substantial re-uptake of Ca^{2+} was observed in these conditions in the *medial*-Golgi (black trace), no Ca^{2+} refilling was observed in cells expressing the ER Ca^{2+} sensor (grey trace). Similar results were obtained when refilling of pre-emptied stores was followed in cells permeabilized with digitonin and perfused with an intracellular-like medium at fixed [Ca^{2+}] (Fig. 24 B).

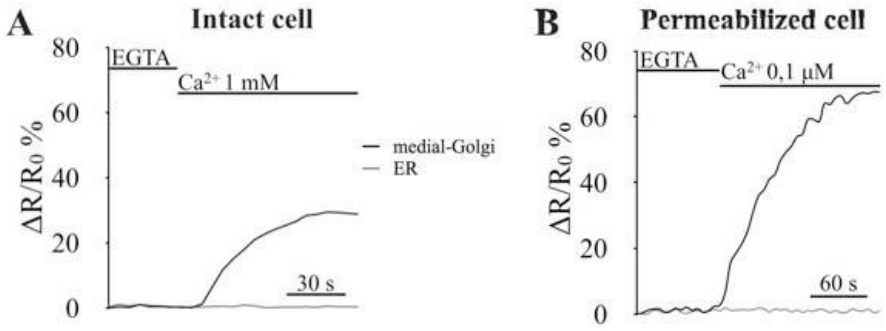

Fig. 24: Representative medial-GA (black trace) and ER (grey trace) Ca^{2+} refilling kinetics in pre-emptied intact SH-SY5Y cells treated with thapsigargin (1 µM) **(A)**. Where indicated, Ca^{2+}-free, EGTA (300 µM)-containing medium was changed with the mKRB containing 1mM $CaCl_2$. Representative medial-GA (black trace) and ER (grey trace) Ca^{2+} refilling kinetics in pre-emptied, digitonin-permeabilized SH-SY5Y cells treated with thapsigargin (1 µM) **(B)**. Where indicated, intracellular-like medium containing EGTA (300 µM) was changed with an intracellular-like medium at 0.1 µM [Ca^{2+}].

We thus hypothesized that the *medial*-Golgi is equipped by both the SERCA and the SPCA-1 pump, known to be present in the trans-GA. To further investigate this Ca^{2+} uptake mechanism in the medial-Golgi, we verified in SH-SY5Y cells expressing the medial-Golgi probe the effect of SPCA1 knock-down by RNA interference (Fig. 25). SH-SY5Y cells treated with specific siRNA against SPCA1 and expressing the mGo-D1cpv were analyzed by Western blotting with an anti-SPCA1 antibody: a reduction in the total SPCA1 protein level of 54 ± 9% (n=3) was revealed in interfered cells, compared to control scramble siRNA-transfected cells (Fig. 25A). Taken into consideration the transfection efficiency in these cells (~70%), this should correspond to a reduction of about 70% of SPCA1 level in the transfected cells.

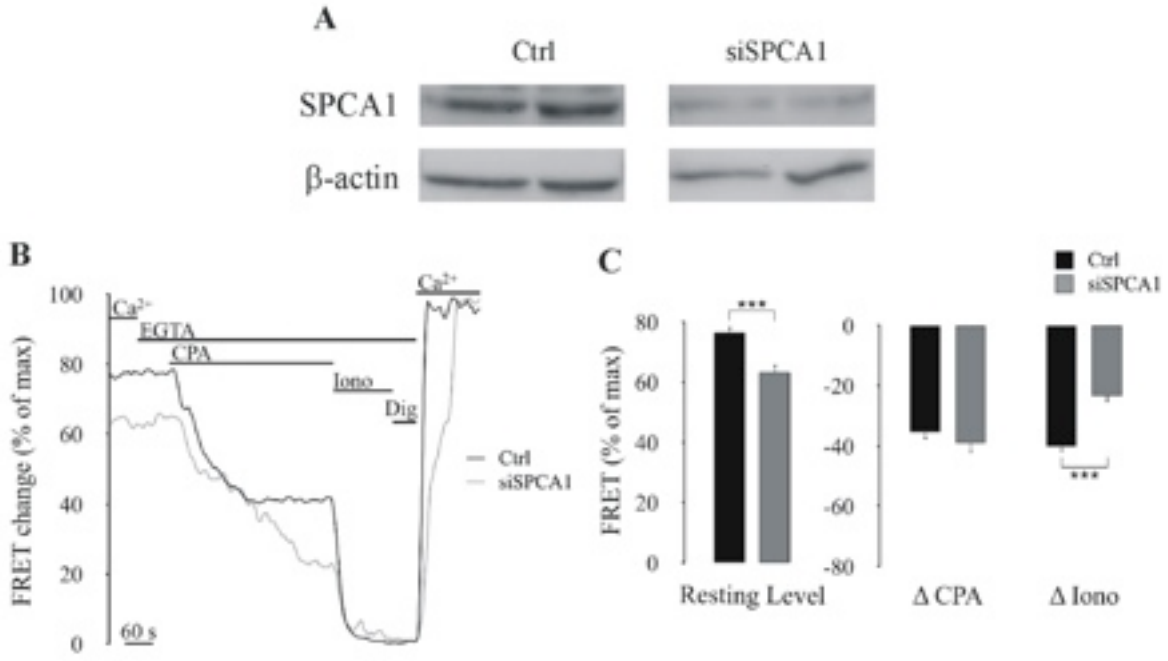

Fig. 25: Western blot of control (Ctrl, scrambe siRNA-trasfected) and interfered (siSPCA1-transfected) SH-SY5Y cell extracts visualized with anti-SPCA1 and anti-actin antibodies **(A)**. A significant reduction in the level of SPCA1 was observed in interfered cells (-54 ± 9%, mean ± s.e.m., n = 3).

Representative FRET changes (% of max) in mGo-D1cpv expressing control (black trace) and interfered (grey trace) SH-SY5Y cells in response to the addition of different stimuli **(B)**. Where indicated, $CaCl_2$ 1 mM, EGTA 300 µM, CPA 20 µM, Iono 1 µM were perfused. Statistical *medial*-Golgi FRET variations in SH-SY5Y cells treated as in B **(C)**.

The effects of SPCA1 down-regulation were then tested on medial-GA Ca^{2+} handling. Figure 25 B showed that SPCA1 knockdown caused a reduction in the FRET value in resting condition and no further effect upon CPA addition, compared to controls (Fig. 25 C); accordingly, the additional drop induced by ionomycin was larger in controls compared to SPCA1 knocked-down cells (Fig. 25 C).

The question that arises as to whether the medial-Golgi is endowed with other Ca^{2+}-releasing channels than the IP_3R.

To investigate the expression of TPCs, SH-SY5Y cells transiently expressing mGo-D1cpv were permeabilized with digitonin in an intracellular-like medium and stimulated with nicotinic acid adenine dinucleotide phosphate (NAADP), a potent Ca^{2+}-releasing second messenger that should specifically activate TPCs (Calcraft et al., 2009). The addition of NAADP (from 10 up to 100 nM) had no

appreciable effect on DR/R0 (data not shown), indicated that the TPCs-mediated Ca^{2+}-releasing mechanism is not present in the medial-Golgi.

To investigate the presence of the RyRs in the *medial*-GA we expressed the mGolgi-D1cpv in a stable cardiac cell line, HL-1 (Figure 26 A), which shows high levels of RyRs, type 2 expression (George et al., 2003). Figure 26 B shows that the addition of depolarizing concentrations of KCl (30 mM) induced a clear drop in $\Delta R/R_0$ (27% ± 0.8%; n = 8); similarly, the addition of caffeine (Caff, 20 mM), either after KCl (Figure 26 B) or alone (Figure 26 C), caused a rapid drop in $\Delta R/R_0$ (-12% ± 1.3% and -10% ± 1.4%, respectively; n = 8).

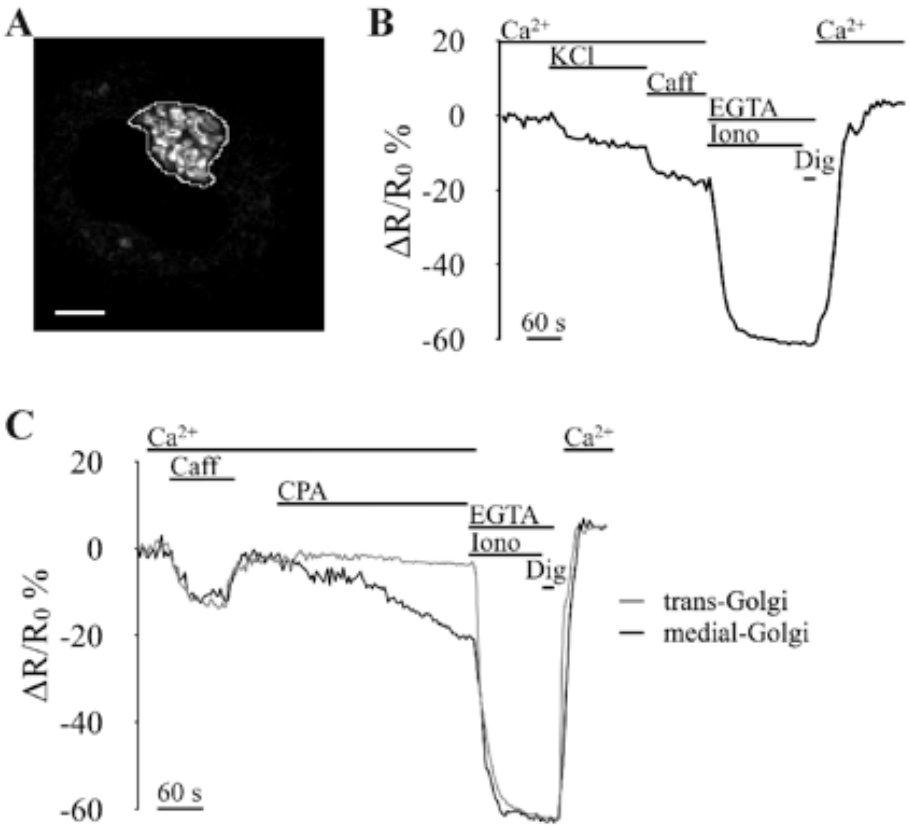

Fig. 26: Ca^{2+} response by *medial*-GA in HL-1 cells upon RyRs stimulation. Image of an HL-1 cell expressing the mGo-D1cpv probe (selected ROI). Bar, 10 µm **(A)**. Representative $\Delta R/R_0$ changes of mGo-D1cpv in HL-1 cells in response to different stimuli. Where indicated, 1 mM $CaCl_2$, 50 mM KCl, 20 mM Caff, 300 µM EGTA, 1 µM Iono, and 50 µM Dig were added through the perfusion system **(B)**. Representative $\Delta R/R_0$ changes in *medial*-Golgi (black trace) and *trans*-Golgi (grey trace) of HL-1 cells in response to different stimuli. Where indicated, 1 mM $CaCl_2$, 20 mM caffeine (Caff), 20 µM CPA, 300 µM EGTA, 1 µM Iono, and 50 mM Dig were added through the perfusion system.

Thus, the medial-Golgi sub-compartment seems to be equipped with IP_3Rs and RyRs and its Ca^{2+} uptake can be mediated by both SERCA and SPCA1 pumps.

2. A new Cameleon probe specifically targeted to ER

In order to specifically evaluate the [Ca^{2+}] within the ER at the single-cell level, we generated a new cameleon Ca^{2+} probe, starting from the ER-D1 cDNA present in the lab (Rudolf et al. 2006), which contains the calreticulin targeting sequence (MLLPVLLLGLLGAAAD) at the 5' of the CFP, and an ER retention sequence (KDEL) at the 3' end of YFP (Fig. 27 A). The central part of the ER-D1 sequence (D1), containing calmodulin and the mutant peptide M13, was substituted with that coming from the D4cpv (Palmer et al. 2006), upon SphI/ SacI enzymatic restriction and following ligation. This strategy was utilized to improve the small dynamic range and low K_d of the original ERD1 probe. The new probe was named ER-D4.

As shown in figure 27 B, in BHK cells transiently transfected with the cDNA for ER-D4 (in green) and immuno-labelled with a *bona fide* marker for the ER (calreticulin, in red), our probe localized in a reticular structure present in all the the cell that perfectly overlaps with the calreticulin signal.

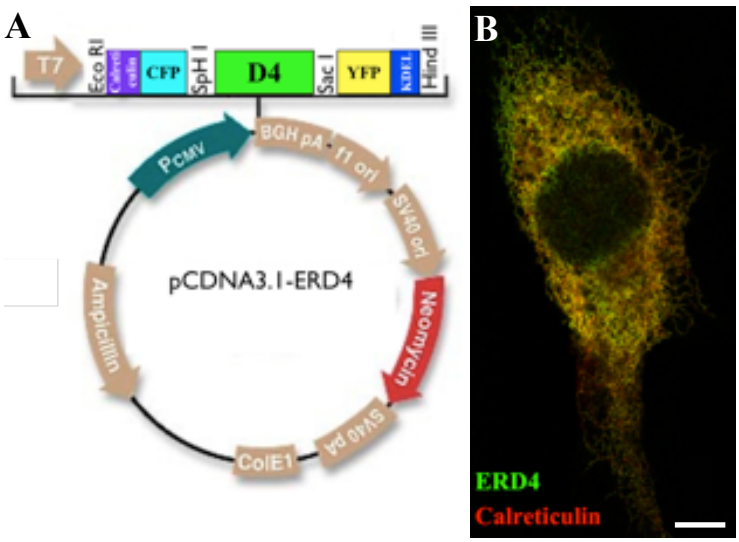

Fig. 27: **(A)** Design of the new construct codifying the ER-D4. **(B)** Confocal fluorescence images of a ER-D4 expressing BHK cell excited at 488 nm (in green) and decorated with antibodies against calreticulin (excited at 555 nm; in red). Bar, 10 µm.

2.1. Calibration of the new ERD4

To define the [Ca^{2+}] within the ER compartment, the *in situ* calibration of the new probe was performed by passive Ca^{2+} loading experiments, permeabilizing the cells with digitonin in an intracellular-like medium, containing different Ca^{2+} concentrations and no energy source (Fig. 28 A).The calculated apparent K_d for the new probe is 305 µM (Fig.28 B) and the mean Ca^{2+} level that matched the YFP/CFP fluorescence emission ratio in SH-SY5Y cells at rest before permeabilization was 475 ± 50 µM (mean ± s.e.m., n = 47).

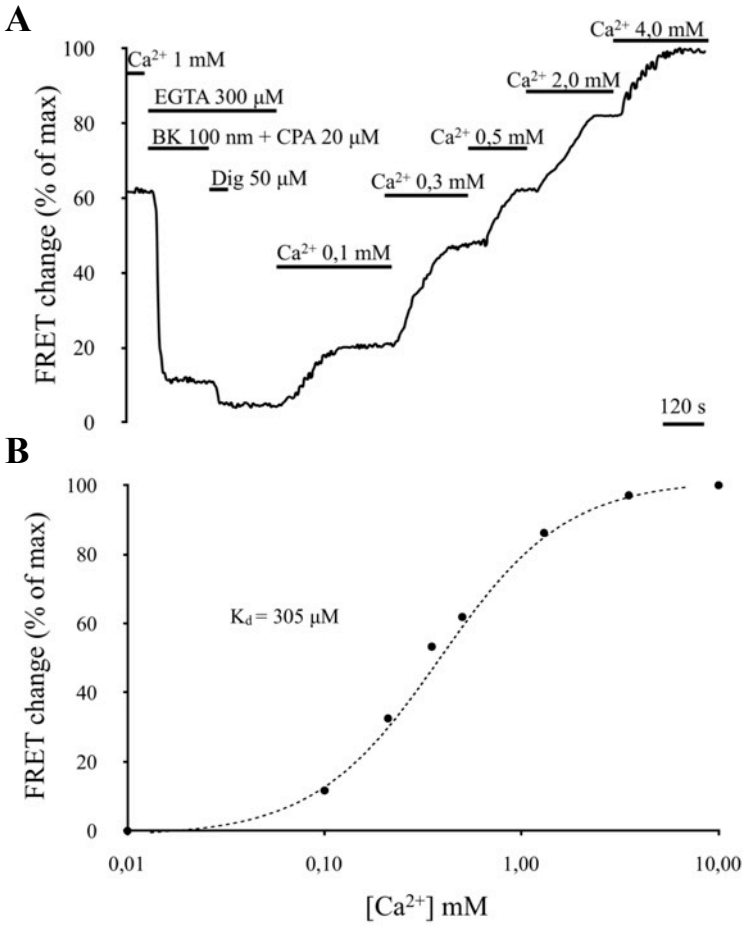

Fig. 28: **(A)** Representative kinetics of FRET changes (% of max) in permeabilized SH-SY5Y cells transiently transfected with ER-D4. Where indicated, digitonin-permeabilized cells were bathed with an intracellular-like medium without energy source and containing different [Ca^{2+}]. **(B)** *In situ* calibration curve for the ER-D4, obtained perfusing the cells with different [Ca^{2+}]-containing intracellular-like medium as described in A. Mean ± s.e.m., n ≥ 27 for each Ca^{2+} concentration.

3. Effects of familial Alzheimer's disease linked-Presenilin (PS) mutants on intracellular Ca^{2+} stores homeostasis

To study in details the effects of FAD-linked PS mutations in ER and *medial*- and *trans*-GA sub-compartments, we transfected the SH-SY5Y human neuroblastoma cell line with the cDNA coding for the ER-D4, the tGo-D1cpv or the mGo-D1cpv cameleon probes and those for different FAD-PS mutated form, PSs wt or the void vector, as control. Upon different protocols, Ca^{2+} measurements were performed.

3.1 Intracellular localization of PS2 in SH-SY5Y cells

In order to study the effect of transient over-expression of PSs in SH-SY5Y cells, we firstly checked whether they co-localized intracellularly with the three cameleon probes used for Ca^{2+} measurements.

Cells over-expressing PS2 (wt or T122R) and the probes were immuno-labelled with an antibody against PS2 (Fig. 29) and observed at the confocal microscope. A good co-localization between the signal coming from the three fluorescent probes and that from the antibodies was found in both conditions, thus suggesting that PS2, both mutated and wt, is expressed at the level of the ER, the *medial*- and the *trans*-GA.

3.2 FAD-linked-PS2 strongly affect the Ca^{2+} level of the ER and *medial*-GA but do not affect the Ca^{2+} level of the *trans*-GA

In order to study the effect of FAD-linked PSs on Ca^{2+} handling of intracellular stores, Ca^{2+} measurements were performed in SH-SY5Y cells transiently transfected with the cDNAs coding for ER-D4, mGo-D1cpv or tGo-D1cpv and

different PS1 or PS2 (wt or FAD- PS1-A246E and FAD-PS2-T122R), or the void vector, as control.

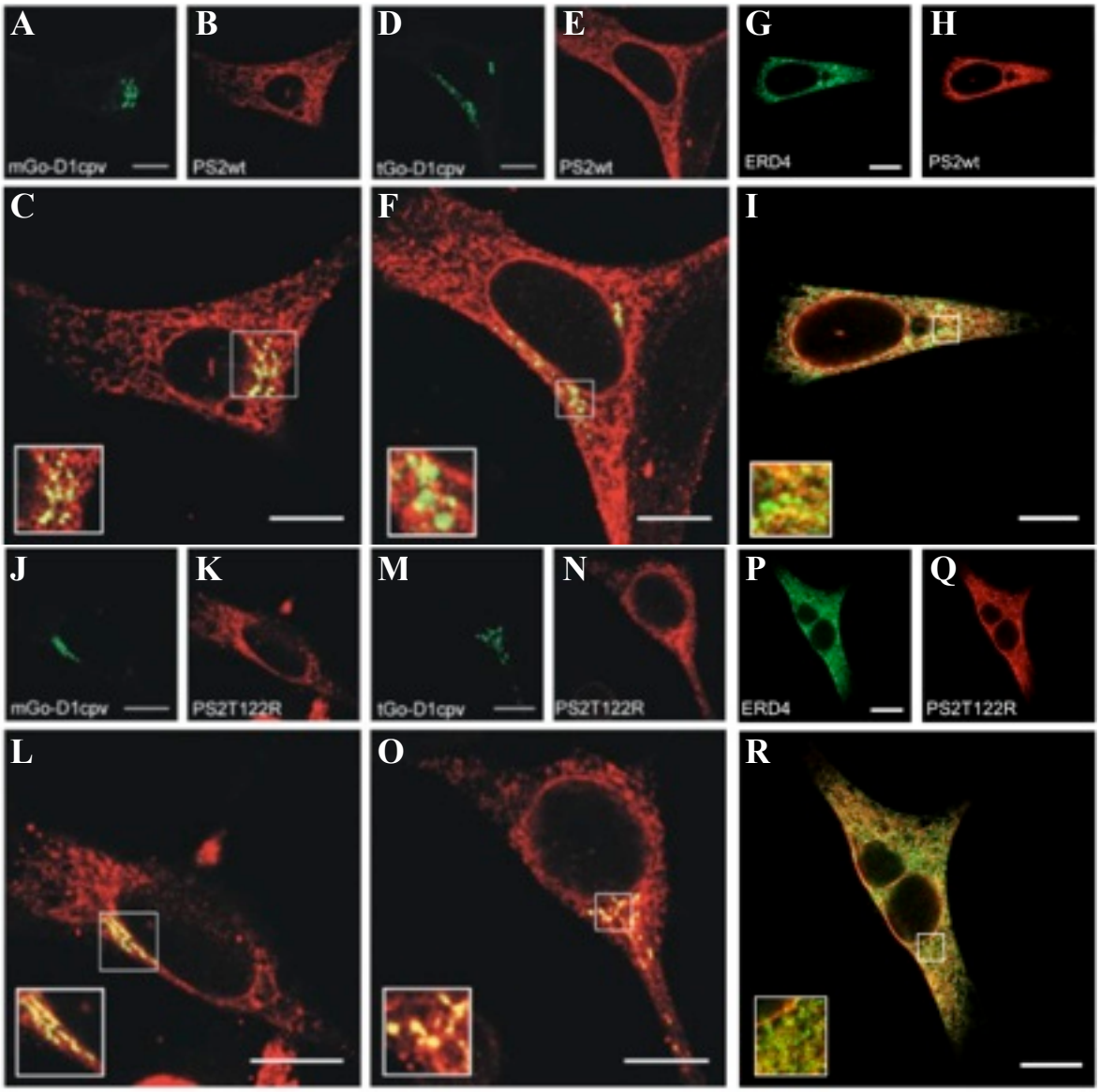

Fig. 29: Confocal fluorescence images corresponding to SH-SY5Y cells expressing the three Ca^{2+} probes excited at 488 nm **(A, D, G, J, M** and **P)** or decorated with antibody against PS2 **(B, E, H, K, N** and **Q)** and excited at 543 nm. Merging of the two previous images **(C, F, I, L, O** and **R)**: the yellow colour indicates overlapping of the green and red signals. Insets show magnifications of selected ROIs. Bar, 10 μm.

The Ca^{2+} content at rest was firsly observed (Fig. 30 and 31), founding that the over-expression of PS2 wt or T122R, but not of PS1 wt or A246E, affects ER the Ca^{2+} level of the ER and that of the medial-GA, being strongly reduced compared to control cells.

Within the ER, a major effect was observed upon of PS2-T122R over-expression: in terms of FRET value (% of the max; Fig. 30 B), a reduction, from about 62 ± 1.7 % (mean ± s.e.m., n = 23), in control cells, to about 46 ± 2,8 % (mean ± s.e.m., n = 14), in cells over-expressing PS2-T122R was observed; in terms of [Ca^{2+}] (Fig. 30C), this represents a reduction from about 475 ± 50 µM (mean ± s.e.m., n = 23) in controls to about 255 ± 40 µM (mean ± s.e.m., n = 14) in PS2-T122R expressing cells. The effect was mimicked by the over-expression of PS2wt, that reduces ER Ca^{2+} content to 286 ± 30 µM (mean ± s.e.m., n = 13), but not by the over-expression of PS1, either wt or A246E (Fig. 30 A and B).

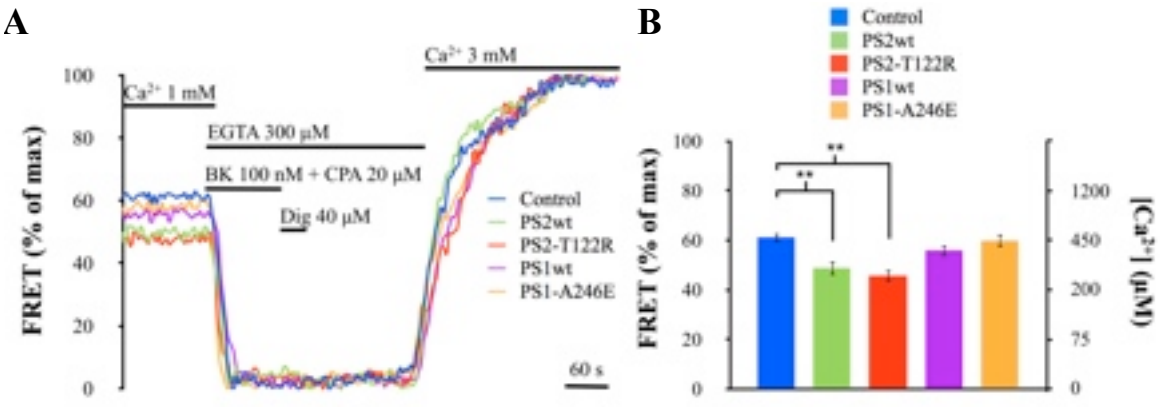

Fig. 30: Representative traces of SH-SY5Y cells co-expressing the ER-D4 probe and either PS2-T122R, PS2wt, PS1-A246E or PS1wt **(A)** in response to different stimuli. **(B)** Averaged ER FRET and [Ca^{2+}] values in resting cells expressing PS2-T122R, PS2wt, PS1-A246E or PS1wt (mean ± s.e.m.; n ≥ 11).

Similar results were obtained with the *medial*-Golgi probe: PS2-T122R over-expression leads to a reduced FRET value at rest, from about 82 ± 1.5 % (mean ± s.e.m., n = 24), in control cells, to about 58 ± 3 % (mean ± s.e.m., n = 15), in cells over-expressing the mutated protein; this represents, a reduction in [Ca^{2+}] within the organelle at rest (Fig. 31 B) from about 235 ± 30 µM (mean ± s.e.m., n = 24) in controls to about 62 ± 6 µM (mean ± s.e.m., n = 15) in over-expressing cells. As for the ER, a similar effect was observed upon over-expression of PS2wt, that reduces ER Ca^{2+} content to 52 ± 7 µM (mean ± s.e.m., n = 10), but not upon over-expression of PS1, either wt or A246E (Fig. 31 A and B).

No differences in Ca^{2+} content has been found in *trans*-GA between control cells and those expressing wt or mutated PS1 or PS2: $[Ca^{2+}]$ within this sub-organelle in resting condition was about 146 ± 15 µM (mean ± s.e.m., n = 16) for controls, 156 ± 19 µM (mean ± s.e.m., n = 15) for PS2-T122R over-expressing cells, 157 ± 14 µM (mean ± s.e.m., n = 17) for PS2wt over-expressing cells, 173 ± 15 µM (mean ± s.e.m., n = 12) for PS1-A246E over-expressing cells and 167 ± 17 µM (mean ± s.e.m., n = 12) for PS1wt over-expressing cells (Fig. 31 C and D).

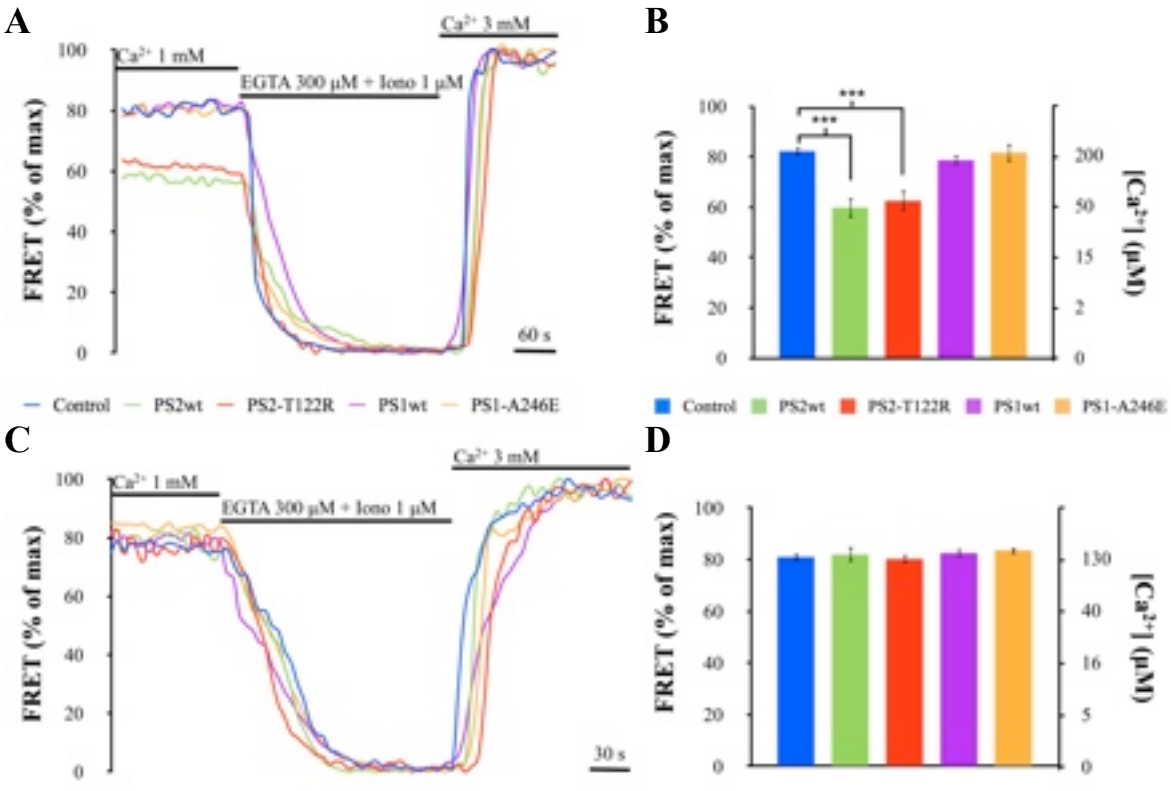

Fig. 31: Representative FRET variations of mGo-D1cpv **(A)** or tGo-D1cpv **(C)** in PS2-T122R, PS2wt, PS1-A246E or PS1wt expressing SH-SY5Y cells in response to different stimuli. Averaged *medial*-Golgi **(B)** and *trans*-Golgi **(D)** FRET and $[Ca^{2+}]$ values in resting cells expressing PS2-T122R, PS2wt, PS1-A246E or PS1wt (mean ± s.e.m.; n ≥ 10).

To verify that the observed PS effects were not due to the over-expression procedure, human fibroblasts from different FAD patients (as well as from healthy age-matched controls) were similarly analysed. In fibroblasts from a FAD patient carrying the PS2-N141I mutation a reduced $[Ca^{2+}]$ was measured

within the ER (Fig. 32) compared to human control fibroblasts from three different individuals (PS2 ctrl 1-3). In terms of FRET changes, a reduction from values of about 75 ± 1%, 72 ± 3 % and 70 ± 3 % (mean ± s.e.m., n ≥ 14), measured in the three controls, to about 60 ± 2 % (mean ± s.e.m., n = 19) in PS2-N141I fibroblasts was observed. In terms of Ca^{2+} this means that while control fibroblasts showed an ER [Ca^{2+}] around 775 ± 50 µM(850 ± 60 µM, 760 ± 80 µM and 695 ± 20 µM, respectively; mean ± s.e.m., n ≥ 14), PS2-N141I fibroblasts showed an ER [Ca^{2+}] of 450 ± 40 µM (mean ± s.e.m., n = 22).

On the contrary, there were no difference in FRET (73 ± 3 % (mean ± s.e.m., n = 14) and 75 ± 2 % (mean ± s.e.m., n = 16), respectively) and [Ca^{2+}] (840 ± 80 µM (mean ± s.e.m., n = 14) and 790 ± 70 µM (mean ± s.e.m., n = 16), respectively (Fig. 32 B); resting values between controls and PS1-A246E human fibroblasts.

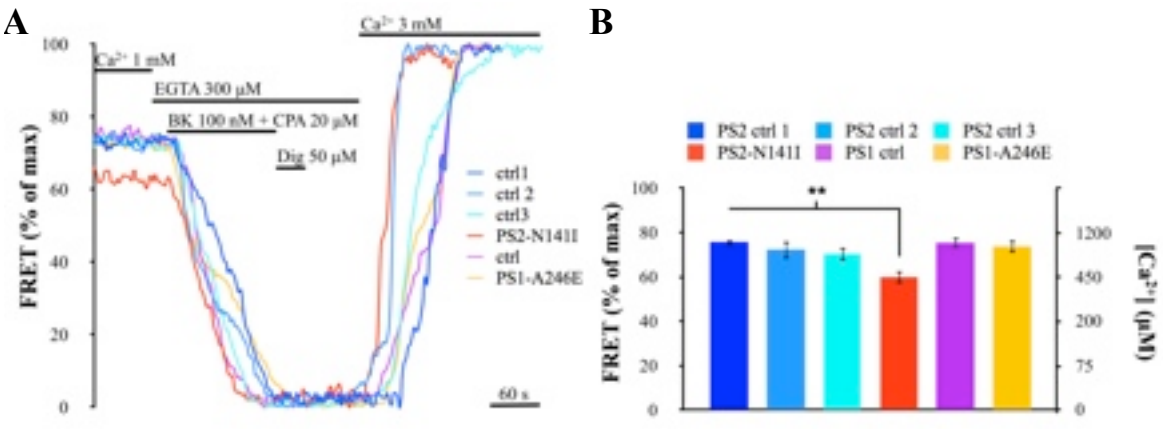

Fig. 32: Representative FRET variations of ER-D4 **(A)** in FAD PS2-N141I, PS1-A246E human fibroblasts and their controls, in response to different stimuli. **(B)** Averaged ER FRET and [Ca^{2+}] values in resting control, PS2-N141I and PS1-A246E fibroblasts (mean ± s.e.m.; n ≥ 14).

As for the ER, PS2-N141I human fibroblasts showed a reduced [Ca^{2+}] in the *medial*-GA (Fig. 33 A and B) compared to control cells (PS2 Ctrl 1). In terms of FRET values, a reduction from 87 ± 1 % (mean ± s.e.m., n = 10) in control fibroblasts, to 69 ± 3 % (mean ± s.e.m., n = 10) in PS2-N141I fibroblasts was observed, corresponding to a *medial*-Go [Ca^{2+}] of 297 ± 30 µM, (mean ± s.e.m., n = 10) in controls and of 84 ± 13 µM (mean ± s.e.m., n = 10) in PS2-N141I

fibroblasts. There were instead no difference in FRET and Ca2+ values between controls and PS1-A246E fibroblasts (Fig. 33 C and D; FRET values of 78 ± 2 % (mean ± s.e.m., n = 10) and 79 ± 2 % (mean ± s.e.m., n = 10); [Ca^{2+}] of 123 ± 5 µM (mean ± s.e.m., n = 10) and 127 ± 9 µM (mean ± s.e.m., n = 10); for control and PS1-A246E fibroblasts, respectively) .

No differences in Ca^{2+} content has been found in *trans*-GA between PS2-N141I or PS1-A246E compared to their respective controls (Fig. 33, panels F, G, H): control and PS2-N141I fibroblasts showed respectively a trans-Golgi Ca^{2+} content at the steady state of 105 ± 7 µM (mean ± s.e.m., n = 10) and 110 ± 12 µM (mean ± s.e.m., n = 10).

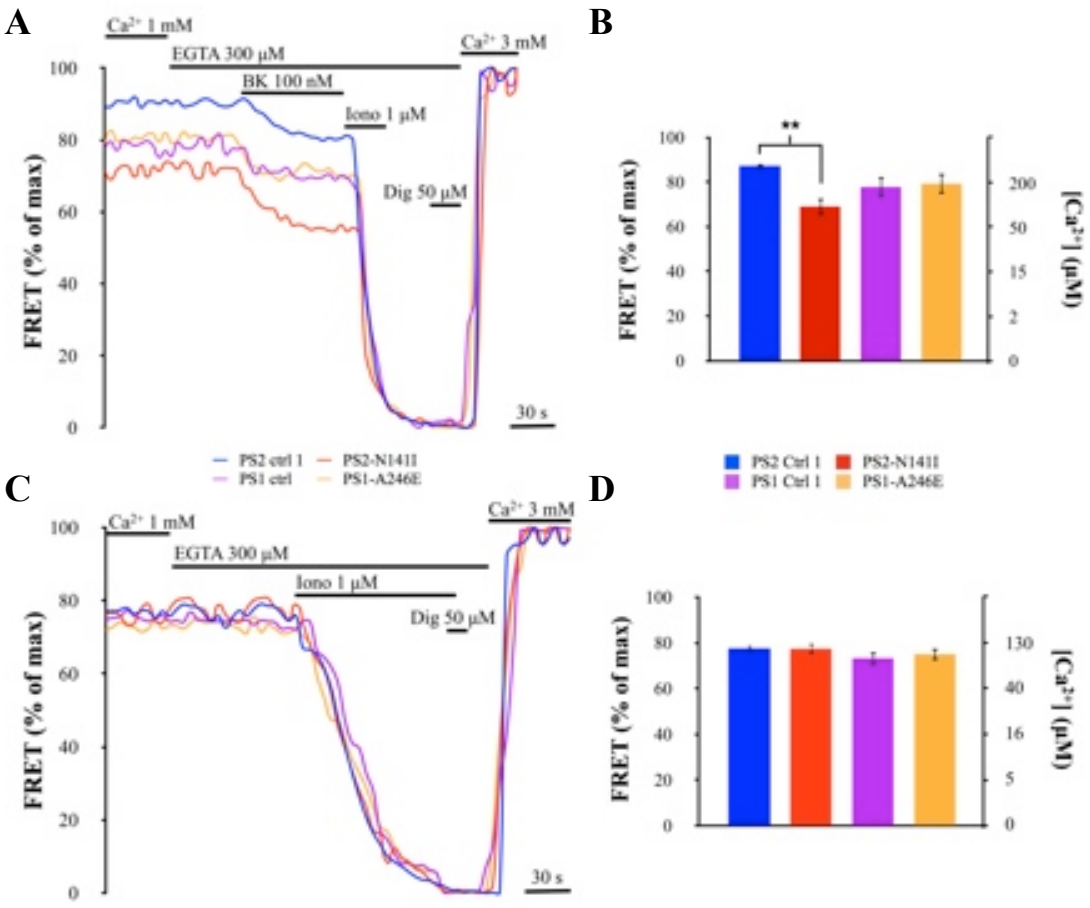

Fig. 33: Representative FRET variations of mGo-D1cpv **(A)** or tGo-D1cpv **(C)** in FAD PS2-N141I and PS1-A246E fibroblasts (and corresponding controls), in response to different stimuli. **(B** and **D)** Averaged FRET and [Ca^{2+}] values of *medial*-GA and *trans*-GA in PS2-N141I and PS1-A246E FAD fibroblasts, and corresponding controls, at rest controls, (mean ± s.e.m.; n ≥ 10).

3.3 FAD-linked-PS2 mutants reduce ER and medial-Golgi Ca^{2+} uptake by inhibiting SERCA activity

In order to investigate how PS2 affects Ca^{2+} homeostasis within the ER and the *medial*-Golgi, we performed some experiments in permeabilized SH-SY5Y cells transiently transfected either with the ER-D4 or the mGo-D1cpv probe and with PS2 wt or T122R, or the void vector as control.

Cells were pre-incubated in a Ca^{2+}-free EGTA-containing (300 μM) medium and the SERCA inhibitor CPA (20 μM) for 10 minutes, to induce intracellular Ca^{2+} stores depletion. Cells were permeabilized in an intracellular-like medium containing EGTA (300 μM) and digitonin (40 μM) for 30 seconds. They were then washed with an intracellular-like medium containing only EGTA (300 μM) and perfused with an intracellular-like medium containing 100 nM Ca^{2+} in the presence of ATP (200 μM; Fig. 34 and 35).

Within the ER, in SH-SY5Y cells, the expression of PS2-T122R, or its wt form, significantly reduced the plateau reached upon Ca^{2+} addition, as well as the Ca^{2+} uptake rate (Fig. 34 A). Indeed, the plateau reached after Ca^{2+} refilling(Fig. 34 B) was of 486 ± 20 μM (mean ± s.e.m., n = 11) in control cells, 364 ± 15 μM (mean ± s.e.m., n = 10) in cells over-expressing PS2 wt and 350 ± 40 μM (mean ± s.e.m., n = 12) in cells over-expressing PS2-T122R; the initial Ca^{2+} uptake rate (calculated as the maximal values of the first derivate of momentaneous $[Ca^{2+}]$) was of 5.93 ± 0.62 μmol Ca^{2+}/s (mean ± s.e.m., n = 11) in control cells, 3.70 ± 0.63 μmol Ca^{2+}/s (mean ± s.e.m., n = 10) in cells over-expressing PS2 wt and 4.14 ± 0.40 μmol Ca^{2+}/s (mean ± s.e.m., n = 12) in cells over-expressing PS2-T122R.

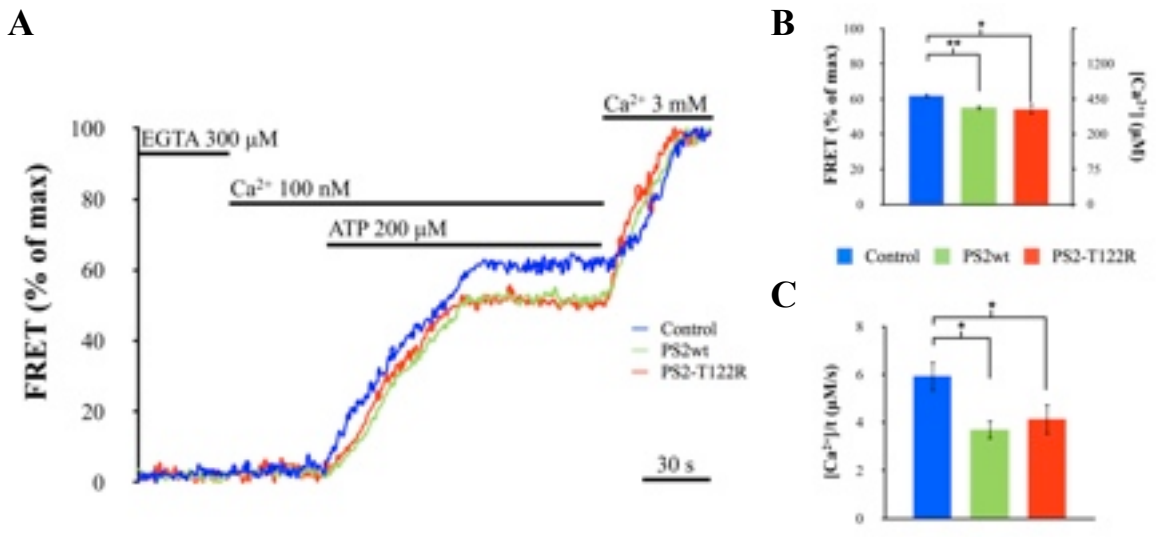

Fig. 34: Representative ER-D4 **(A)** FRET changes in PS2-T122R or PS2wt expressing SH-SY5Y cells, in response to different stimuli. **(B)** Averaged FRET and [Ca^{2+}] values reached in the ER upon Ca^{2+} refilling and **(C)** averaged [Ca^{2+}]/s values for the first 10 s of Ca^{2+} uptake in control, PS2-T122R and PS2wt expressing SH-SY5Y cells (mean ± s.e.m.; n ≥ 10).

Similarly, in the medial-GA, the expression of PS2-T122R significantly reduced both the refilling reached plateau and the initial Ca^{2+} uptake rate (fig. 34 A, B; a reached plateau values of 148 ± 20 µM (mean ± s.e.m., n = 13) and of 35 ± 6 µM (mean ± s.e.m., n = 15); an initial Ca^{2+} uptake rate of 1.64 ± 0.35 µmol Ca^{2+}/s (mean ± s.e.m., n = 13) and 0.63 ± 0.06 µmol Ca^{2+}/s (mean ± s.e.m., n = 15) in controls and PS2-T122R expressing cells, respectively.

Medial-Golgi Ca^{2+} uptake were affected also upon over-expression of wt PS2, although its effect was weaker than that induced by the FAD-mutant (Fig. 35), with a reached plateau after refilling (Fig. 35 B) of 54 ± 5 µM (mean ± s.e.m., n = 13) and an initial Ca2+ uptake rate (Fig. 35 C) of 0.85 ± 0.07 µmol Ca^{2+}/s (mean ± s.e.m., n = 13).

The over-expression of PS2-T122R or PS2 wt, does not alter, within the *trans*-Golgi, neither the plateau reached after refilling, (Fig. 35 E) neither the initial uptake rate (Fig. 35 F).

These results thus suggest that the over-expression of the FAD-linked PS2-T122R (and similarly of wt PS2) decreases ER and *medial*-Golgi [Ca^{2+}] by inhibiting SERCA activity, whereas it doesn't affect SPCA1 activity and, consequently, trans-Golgi [Ca^{2+}].

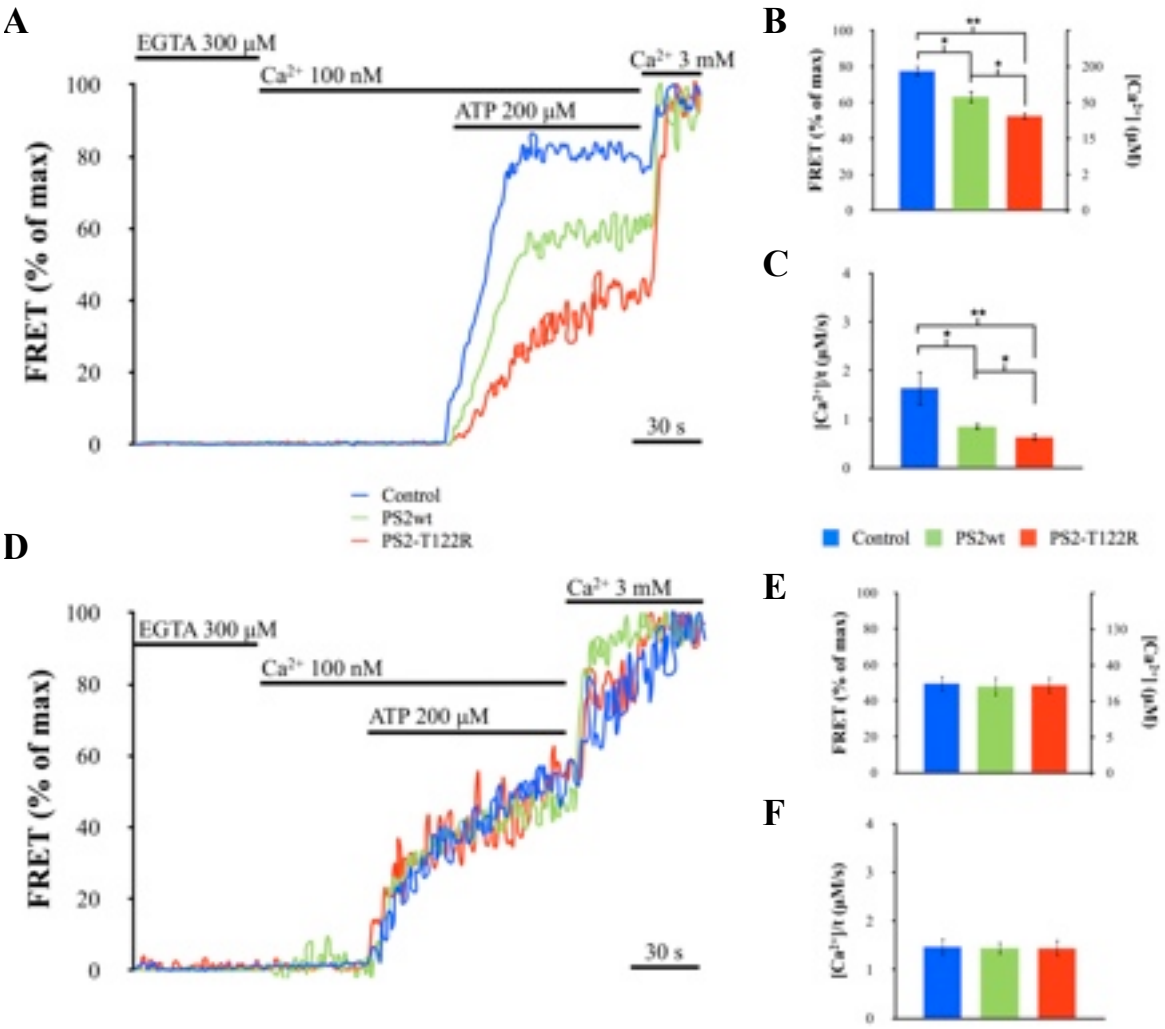

Fig. 35: Representative FRET variations of mGo-D1cpv **(A)** and tGo-D1cpv **(D)** in PS2-T122R or PS2wt expressing SH-SY5Y cells, in response to different stimuli. Averaged FRET and [Ca^{2+}] values of *medial*-GA **(B)** or *trans*-GA **(E)** plateau reached after refilling and **(C** and **F)** averaged [Ca^{2+}]/s values for the first 10 s of Ca^{2+} uptake in control, PS2-T122R and PS2wt expressing SH-SY5Y cells (mean ± s.e.m.; n ≥ 13).

Similar results for the ER and the medial-GA have been obtain in fibroblasts from the FAD_PS2-N141I patient compared to controls (Fig. 36).

PS2-N141I human fibroblasts transiently expressing ER-D4 or mGo-D1cpv, have shown both a significantly reduced plateau reached upon Ca^{2+} refilling and reduced Ca^{2+} uptake rate (Fig. 36 A and D). Indeed, for the ER, the plateau values (Fig. 36 B) were of 805 ± 50 µM, 760 ± 40 µM, 755 ± 50 µM (mean ±

s.e.m., n ≥ 10) in the three controls (PS2 ctrl 1-3) and 507 ± 40 µM (mean ± s.e.m., n = 9) in PS2-N141I fibroblasts. Within the *medial*-GA, the plateau reached after refilling (Fig. 36 E) was of 42 ± 3 µM, 45 ± 6 µM, 45 ± 4 µM (mean ± s.e.m., n ≥ 6) in the three controls (PS2 ctrl 1-3) and 14 ± 2 µM (mean ± s.e.m., n = 4) in PS2-N141I fibroblasts. As in SH-SY5Y cells, the ER initial Ca^{2+} uptake rate (Fig. 36 C) in PS2 control fibroblasts (ctrl 1-3) was, respectively, of 6.9 ± 0.33 µmol Ca^{2+}/s (mean ± s.e.m., n = 10), 6.56 ± 0.47 µmol Ca^{2+}/s (mean ± s.e.m., n = 11), 6.71 ± 0.42 µmol Ca^{2+}/s (mean ± s.e.m., n = 10) and of 3.9 ± 0.46 µmol Ca^{2+}/s (mean ± s.e.m., n = 9) in PS2-N141I fibroblasts. Within the *medial*-GA (Fig. 36 E) the same parameter was of 0.99 ± 0.14 µmol Ca^{2+}/s, 0.92 ± 0.16 µM Ca^{2+}/s, 0.96 ± 0,1 µmol Ca^{2+}/s (mean ± s.e.m., n ≥ 6), in the three controls (PS2 ctrl 1-3) and 0,41 ± 0,07 µmol Ca^{2+}/s (mean ± s.e.m., n = 4) in PS2-N141I fibroblasts.

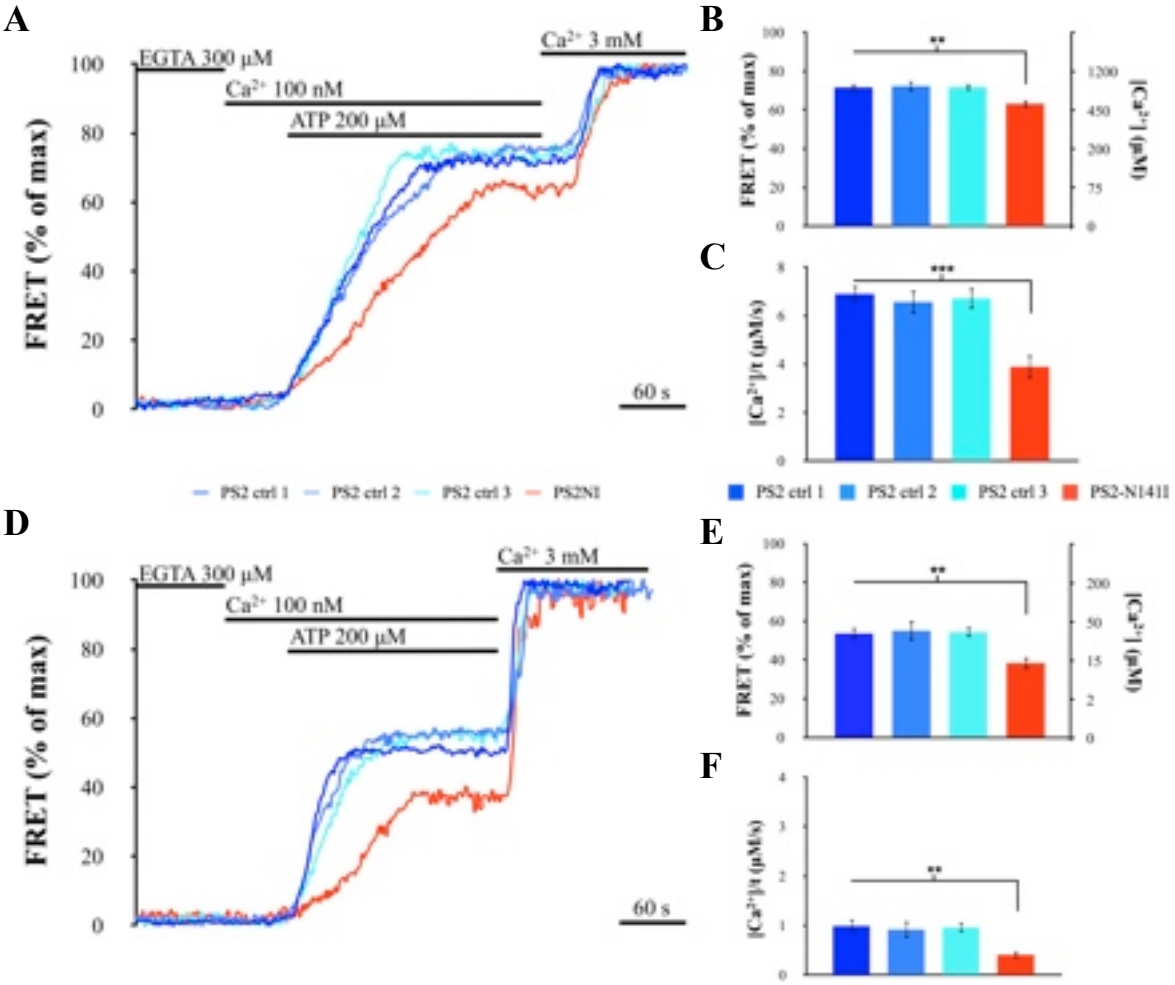

Fig. 36: Representative FRET variations of ER-D4 **(A)** and mGo-D1cpv **(D)** in PS2-N141I fibroblasts and corresponding controls, in response to different stimuli. Averaged FRET and [Ca^{2+}] values of ER **(B)** or *medial*-GA **(E)** plateau reached after Ca^{2+} refilling and **(C** and **F)** avereged [Ca^{2+}]/s values for the first 10s of the Ca^{2+} uptake in controls and PS2-N141I fibroblasts (mean ± s.e.m.; n ≥ 4).

3.4 FAD-linked PS2 increases *medial*-Golgi, but not ER Ca^{2+} leak

In addition to the Ca^{2+} uptake, also the Ca^{2+} leak of an organelle could determined its steady-state [Ca^{2+}].

In order to study if organelles leak of Ca^{2+} were also affected by the over-expression of FAD-linked PS2 mutants, control SH-SY5Y cells were pre-treated in extracellular medium containing EGTA (300 µM), at 4 C° for 20 minutes before starting Ca^{2+} measurement, to match the Ca^{2+} content within the ER or the

medial-GA of over-expressing PS2 (wt and T122R) cells (Fig. 37 A, B, D and E). Upon this protocol, control cells showed an initial ER [Ca^{2+}] of about of 264 ± 15 µM (mean ± s.e.m., n = 9), very similar to the Ca^{2+} ER levels found in PS2 (wt and T122R)-expressing cells (264 ± 9 µM (mean ± s.e.m., n = 9) and 275 ± 11 µM (mean ± s.e.m., n = 7), respectively; Fig. 37 B).

In the same way, control cells showed an initial *medial*-Go [Ca^{2+}] of about 45 ± 4 µM (mean ± s.e.m., n = 9), similar to those of PS2 (wt and T122R) expressing cells (47 ± 5 µM (mean ± s.e.m., n = 10) and 44 ± 4 µM (mean ± s.e.m., n = 10), respectively; Fig. 37 E).

The over-expression of PS2 wt increased spontaneous Ca^{2+} leak from the *medial*-Golgi after perfusing an extracellular medium containing CPA and EGTA, to visualize it (Fig. 37 D and F). A similar, but weaker effect was observed upon the over-expression of PS2-T122R. Indeed, the initial leak rate (calculated as the minimal values of the first derivate of the momentaneous [Ca^{2+}]) were -0.2 ± 0.03 µmol Ca^{2+}/s (mean ± s.e.m., n = 9), -0.4 ± 0.07 µmol Ca^{2+}/s (mean ± s.e.m., n = 10) and -0.7 ± 0.08 µmol Ca^{2+}/s (mean ± s.e.m., n = 11) for control, PS2-T122R and PS2 wt over-expressing cells, respectively (Fig. 37 F).

Contrariwise, similar experiments in SH-SY5Y cells with the ER probe demonstrated that the over-expression of both PS2 wt and mutated does not affect ER Ca^{2+} leak (Fig. 37 A and C): the calculated initial leak rate was -2.65 ± 0.18 µmol Ca^{2+}/s (mean ± s.e.m., n = 9), -2.95± 0.23 µmol Ca^{2+}/s (mean ± s.e.m., n = 7) and -2.99 ± 0.36 µmol Ca^{2+}/s (mean ± s.e.m., n = 8) for control, PS2-T122R and PS2 wt over-expressing cells, respectively(Fig. 37 C).

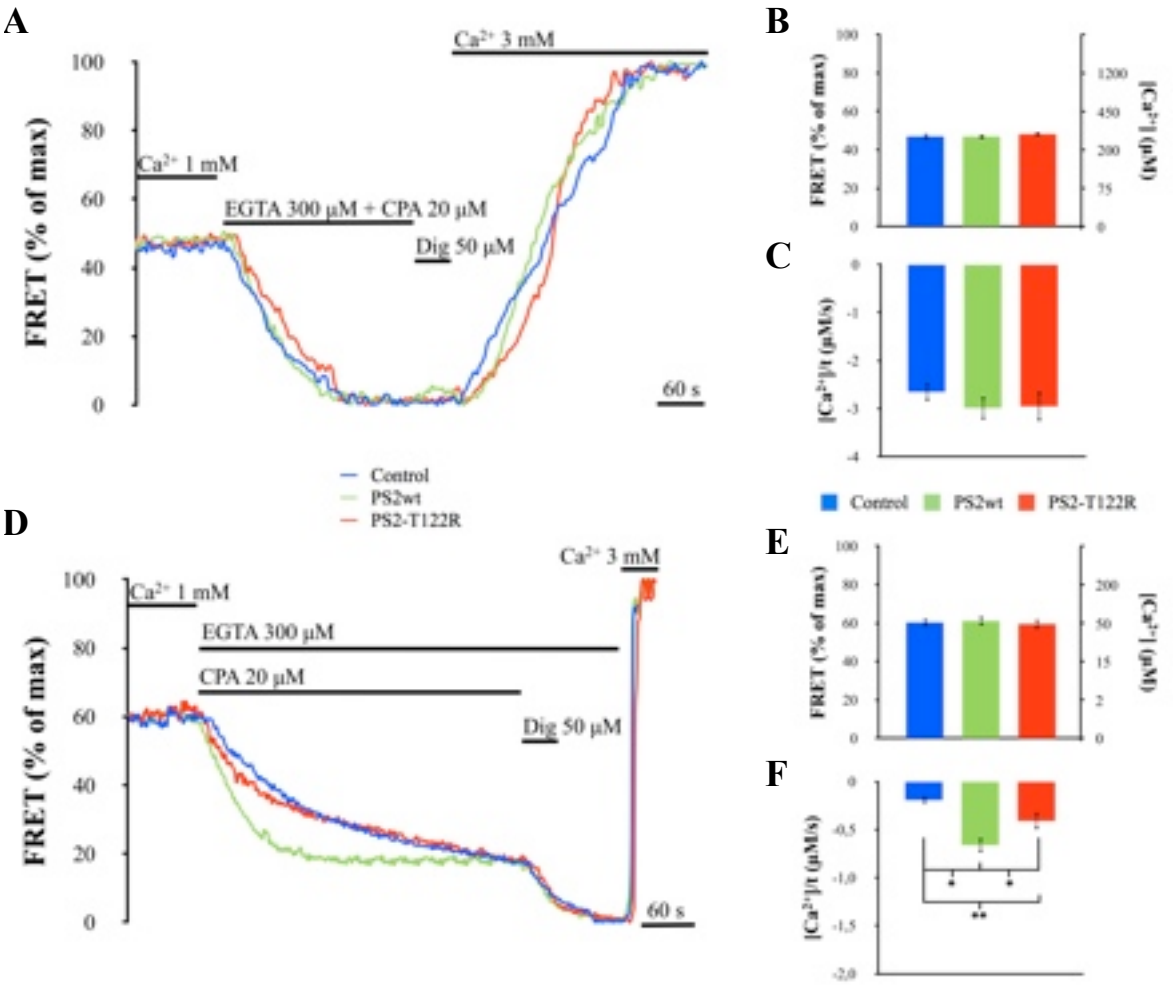

Fig. 37: Representative FRET variations of ER **(A)** and mGo-D1cpv **(D)** in PS2-T122R or PS2 wt expressing SH-SY5Y cells, in response to different stimuli. Averaged FRET and $[Ca^{2+}]$ values of ER **(B)** or *medial*-GA **(E)** at initial $[Ca^{2+}]$ level and **(C** and **F)** averaged $[Ca^{2+}]/s$ values for the first 10s of Ca^{2+} leak in PS2-T122R, PS2wt expressing or control SH-SY5Y cells (mean ± s.e.m.; n ≥ 13).

Discussion and conclusions

Direct information on the Ca^{2+} homeostatic mechanisms in the GA of living cells has been obtained for the first time in the 90's, using an aequorin chimeric construct localized to this organelle lumen (Pinton P. et al., 1998). In this paper it has been demonstrated that the GA (as a whole) behaves, in terms of Ca^{2+} handling, similarly to the ER.

More recently, in our lab, using a novel GFP-based Ca^{2+} probe selectively localized to the *trans*-Golgi, tGo-D1cpv, it has been demonstrated that this GA sub-compartment is endowed with unique characteristics that differ completely from those of the ER. In particular, it has been shown that the *trans*-Golgi is IP_3-insensitive and utilizes solely SPCA1 for its Ca^{2+} uptake (Lissandron V. et al., 2010).

During my PhD, another cameleon Ca^{2+} probe able to measure the $[Ca^{2+}]$ in the *medial*-GA has been generated in the lab; this probe has revealed additional complexity and heterogeneity in the Ca^{2+} handling of the entire organelle. Indeed, the characteristics, and the molecular components involved, of the Ca^{2+} handling in this latter GA sub-compartment are totally different from those of the trans-GA. The *medial*-GA appears to accumulate Ca^{2+} within its lumen taking advantage of both SERCA and SPCA1 and it is an IP_3- and Ry-sensitive Ca^{2+} store. Thus, within the GA in a space of a few microns, and despite its continuous inter-mixing dynamics, there are separate functional entities with clearly distinct Ca^{2+} handling mechanisms.

In the second part of my PhD, we generated a cameleon Ca^{2+} probe targeted to the ER, with appropriate features to measure its $[Ca^{2+}]$, named ER-D4.

Using the two new probes and that targeted to the trans-Golgi, the specific effect on intracellular Ca^{2+} stores of the expression of FAD-linked PS mutants was evaluated. Indeed, impairment of cellular Ca^{2+} signalling has been causally associated to ageing and several neuronal disorders, including AD (Mattson M.P. et al., 2000). In particular, previous data from our lab have demonstrated that FAD-PS2 mutations reduce ER and GA Ca^{2+} levels, in particular by inhibiting SERCA activity (Zatti et al., 2006 and Brunello et al., 2009).

My results further indicate that the expression of FAD-linked PS2 mutants (but not PS1) cause dysregulations in ER and *medial*-Golgi Ca^{2+} handling. In particular, they strengthen the idea that FAD-PS2 mutants act on intracellular Ca^{2+} content by affecting SERCA-2 activity, thus reducing stored Ca^{2+} and thus its release in the cytosol upon different cell stimulations.

The result of a decreased intracellular store Ca^{2+} content in the presence of FAD-PS2 mutants is however a debated issue. On one hand, Foskett' s group proposed that PSs, both PS1 and PS2, can regulate the sensitivity of the IP_3R, with their FAD mutants increasing its open probability at low IP_3 concentrations; this molecular effect results in an exaggerated Ca^{2+} signals in response to agonist stimulation, as well as in a higher degree of constitutive Ca^{2+} signalling, without however affecting intracellular store Ca^{2+} content (Cheung K.H. et al., 2010). On the contrary, data from another group sustained the "Ca^{2+} overload" hypothesis, in which an increased Ca^{2+} content in intracellular stores in the presence of FAD-PSs mutants is observed. According to this hyphothesis, wt PS holoprotein forms ER Ca^{2+} channels that comprise a passive ER Ca^{2+} leak, while FAD-PSs mutants have lost this functionality and thus cause an ER Ca^{2+} overload (Nelson O. et al., 2010).

Recently, a new study has shown that PS2, but not PS1, emerges from a broad screening as a protein able to cause an ER Ca^{2+} leak (Bandara S. et al., 2013), and thus a reduction in ER Ca^{2+} content, sustaining our data. Moreover, the fact that in our experiments PS2 wt behaves as the FAD mutant forms only when it is largely over-expressed, suggest that FAD-PS2 effect on Ca^{2+} homeostasis is due to a toxic "gain of function", as demonstrated for other PS features (Haas C. et al., 1999).

The main question is whether and how this alteration may contribute to the pathogenesis of FAD. A reduced ER Ca^{2+} release is expected to influence negatively ER-mitochondria Ca^{2+} transfer, with a reduction in mitochondrial functions but also an increased resistance to apoptotic stimuli. Indeed, as demonstrated in several models of cell death, a reduction in the ER Ca^{2+} content is partially protective against a variety of cytotoxic insults (Pinton P. et al., 2001). In our lab, however, it has been previously demonstrated that endogenous

PS2 and, more potently FAD-PS2 mutants (but not FAD-PS1 mutants), have an additional effect, increasing the physical tethering between ER and mitochondria and their Ca^{2+} cross-talk (Zampese E. et al. 2011). This latter feature further complicates the possible PS2 mechanism of action, since the stronger ER-mitochondrial tethering could compensate the reduced ER Ca^{2+} content, locally inducing a mitochondrial Ca^{2+} overload that, in concomitance with other toxic stimuli, *i.e.*, Aβ peptide, could be detrimental for cell life. Indeed, it has been demonstrated that a chronic mitochondrial Ca^{2+} overload may activate the apoptotic pathway (Pizzo P. et al., 2012).

Alternatively, the reduced store Ca^{2+} content induced by the expression of FAD-PS2 mutants, but not of FAD-PS1 mutants, may in someway be protective against a variety of cytotoxic insults, avoiding mitochondria Ca^{2+} overload. The increased ER-mitochondria apposition caused by FAD-PS2, on the other hand, could be necessary to maintain the proper ER-mitochondria Ca^{2+} transfer needed for cell viability even in the presence of a reduced ER Ca^{2+} content. This hypothesis could explain the late-onset and less aggressive AD phenotype linked to PS2 mutations, compared to that linked to PS1 mutations, being these latter unable to modify ER Ca^{2+} content.

Whether the abnormalities in Ca^{2+} homeostasis caused by FAD-PS2 mutants expression, both as reduced Ca^{2+} store content and favoured mitochondria Ca^{2+} uptake, could have a key role in cell viability, toxicity and eventually cell death will be the topic of further investigations.

We here show evidence that the PS2-T122R mutation causes a reduction in ER and *medial*-Golgi Ca^{2+} content.

Abbreviations

[Ca^{2+}]: Calcium concentration

AA: Amino acids

Aβ: Amyloid-β

AD: Alzheimer's disease

ADAM: α disintegrin and metalloproteinase

AICD: APP intracellular domain

APH1: Anterior pharynx-defective1

APP: Amyloid precursor protein

BACE1: β-site APP cleaving enzyme 1

BK: Bradykinin

Ca^{2+}: Calcium

Caff: Caffeine

CaM: Calmodulin

CARP: carbonic anhydrase-related protein

cDNA: complementary DNA

CFP: Cyan fluorescent proteins

CGN: Cis Golgi network

CICR: Ca^{2+}-induced Ca^{2+} release

CNS: Central nervous sisystem

CNX: Calnexin

CPA: Cyclopiazonic acid

CRAC: Ca^{2+} release-activated Ca^{2+} channel

CRT: Calreticulin

CSQ: Calsequestrin

Dig: Digitonin

E-C: Exitation - contraction

ER: Endoplasmic reticulum

FAD: Familial Alzheimer's disease

FP: Fluorescent protein

FRET: Fluorescence resonance energy transfer

GA: Golgi apparatus

GECIs: Genetically encoded Ca^{2+} sensors

GRP78: Glucose-related protein78

GRP94: Glucose-related protein94

IP_3R: IP_3 receptor

Iono: Ionomycin

K_d: Dissociation constant

LOAD: “late-onset” AD

M13: CaM binding peptide of myosin light chain kinase M13

MBDs: Microtubule-binding domains

MCU: Mitochondrial Ca^{2+} uniporter

mGoD1cpv: Medial Golgi-D1cpv

mKRB: Modified Krebs-Ringer buffer

NAADP: Nicotinic acid adenine dinucleotide phosphate

NFT: Neurofibrillary tangle

PEN2: Presenilin enhancer 2

PIP_2: Phosphatidyl inositol bis-phosphate

PLC: Phospholipase C

PP1: Protein phosphatase 1

PP2A: Protein phosphatase 2A

PS: Presenilin

PS1: Presenilin-1

PS2: Presenilin-2

Ry: Ryanodine

RyRs: Ryanodine receptors

sAPP-α: Secreted Extracellular Domain

SERCA: Sarco/endoplasmic reticulum calcium ATPase

SOCCs: Store-operated Ca^{2+} channels

SPCA1: Secretory pathway Ca^{2+} ATPase1

SR: Sarcoplasmic reticulum

STIM1: stromal interacting molecule

t-BHQ: 2,5-di-(ter-butyl)-1,4-benzohydroquinone

Tg: Thapsigargin

TGN: Trans Golgi network

TPC: Two pore channel

VOCCs: Voltage-operated Ca^{2+} channels

wt: Wild type

YC: Yellow cameleon

YFP: Yellow fluorescent proteins

References

- Adler J. and Parmryd I., Quantifying colocalization by correlation: the Pearson correlation coefficient is superior to the Mander's overlap coefficient. *Cytometry A*, Vol.77: 733-742, 2010.
- Bandara S., Malmersjö S., Meyer T, .Regulators of calcium homeostasis identified by inference of kinetic model parameters from live single cells perturbed by siRNA. *Sci Signal*, Vol.6, 2013
- Barker W.W., Luis C.A., Kashuba A., Luis M., Harwood D.G., Loewenstein D., Waters C., Jimison P., Shepherd E., Sevush S., Graff-Radford N., Newland D., Todd M., Miller B., Gold M., Heilman K., Doty L., Goodman I., Robinson B., Pearl G., Dickson D., Duara R., Relative frequencies of Alzheimer disease, Lewy body, vascular and frontotemporal dementia, and hippocampal sclerosis in the State of Florida Brain Bank. *Alzheimer Dis Assoc Disord*, Vol.16: 203–212, 2002.
- Beam K.G. and Bannister R.A., Looking for answers to EC coupling's persistent questions. *J Gen Physiol*, Vol.136: 7–12, 2010.
- Behbahani H. et al., Differential role of Presenilin-1 and -2 on mitochondrial membrane potential and oxygen consumption in mouse embryonic fibrobroblasts. *J Neurosci Res*, Vol.84: 891–902, 2006.
- Berridge M.J., Bootman M.D. and Roderick H.L., Calcium signalling: dynamics, homeostasis and remodelling. *Nat Rev Mol Cell Biol,* Vol.4: 517-529, 2003.
- Braak H. and Braak E., Frequency of stages of Alzheimer-related lesions in different age categories. *Neurobiol Aging*, Vol.18: 351–357, 1997.
- Breton C., Mucha J., Jeanneau C., Structural and functional features of glycosyltransferases. *Biochimie*, Vol.83: 713–718, 2001.
- Brini M. and Carafoli E., Calcium pumps in health and disease. *Physiol Rev*, Vol.89: 1341-1378, 2009.
- Brunello L., Zampese E., Florean C., Pozzan T., Pizzo P., Fasolato C., Presenilin-2 dampens intracellular Ca^{2+} stores by increasing Ca^{2+} leakage and reducing Ca^{2+} uptake. *J Cell Mol Med*, Vol.13: 3358-69, 2009.

- Buxbaum J.D., Choi E.K., Luo Y., Lilliehook C., Crowley A.C., Merriam D.E., Wasco W., Calsenilin: a calcium-binding protein that interacts with the presenilins and regulates the levels of a presenilin fragment. *Nat Med*, Vol.4: 1177-81, 1998.
- Cahalan M.D., STIMulating store-operated Ca^{2+} entry. *Nat Cell Biol*, Vol.11: 669–677, 2009.
- Cai H., Wang Y., McCarthy D., Wen H., Borchelt D.R., Price D.L. and Wong P.C., BACE1 is the major beta-secretase for generation of Abeta peptides by neurons. *Nat Neurosci*, Vol.4: 233–234, 2001.
- Calcraft P.J., Ruas M., Pan Z., Cheng X., Arredouani A., Hao X., Tang J., Rietdorf K., Teboul L., Chuang K.T., Lin P., Xiao R., Wang C., Zhu Y., Lin Y., Wyatt C.N., Parrington J., Ma J., Evans A.M., Galione A., Zhu M.X., NAADP mobilizes calcium from acidic organelles through two-pore channels. *Nature*, Vol.459: 596–600, 2009.
- Callewaert G., Parys J.B., De Smedt H., Raeymaekers L., Wuytack F., Vanoevelen J., Van Baelen K., Simoni A., Rizzuto R., Missiaen L., Similar Ca^{2+}-signaling properties in keratinocytes and in COS-1 cells overexpressing the secretory-pathway Ca^{2+}-ATPase SPCA1. *Cell Calcium*, Vol.34: 157–162, 2003.
- Carafoli E., Calcium - a universal carrier of biological signals. *FEBS J*, Vol. 272: 1073-1089, 2005.
- Catterall W.A., Excitation-contraction coupling in vertebrate skeletal muscle: a tale of two calcium channels. *Cell*, Vol.64: 871–874, 1991.
- Catterall W.A., Voltage-gated calcium channels, *Cold Spring Harb Perspect Biol*, Vol.3: 3947-3960, 2011.
- Chanat E. and Huttner W.B., Milieu-induced, selective aggregation of regulated secretory proteins in the trans-Golgi network. *J Cell Biol*, Vol.115: 1505–1519, 1991.
- Chandra S., Kable E.P., Morrison G.H., Webb W.W., Calcium sequestration in the Golgi apparatus of cultured mammalian cells revealed by laser scanning confocal microscopy and ion microscopy. *J Cell Sci*, Vol.100: 747–752, 1991.

- Cheung K.H., Mei L., Mak D.O., Hayashi I., Iwatsubo T., Kang D.E., Foskett J.K., Gain-of-function enhancement of IP_3 receptor modal gating by familial Alzheimer's disease-linked presenilin mutants in human cells and mouse neurons. *Sci signal*, Vol.3, 2010.
- Choe C.U. and Ehrlich B.E., The inositol 1,4,5-trisphosphate receptor (IP3R) and its regulators: sometimes good and sometimes bad teamwork. *Sci STKE*, Vol.15, 2006.
- Chung S.H., Aberrant phosphorylation in the pathogenesis of Alzheimer's disease. *BMB Rep*, Vol.42: 467–474, 2009.
- Cifuentes F., González C.E., Fiordelisio T., Guerrero G., Lai F.A., Hernández-Cruz A., A ryanodine fluorescent derivative reveals the presence of high-affinity ryanodine binding sites in the Golgi complex of rat sympathetic neurons, with possible functional roles in intracellular Ca^{2+} signaling. *Cell Signal,* Vol.13: 353–362, 2001.
- Clapham D.E., Calcium Signaling. *Cell*, Vol.131: 1047-1058, 2007.
- Csala M., Bánhegyi G., Benedetti A., Endoplasmic reticulum: a metabolic compartment. *FEBS Lett*, Vol.580: 2160-2165, 2006.
- Cole S.L., Vassar R., The Alzheimer's disease beta-secretase enzyme, BACE1. Mol Neurodegener, Vol.2: 22, 2007.
- Cupers P., Bentahir M., Craessaerts K., Orlans I., Vanderstichele H., Saftig P., De Strooper B., Annaert W., The discrepancy between presenilin subcellular localization and gamma-secretase processing of amyloid precursor protein. *J Cell Biol*, Vol.154: 731-740, 2001.
- da Silva C.P. and Guse A.H., Intracellular Ca^{2+} release mechanisms: multiple pathways having multiple functions within the same cell type? *Biochim Biophys Acta*, Vol.1498: 122-133, 2000.
- de Brito O.M. and Scorrano L., Mitofusin 2 tethers endoplasmic reticulum to mitochondria. *Nature*, Vol.456: 605–610, 2008.
- De Stefani D., Raffaello A., Teardo E., Szabò I., Rizzuto R., A forty-kilodalton protein of the inner membrane is the mitochondrial calcium uniporter. *Nature*, Vol.476: 336-340, 2011.

- Demaurex N., Calcium measurements in organelles with Ca^{2+}-sensitive fluorescent proteins. *Cell Calcium*, Vol.38: 213–222, 2005.
- Drago I., Giacomello M., Pizzo P., Pozzan T., Calcium dynamics in the peroxisomal lumen of living cells. *J Biol Chem*, Vol.283: 14384-90, 2008.
- Ehehalt R., Michel B., De Pietri Tonelli D., Zacchetti D., Simons K., Keller P., Splice variants of the beta-site APP-cleaving enzyme BACE1 in human brain and pancreas. *Biochem Biophys Res Commun*, Vol.293: 30–37, 2002.
- Fasolato C., Innocenti B., Pozzan T., Receptor-activated Ca^{2+} influx: how many mechanisms for how many channels? *Trends Pharmacol Sci*, Vol.15: 77-82, 1994.
- Foskett J.K., White C., Cheung K., Mak D.O., Inositol triphosphate receptor Ca^{2+} release channels. *Physiol Rev*, Vol.87: 593-658, 2007.
- Francis R., McGrath G., Zhang J., Ruddy D.A., Sym M., Apfeld J., Nicoll M., Maxwell M., Hai B., Ellis M.C., Parks A.L., Xu W., Li J., Gurney M., Myers R.L., Himes C.S., Hiebsch R., Ruble C., Nye J.S., Curtis D., aph-1 and pen-2 are required for Notch pathway signaling, gamma-secretase cleavage of betaAPP, and presenilin protein accumulation. *Dev Cell*, Vol.3: 85–97, 2002.
- Furukawa K., Guo Q., Schellenberg G.D., Mattson M.P., Presenilin-1 mutation alters NGF-induced neurite outgrowth, calcium homeostasis, and transcription factor (AP-1) activation in PC12 cells. *J Neurosci Res*, Vol.52: 618-24, 1998.
- Giacomello M., Drago I., Pizzo P., Pozzan T., Mitochondrial Ca^{2+} as a key regulator of cell life and death. *Cell Death Differ*, Vol.14: 1267-1274, 2007.
- Giacomello M., Barbiero L., Zatti G., Squitti R., Binetti G., Pozzan T., Fasolato C., Ghidoni R., Pizzo P., Reduction of Ca^{2+} stores and capacitative Ca^{2+} entry is associated with the familial Alzheimer's disease presenilin-2 T122R mutation and anticipates the onset of dementia. *Neurobiol Dis*, Vol.18: 638-48, 2005.
- Glenner G.G. and Wong C.W., Alzheimer’s disease: initial report of the purification and characterization of a novel cerebrovascular amyloid protein. *Biochem Biophys Res Commun*, Vol.120: 885–890, 1984.
- Goedert M., Oskar Fischer and the study of dementia. *Brain*, Vol.132: 1102–1111, 2009.

- Green K.N., Demuro A., Akbari Y., Hitt B.D., Smith I.F., Parker I., LaFerla F.M., SERCA pump activity is physiologically regulated by presenilin and regulates amyloid beta production. *J Gen Physiol*, Vol.132, 2008.
- Guo Q., Christakos S., Robinson N., Mattson M.P., Calbindin D28k blocks the proapoptotic actions of mutant presenilin 1: reduced oxidative stress and preserved mitochondrial function. *Proc Natl Acad Sci USA*, Vol.95: 3227-32, 1998.
- Haass, C., De Strooper, B., The presenilins in Alzheimer's disease—Proteolysis holds the key. *Science*. Vol.286: 916–919, 1999.
- Hamilton S.L. and Serysheva I.I., Ryanodine receptor structure: progress and challenges. *J Biol Chem*, Vol.284: 4047-4051, 2008.
- Hattori M., Suzuki A.Z., Higo T., Miyauchi H., Michikawa T., Nakamura T., Inoue T., Mikoshiba K., Distinct roles of inositol 1,4,5-trisphosphate receptor types 1 and 3 in Ca^{2+} signaling. *J Biol Chem*, Vol.279: 11967–11975, 2004.
- Holsinger R.M., McLean C.A., Beyreuther K., Masters C.L., Evin G., Increased expression of the amyloid precursor beta-secretase in Alzheimer's disease. *Ann Neurol*, Vol.51: 783–786, 2002.
- Holtzman D.M., Morris John C., Goate A., Alzheimer's disease: the challenge of the second century. *Sci Transl Med*, Vol.6: 77-112, 2011.
- Ionescu L., Cheung K.H., Vais H., Mak D.O., White C., Foskett J.K., Graded recruitment and inactivation of single $InsP_3$ receptor Ca^{2+}-release channels: implications for quantal Ca^{2+}release. *J Physiol*, Vol.573: 645–662, 2006.
- Joseph S.K., Boehning D., Pierson S., Nicchitta C.V., Membrane insertion, glycosylation, and oligomerization of inositol trisphosphate receptors in a cell-free translation system. *J Biol Chem*, Vol.272: 1579–1588, 1997.
- Jung D.H., Mo S.H., Kim D.H., Calumenin, a multiple EF-hands Ca^{2+}-binding protein, interacts with ryanodine receptor-1 in rabbit skeletal sarcoplasmic reticulum, *Biochem Biophys Res Commun*, Vol.343: 34–42, 2006.
- Kang J., Lemaire H.G., Unterbeck A., Salbaum J.M., Masters C.L., Grzeschik K.H., Multhaup G., Beyreuther K., Müller-Hill B., The precursor of Alzheimer's disease amyloid A4 protein resembles a cell-surface receptor. *Nature*, Vol.325: 733–736, 1987.

- Karabinos A., Bhattacharya D., Morys-Wortmann C., Kroll K., Hirschfeld G., Kratzin H.D., Barnikol-Watanabe S., Hilschmann N., The divergent domains of the NEFA and nucleobindin proteins are derived from an EF-hand ancestor. *Mol Biol Evol*, Vol.13: 990–998, 1996.
- Kaufman R.J., Swaroop M., Murtha-Riel P., Depletion of manganese within the secretory pathway inhibits O-linked glycosylation in mammalian cells. *Biochemistry*, Vol.33: 9813–9819, 1994.
- Kayed R., Head E., Thompson J.L., McIntire T.M., Milton S.C., Cotman C.W., Glabe C.G., Common structure of soluble amyloid oligomers implies common mechanism of pathogenesis. *Science*, Vol.300: 486–489, 2003.
- Koike H., Tomioka S., Sorimachi H., Saido T.C., Maruyama K., OkuyamaA., Fujisawa-Sehara A., Ohno S., Suzuki K., Ishiura S., Membrane-anchored metalloprotease MDC9 has an alpha-secretase activity responsible for processing the amyloid precursor protein. *Biochem J*, Vol.343: 371–375, 1999.
- Kojro E., Gimpl G., Lammich S., Marz W., Fahrenholz F., Low cholesterol stimulates the nonamyloidogenic pathway by its effect on the alpha-secretase ADAM 10. *Proc Natl Acad Sci USA*, Vol.98: 5815–5820, 2001.
- Lamb G.D., Excitation–contraction coupling in skeletal muscle: comparisons with cardiac muscle. *Clin Exp Pharmacol Physiol*, Vol.27: 216–224, 2000.
- LaPointe N.E., Morfini G., Pigino G., Gaisina I.N., Kozikowski A.P., Binder L.I., Brady S.T., The amino terminus of tau inhibits kinesin-dependent axonal transport: implications for filament toxicity. *J Neurosci Res*, Vol.87: 440–451, 2009.
- Lee S.F., Shah S., Li H., Yu C., Han W., Yu G., Mammalian APH-1 interacts with presenilin and nicastrin and is required for intramembrane proteolysis of amyloid-beta precursor protein and Notch. *J Biol Chem*, Vol.277: 45013–45019, 2002
- Leite M.F., Thrower E.C., Echevarria W., Koulen P., Hirata K., Bennett A.M., Ehrlich B.E., Nathanson M.H., Nuclear and cytosolic calcium are regulated independently. *Proc Natl Acad Sci USA*, Vol.100: 2975–2980, 2003.
- Levy E., Carman M.D., Fernandez-Madrid I.J., Power M.D., Lieberburg I., van Duinen S.G., Bots G.T., Luyendijk W., Frangione B., Mutation of the

Alzheimer's disease amyloid gene in hereditary cerebral hemorrhage, Dutch type. *Science*, Vol.248: 1124–1126, 1990.

- Levy-Lahad E., Wasco W., Poorkaj P., Romano D.M., Oshima J., Pettingell W.H., Yu C.E., Jondro P.D., Schmidt S.D., Wang K., et al., Candidate gene for the chromosome 1 familial Alzheimer's disease locus. *Science*, Vol.269: 973–977, 1995.
- Lewis R.S., The molecular choreography of a store-operated calcium channel. *Nature*, Vol.446: 284-287, 2007.
- Lin P., Le-Niculescu H., Hofmeister R., McCaffery J.M., Jin M., Hennemann H., McQuistan T., De Vries L., Farquhar M.G., The mammalian calcium-binding protein, nucleobindin (CALNUC) is a Golgi resident protein. *J Cell Biol*, Vol.141: 1515–1527, 1998.
- Lin P., Yao Y., Hofmeister R., Tsien R.Y., Farquhar M.G., Overexpression of CALNUC (nucleobindin) increases agonist and thapsigargin releasable Ca^{2+} storage in the Golgi. *J Cell Biol*, Vol.145: 279–289, 1999.
- Liou J., Kim M.L., Heo W.D., Jones J.T., Myers J.W., Ferrell J.E. Jr, Meyer T., STIM is a Ca^{2+} sensor essential for Ca^{2+}-store-depletion triggered Ca^{2+} influx. *Curr Biol*, Vol.15: 1235-1241, 2005.
- Lissandron V., Podini P., Pizzo P., Pozzan T., Unique characteristics of Ca^{2+} homeostasis of the trans-Golgi compartment. *Proc Natl Acad Sci USA*, Vol. 107: 9198–9203, 2010.
- Lucin K.M. and Wyss-Coray T., Immune activation in brain aging and neurodegeneration: too much or too little? *Neuron*, Vol.64: 110–122, 2009.
- Luo W.J., Wang H., Li H., Kim B.S., Shah S., Lee H.J., Thinakaran G., Kim T.W., Yu G. and Xu H., PEN-2 and APH-1 coordinately regulate proteolytic processing of presenilin 1. *J Biol Chem*, Vol.278: 7850–7854, 2003.
- Mak D.O., McBride S., Foskett J.K., Inositol 1,4,5-trisphosphate activation of inositol trisphosphate receptor Ca^{2+} channel by ligand tuning of Ca^{2+} inhibition. *Proc Natl Acad Sci USA*, Vol. 95: 15821–15825, 1998.
- Martin L., Latypova X., Terro F., Post-translational modifications of tau protein: implications for Alzheimer's disease. *Neurochem Int*, Vol.58: 458–471, 2011.

- Mattson, M.P., LaFerla, F.M., Chan, S.L., Leissring, M.A., Shepel, P.N., Geiger, D., Calcium signaling in the ER: its role in neuronal plasticity and neurodegenerative disorders. *Trends Neurosci*, Vol.23: 222 – 229, 2000.
- McCombs J.E. and Palmer A.E., Measuring calcium dynamics in living cells with Genetically Encodable Calcium Indicators. *Methods*, Vol.46: 152–159, 2008.
- Meldolesi J. and Pozzan T., The endoplasmic reticulum Ca^{2+} store: a view from the lumen. *Trends Biochem Sci*, Vol.23: 10-14, 1998.
- Michikawa T., Hirota J., Kawano S., Hiraoka M., Yamada M., Furuichi T., Mikoshiba K., Calmodulin mediates calcium-dependent inactivation of the cerebellar type 1 inositol 1,4,5-trisphosphate receptor. *Neuron*, Vol.23: 799–808, 1999.
- Mignery G.A., Newton C.L., Archer B.T. 3rd, Südhof T.C., Structure and expression of the rat inositol 1,4,5-trisphosphate receptor. *J Biol Chem*, Vol. 265: 12679–12685, 1990.
- Missiaen L., Van Acker K., Van Baelen K., Raeymaekers L., Wuytack F., Parys J.B., De Smedt H., Vanoevelen J., Dode L., Rizzuto R., Callewaert G., Calcium release from the Golgi apparatus and the endoplasmic reticulum in HeLa cells stably expressing targeted aequorin to these compartments. *Cell Calcium*, Vol.36: 479–487, 2004.
- Mitchell K.J., Pinton P., Varadi A., Tacchetti C., Ainscow E.K., Pozzan T., Rizzuto R., Rutter G.A., Dense core secretory vesicles revealed as a dynamic Ca^{2+} store in neuroendocrine cells with a vesicle-associated membrane protein aequorin chimaera. *J Cell Biol*, Vol.155: 41–51, 2001.
- Miyawaki A., Llopis J., Heim R., McCaffery J.M., Adams J.A., Ikura M., Tsien R.Y., Fluorescent indicators for Ca^{2+} based on green fluorescent proteins and calmodulin. *Nature*, Vol.388: 882–887, 1997.
- Nagai T., Yamada S., Tominaga T., Ichikawa M., Miyawaki A., Expanded dynamic range of fluorescent indicators for Ca^{2+} by circularly permuted yellow fluorescent proteins. *Proc Natl Acad Sci USA*, Vol.101: 10554–10559, 2004.
- Nelson O., Supnet C., Liu H., Bezprozvanny I., Familial Alzheimer's disease mutations in presenilins. Effects on endoplasmic reticulum calcium

homeostasis and correlation with clinical phenotypes. *J. Alzheimer's Dis*, Vol. 21: 781–793, 2010.

- Oda K., Calcium depletion blocks proteolytic cleavages of plasmaprotein precursors which occur at the Golgi and/or trans-Golgi network. Possible involvement of Ca^{2+}-dependent Golgi endoproteases. *J Biol Chem*, Vol.267: 17465–17471, 1992.
- Oldershaw K.A. and Taylor C.W., 2,5-Di-(tert-butyl)-1,4-benzohydroquinone mobilizes inositol 1,4,5-trisphosphate-sensitive and -insensitive Ca^{2+} stores. *FEBS Lett*, Vol.274: 214-216, 1990.
- Ozer R.S. and Halpain S., Phosphorylation-dependent localization of microtubule- associated protein MAP2c to the actin cytoskeleton. *Mol Biol Cell*, Vol.11: 3573–3587, 2000.
- Pack-Chung E., Meyers M.B., Pettingell W.P., Moir R.D., Brownawell A.M., Cheng I., Tanzi R.E., Kim T.W., Presenilin 2 interacts with sorcin, a modulator of the ryanodine receptor. *J Biol Chem*, Vol.275: 14440-5, 2000.
- Palmer A.E., Giacomello M., Kortemme T., Hires S.A., Lev-Ram V.,Baker D., Tsien R.Y., Ca^{2+} indicators based on computationally redesigned calmodulin-peptide pairs. *Chem Biol*, Vol.13: 521–530, 2006.
- Palmer A.E., Jin C., Reed J.C. and Tsien R.Y., Bcl-2-mediated alterations in endoplasmic reticulum Ca^{2+} analyzed with an improved genetically encoded fluorescent sensor. *Proc Natl Acad Sci USA*, Vol.101: 17404–17409, 2004.
- Patel S., Joseph S.K., Thomas A.P., Molecular properties of inositol 1,4,5-trisphosphate receptors. *Cell Calcium*, Vol.25: 247–264, 1999.
- Pietrobon D., Di Virgilio F., Pozzan T., Structural and functional aspects of calcium homeostasis in eukaryotic cells. *Eur J Biochem*, Vol.193: 599-622, 1990.
- Pizzo P., Lissandron V., Capitanio P., Pozzan T., Ca^{2+} signalling in the Golgi apparatus. *Cell Calcium*, Vol.50: 184-92, 2011.
- Pizzo P, Drago I, Filadi R and Pozzan T., Mitochondrial Ca^{2+} homeostasis: mechanism, role, and tissue specificities. *Pflügers Arch*, Vol.464: 3-17, 2012.
- Pezzati R., Bossi M. , Podini P., Meldolesi J., Grohovaz F., High-resolution calcium mapping of the endoplasmic reticulum-Golgi-exocytic membrane

system. Electron energy loss imaging analysis of quick frozen-freeze dried PC12 cells. *Mol Biol Cell*, Vol.8: 1501–1512, 1991.

- Pinton, P., Ferrari, D., Rapizzi, E., Di Virgilio, F., Pozzan, T., Rizzuto, R., The Ca^{2+} concentration of the endoplasmic reticulum is a key determinant of ceramide-induced apoptosis: significance for the molecular mechanism of Bcl-2 action. *EMBO J*, Vol.20: 2690–2701.
- Pinton P., Pozzan T., Rizzuto R., The Golgi apparatus is an inositol 1,4,5-trisphosphate-sensitive Ca^{2+} store, with functional properties distinct from those of the endoplasmic reticulum. *EMBO J*, Vol.17: 5298–5308, 1998.
- Ponting C.P., Novel repeats in ryanodine and IP3 receptors and protein O-mannosyltransferases. *Trends Biochem Sci*, Vol.25: 48–50, 2000.
- Postina R., Schroeder A., Dewachter I., Bohl J., Schmitt U., Kojro E., Prinzen C., Endres K., Hiemke C., Blessing M., Flamez P., Dequenne A., Godaux E., van Leuven F., Fahrenholz F., A disintegrin-metalloproteinase prevents amyloid plaque formation and hippocampal defects in an Alzheimer disease mouse model. *J Clin Invest*, Vol.113: 1456–1464, 2004.
- Pozzan T., Rizzuto R., Volpe P., Meldolesi J., Molecular and cellular physiology of intracellular calcium stores. *Physiol Rev*, Vol.74: 595-636, 1994.
- Prins D. and Michalak M., Organellar calcium buffers. *Cold Spring Harb Perspect Biol*, Vol.3: 1-16, 2011.
- Pritchard S.M., Dolan P.J., Vitkus A., Johnson G.V., The toxicity of tau in Alzheimer disease: turnover, targets and potential therapeutics. *J Cell Mol Med*, Vol.15: 1621-1635, 2011.
- Putney J.W. Jr., Recent breakthroughs in the molecular mechanism of capacitative calcium entry (with thoughts on how we got here). *Cell Calcium*, Vol.42: 103–110, 2007.
- Ramos-Franco J., Galvan D., Mignery G.A., Fill M., Location of the permeation pathway in the recombinant type 1 inositol 1,4,5-trisphosphate receptor. *J Gen Physiol*, Vol.114: 243–250, 1999.
- Raychaudhury B., Gupta S., Banerjee S., Datta S.C., Peroxisome is a reservoir of intracellular calcium. *Biochim Biophys Acta*, Vol.1760: 989–992, 2006.

- Rizzuto R., Simpson A.W., Brini M., Pozzan T., Rapid changes of mitochondrial Ca^{2+} revealed by specifically targeted recombinant aequorin. *Nature*, Vol.358: 325–327, 1992.
- Rizzuto R., Brini M., Murgia M., Pozzan T., Microdomains with high Ca^{2+} close to IP_3-sensitive channels that are sensed by neighboring mitochondria. *Science*, Vol.262: 744-747, 1993.
- Rizzuto R., Brini M., Pozzan T., Targeting recombinant aequorin to specific intracellular organelles. *Methods Cell Biol*, Vol.40: 339–358, 1994.
- Rizzuto R. and Pozzan T., Microdomains of intracellular Ca^{2+}: molecular determinants and functional consequences. *Physiol Rev*, Vol.86: 369-408, 2006.
- Roderick H.L., Berridge M.J., Bootman M.D. Calcium-induced calcium release. *Curr Biol*, Vol.13: R425, 2003.
- Soboloff J., Madesh M., Gill D.L., Sensing cellular stress through STIM proteins. *Nat Chem Biol*, Vol.7: 488–492, 2011.
- Sahoo S.K., Kim T., Kang G.B., Lee J.G., Eom S.H., Kim do H., Characterization of calumenin-SERCA2 interaction in mouse cardiac sarcoplasmic reticulum. *J Biol Chem*, Vol.284: 31109–31121, 2009.
- Schäfer W., Stroh A., Berghöfer S., Seiler J., Vey M., Kruse M.L., Kern H.F., Klenk H.D., Garten W., Two independent targeting signals in the cytoplasmic domain determine trans-Golgi network localization and endosomal trafficking of the proprotein convertase furin. *EMBO J*, Vol.14: 2424–2435, 1995.
- Scherer P.E., Lederkremer G.Z., Williams S., Fogliano M., Baldini G., Lodish H.F., Cab45, a novel Ca^{2+}-binding protein localized to the Golgi lumen. *J Cell Biol*, Vol.133: 257–268, 1996.
- Schrader M. and Yoon Y., Mitochondria and peroxisomes: are the ‘big brother’ and the ‘little sister’ closer than assumed? *Bioessays*, Vol.29: 1105–1114, 2007.
- Seidler N.W., Jona I., Vegh M., Martonosi A., Cyclopiazonic acid is a specific inhibitor of the Ca^{2+}-ATPase of sarcoplasmic reticulum. *J Biol Chem*, Vol. 264:17816-17823, 1989.

- Sengupta A., Kabat J., Novak M., Wu Q., Grundke-Iqbal I., Iqbal K., Phosphorylation of tau at both Thr 231 and Ser 262 is required for maximal inhibition of its binding to microtubules. *Arch Biochem Biophys*, Vol.357: 299–309, 1998.
- Sherrington R., Rogaev E.I., Liang Y., Rogaeva E.A., Levesque G., Ikeda M., Chi H., Lin C., Li G., Holman K., Tsuda T., Mar L., Foncin J.F., Bruni A.C., Montesi M.P., Sorbi S., Rainero I., Pinessi L., Nee L., Chumakov I., Pollen D., Brookes A., Sanseau P., Polinsky R.J., Wasco W., Da Silva H.A., Haines J.L., Perkicak-Vance M.A., Tanzi R.E., Roses A.D., Fraser P.E., Rommens J.M., St George-Hyslop P.H., Cloning a gene bearing missense mutations in early-onset familial Alzheimer's disease. *Nature*, Vol.375: 754–760, 1995.
- Shirotani K., Edbauer D., Capell A., Schmitz J., Steiner H., Haass C., Gamma-Secretase activity is associated with a conformational change of nicastrin. *J Biol Chem*, Vol.278: 16474, 2003.
- Sinha S., Anderson J.P., Barbour R., Basi G.S., Caccavello R., Davis D., Doan M., Dovey H.F., Frigon N., Hong J., Jacobson-Croak K., Jewett N., Keim P., Knops J., Lieberburg I., Power M., Tan H., Tatsuno G., Tung J., Schenk D., Seubert P., Suomensaari S.M., Wang S., Walker D., Zhao J., McConlogue L., John V., Purification and cloning of amyloid precursor protein beta-secretase from human brain. *Nature*, Vol.402: 537–540, 1999.
- Small S.A. and Duff K., Linking Abeta and tau in late-onset Alzheimer's disease: a dual pathway hypothesis. *Neuron*, Vol.60: 534–42, 2008.
- Stutzmann G.E., Smith I., Caccamo A., Oddo S., Laferla F.M., Parker I., Enhanced ryanodine receptor recruitment contributes to Ca^{2+} disruptions in young, adult, and aged Alzheimer's disease mice. *J Neurosci*, Vol.26: 5180-9, 2006.
- Takasugi N., Tomita T., Hayashi I., Tsuruoka M., Niimura M., Takahashi Y., Thinakaran G., Iwatsubo T., The role of presenilin cofactors in the gamma-secretase complex. *Nature*, Vol.422: 438–441, 2003.
- Tanzi R.E., Gusella J.F., Watkins P.C., Bruns G.A., St George-Hyslop P., Van Keuren M.L., Patterson D., Pagan S., Kurnit D.M., Neve R.L., Amyloid beta

protein gene: cDNA, mRNA distribution, and genetic linkage near the Alzheimer locus. *Science*, Vol.235: 880–884, 1987.

- Tarassishin L., Yin Y.I., Bassit B., Li Y.M., Processing of Notch and amyloid precursor protein by gamma-secretase is spatially distinct. *Proc Natl Acad Sci USA*, Vol.101: 17050-17055, 2004.
- Thastrup O., Cullen P.J., Drøbak B.K., Hanley M.R., Dawson A.P., Thapsigargin, a tumor promoter, discharges intracellular Ca^{2+} stores by specific inhibition of the endoplasmic reticulum Ca^{2+}-ATPase. *Proc Natl Acad Sci USA*, Vol.87:2466-2470, 1990.
- Thinakaran G., Borchelt D.R., Lee M.K., Slunt H.H., Spitzer L., Kim G., Ratovitsky T., Davenport F., Nordstedt C., Seeger M., Hardy J., Levey A.I., Gandy S.E., Jenkins N.A., Copeland N.G., Price D.L., Sisodia S.S., Endoproteolysis of presenilin 1 and accumulation of processed derivatives in vivo. *Neuron*, Vol.17: 181–190, 1996.
- Thyberg J. and Moskalewski S., Role of microtubules in the organization of the Golgi complex. *Exp Cell Res*, Vol.246: 263-79, 1999.
- Vaca L., SOCIC: the store-operated calcium influx complex. *Cell Calcium*, Vol.47: 199–209, 2010.
- Vanoevelen J., Raeymaekers L., Parys J.B., De Smedt H., Van Baelen K., Callewaert G., Wuytack F., Missiaen L., Inositol trisphosphate producing agonists do not mobilize the thapsigargin-insensitive part of the endoplasmic-reticulum and Golgi Ca^{2+} store. *Cell Calcium*, Vol.35: 115–121, 2004.
- Vetrivel K.S., Cheng H., Lin W., Sakurai T., Li T., Nukina N., Wong P.C., Xu H., Thinakaran G., Association of gamma-secretase with lipid rafts in post-Golgi and endosome membranes. *J Biol Chem*, Vol.279: 44945-54, 2004.
- Vetrivel K.S., Zhang Y.W., Xu H., Thinakaran G. Pathological and physiological functions of presenilins. *Mol Neurodegener*, Vol.1: 4, 2006.
- Wang H.J., Guay G., Pogan L., Sauve R., Nabi I.R., Calcium regulates the association between mitochondria and a smooth subdomain of the endoplasmic reticulum. *J Cell Biol*, Vol.150: 1489–1498, 2000.

- Weingarten M.D., Lockwood A.H., Hwo S.Y., Kirschner M.W., A protein factor essential for microtubule assembly. *Proc Natl Acad Sci USA*, Vol.72: 1858–1862, 1975.
- Wuytack F., Raeymaekers L., Missiaen L., Molecular physiology of the SERCA and SPCA pumps. *Cell Calcium*, Vol.32: 279-305, 2002.
- Yang S.N. and Berggren P.O., The role of voltage-gated calcium channels in pancreatic beta-cell physiology and pathophysiology. *Endocr Rev*, Vol.27: 621–676, 2006.
- Yu G., Nishimura M., Arawaka S., Levitan D., Zhang L., Tandon A., Song Y.Q., Rogaeva E., Chen F., Kawarai T., Supala A., Levesque L., Yu H., Yang D.S., Holmes E., Milman P., Liang Y., Zhang D.M., Xu D.H., Sato C., Rogaev E., Smith M., Janus C., Zhang Y., Aebersold R., Farrer L.S., Sorbi S., Bruni A., Fraser P., St George-Hyslop P., Nicastrin modulates presenilin-mediated notch/glp-1 signal transduction and beta-APP processing. *Nature*, Vol.407, 48–54, 2000
- Zampese E, Fasolato C, Kipanyula M.J., Bortolozzi M., Pozzan T and Pizzo P., Presenilin-2 modulates endoplasmic reticulum (ER)–mitochondria interactions and Ca^{2+} cross-talk. *PNAS*, Vol. 108: 2777-2782.
- Zampese E. and Pizzo P., Intracellular organeles in the saga of Ca^{2+} homeostasis: different molecules for different purpose? *Cell Mol Life Sci*, Vol. 69: 1077-1104, 2011.
- Zampese E., Brunello L., Fasolato C., Pizzo P., Ca^{2+} dysregulation mediated by presenilins in Familial Alzheimer's Disease: Causing or modulating factor? *Curr Trends Neurol*, Vol.3: 1-9, 2009.
- Zatti G., Burgo A., Giacomello M., Barbiero L., Ghidoni R., Sinigaglia G., Florean C., Bagnoli S., Binetti G., Sorbi S., Pizzo P., Fasolato C., Presenilin mutations linked to familial Alzheimer's disease reduce endoplasmic reticulum and Golgi apparatus calcium levels. *Cell Calcium*, Vol.39: 539-50, 2006.
- Zatti G., Ghidoni R., Barbiero L., Binetti G., Pozzan T., Fasolato C., Pizzo P., The presenilin 2 M239I mutation associated with familial Alzheimer's disease reduces Ca^{2+} release from intracellular stores. *Neurobiol Dis*, Vol.15: 269-278, 2004.

- Zerfaoui M., Fukuda M., Langlet C., Mathieu S., Suzuki M., Lombardo D., El-Battari A., The cytosolic and transmembrane domains of the beta 1,6 N-acetylglucosaminyltransferase (C2GnT) function as a cis to medial/Golgi-targeting determinant. *Glycobiology*, Vol.12: 15-24, 2002.
- Zhang H., Ma Q., Zhang Y.W., Xu H., Proteolytic processing of Alzheimer's β-amyloid precursor protein. *J Neurochem*, Vol.120: 9–21, 2012.
- Zhang Y.W., Thompson R., Zhang H., Xu H., APP processing in Alzheimer's disease. *Mol Brain*, Vol.4: 3, 2011.

Scientific curriculum

Pubblications

- Bonza M.C., Loro G., Behera S., **Wong A.**, Kudla J., Costa A., Analyses of Ca^{2+} accumulation and dynamics in the endoplasmic reticulum of Arabidopsis root cells using a genetically encoded cameleon sensor. *Plant Physiology*, Vol.163: 1230–1241, 2013.
- **Wong A.K.**, Capitanio P., Lissandron V., Bortolozzi M., Pozzan T. and Pizzo P., Heterogeneity of Ca^{2+} handling among and within Golgi compartments. *J Mol Cell Biol*, Vol.4:266-276, 2013.
- Kipanyula M.J., Contreras L., Zampese E., Lazzari C., **Wong A.K.**, Pizzo P., Fasolato C., Pozzan T., Ca^{2+} dysregulation in neurons from transgenic mice expressing mutant presenilin 2. *Aging Cell*, Vol.5: 885-893, 2012.